# The *Skyscraper Revolution*: Global Economic Development and Land Savings*

Gabriel M. Ahlfeldt † Nathaniel Baum-Snow ‡ Remi Jedwab §

March 9, 2026

**Abstract**

Tall buildings make up over 20% of real estate by value in the world's largest cities. Nonetheless, many governments constrain tall building construction, hindering urbanization and growth. Quantification for all cities worldwide using a canonical land use model disciplined with reduced form elasticity estimates indicates that eliminating existing height constraints would generate a welfare gain of 3.7% in developing economies. Aggregate land values would decline by 3.9%, incentivizing landowners to support height restrictions. Estimated elasticities of city population and built area with respect to aggregate city building heights are 0.13 and -0.16, reinforcing the quantitative evidence that tall buildings facilitate urban growth and compactness. Interactions between static demand factors and the geography of bedrock isolate 1975-2015 tall building construction driven by technology-induced reductions in the cost of height. Using indirect inference, we estimate a (congestion) elasticity of consumer welfare to urban density of -0.11.

Key words: Urban Density; Tall Buildings; Sustainable Urbanization; Urban Growth; Commercial Real Estate; Housing Supply; Urban Sprawl; Land Savings; Housing Affordability; Geographic Constraints

JEL: R11, R12, R14, R31, R33, O18, O13

*We thank the editor, five anonymous referees, David Albouy, Milena Almagro, Jason Barr, Adrien Bilal, Jan Brueckner, Filipe Campante, Donald Davis, Klaus Desmet, Rebecca Diamond, Jonathan Dingel, Gilles Duranton, Fernando Ferreira, Edward Glaeser, Marco Gonzalez-Navarro, Gabriel Kreindler, Jessie Handbury, Mariaflavia Harari, Matthew Kahn, Jeffrey Lin, John Morrow, David Nagy, Elias Papaioannou, Charly Porcher, Daniel Ramos-Menchelli, Lindsay Relihan, Tanner Regan, Frederic Robert-Nicoud, Jorge De la Roca, Stephen L. Ross, Alexander Rothenberg, Nick Tsivanidis, Matthew Turner, Tony Venables, C. Luke Watson, and numerous seminar audiences for helpful comments.

†London School of Economics and Humboldt University in Berlin. Email: g.ahlfeldt@lse.ac.uk

‡University of Toronto. Email: nate.baum.snow@rotman.utoronto.ca

§George Washington University and NYU Marron Institute of Urban Management. Email: jedwab@gwu.edu

# 1 Introduction

Chicago's ten-storey 42-meter tall Home Insurance Building, built in 1885 and often called the world's first "skyscraper" (Schleier, 1986), was an early example of the use of technologies that would prove to transform cities around the world. Since then, continued technological improvements that have lowered the cost of building tall have facilitated the construction of the more than 16,000 km of buildings of over 55 meters (∼13-14 floors) in cities worldwide, or about four times the Euclidean distance between Los Angeles and New York City. Most of this construction has occurred since 1975 for residential use, and much in developing economies. With the equivalent of almost 43,000 Empire State Buildings, the stock of tall buildings worldwide holds an aggregate asset value of more than 15 trillion dollars. Indeed, a look at many global cities today leaves no doubt that the *Skyscraper Revolution* has been transformative (Glaeser, 2012). The mean aggregate height of tall buildings across cities of over 5 million inhabitants is greater than 100 km. In cities of over 1 million people, tall buildings account for ∼10% of the physical stock and almost 20% of aggregate construction costs for existing structures.[1]

With structural change out of agriculture, many cities in the developing world face strong urbanization pressures (Bryan et al., 2020). Moreover, many nations face a housing crisis that is exacerbated by supply constraints (Knoll et al., 2017; Glaeser and Gyourko, 2018). Some nations and cities are laissez-faire about vertical development, or even "invest" in their skyline through direct subsidy, public-private partnerships, public land donations, or tax incentives.[2] Others restrict vertical development through floor area ratio caps, height limits, and land use planning restrictions (Brueckner et al., 2017). Given the considerable amount of government involvement in the tall building sector, it is essential to study the consequences of vertical development.

This paper evaluates the economic effects of the skyscraper revolution and quantifies the economic costs of height restrictions that may have held back some of its potential transformative effects. We depart from a literature that views tall buildings as a mere consequence of urbanization. Instead, we shed light on the role tall buildings play as catalysts of urbanization. Cities that expand vertically can accommodate more workers in productive locations, fostering structural change, increasing output, and enhancing welfare. Land use regulations that prevent economically viable vertical growth may thus lead to spatial misallocation (Hsieh and Moretti, 2019) and delay economic development (Gechter and Tsivanidis, 2023; Anagol et al., 2024).

We quantify the benefits associated with 1975-2015 reductions in the "cost of height", the elasticity of tall building construction cost per unit of floor area with respect to height. Our empirical analysis recovers causal effects of the component of 1975-2015 tall building construction driven by reductions in the cost of height on urban population growth, urban form, and land use. Innovations to the tall building sector in the 1960s and 1970s, including the development of reinforced concrete, computer aided design and engineering, and improved crane technologies, reduced tall building construction costs in developing economies in particular, thereby facilitating their "Skyscraper Revolution". Using data from 11,257 urban agglomerations worldwide in

[1] Building volumes data indicate that fractions of the building stock in buildings over 55 m tall are 80% in Hong Kong, 58% Seoul, 39% in Singapore, 35% in Mumbai, 32% in Taipei, 30% in Moscow, 29% in Dubai, 27% in Kuala Lumpur, 26% in Sao Paulo, 22% in Hanoi, 17% in Manila, 16% in Bogota, and 12% in New York.

[2] In our data, One World Trade Center cost $3.9 billion, one-third of which was covered by New York's Port Authority and the State of New York. The Clock Towers (Saudi Arabia), the Petronas Towers (Malaysia), the Iconic Tower (Egypt), the AD Plaza (Kazakhstan), the Burj Khalifa (UAE), Tour F (Ivory Coast) and Taipei 101 (Taiwan) cost governments 2.2%, 2.0%, 0.8%, 0.7%, 0.6%, 0.6% and 0.5% of national GDP, respectively.

developing economies, we find average elasticities of city population and built-up land area to total city tall building heights of 0.13 and –0.16, respectively. Remarkably, we find similar population effects in developed countries for the historical 1850 to 1975 period.

To recover the realized and potential benefits of the skyscraper revolution, we confront a quantitative urban land use model with reduced-form moments from the data. As in the standard urban model (Brueckner, 1987), we assume a monocentric city structure with equilibrium rent and density falling in distance from an exogenous historic center. Unlike in the standard model, we allow for endogenous land use (Duranton and Puga, 2015) and wages, which are influenced by agglomeration economies and imperfectly elastic labor supply to the city. Residential and commercial real estate developers face costs that are convex in building height and depend on city characteristics, creating a congestion force that limits density. Each city's hinterland hosts potential in-migrants, with migration responses depending on idiosyncratic preference heterogeneity between rural and urban locations and the stock of potential migrants. Using simulated method of moments, we estimate the (congestion) elasticity of urban consumer amenities to city density to be –0.11 by matching reduced form migration and built area responses to aggregate city height supply shocks for cities with minimal height constraints.

Reductions in the cost of height increase welfare by allowing cities to accommodate greater populations in denser residential *and* work locations. Productivity and wages rise through agglomeration forces. Conditional on urban population, rents decline because of lower construction costs, though with sufficiently large endogenous population responses, rents may increase. Commuting costs decline because of greater urban compactness.

For each city worldwide, we quantify the model to rationalize the observed 2015 population conditional on local construction costs and height constraints. Calibration to an equilibrium constrained by height restrictions is novel to the literature and allows us to predict the aggregate effects on labor and land markets of removing existing height constraints. We infer height restrictions by comparing each city's 2015 aggregate height of tall buildings to that for the $95^{th}$ percentile city with similar observed characteristics. Counterfactual exercises indicate 3.7% greater average worker (consumer) welfare in developing economies in environments with no height restrictions relative to the 2015 equilibrium. Due to the positive effects on real estate supply near city centers of relaxing height restrictions, cities become more compact. Increases in real wages account for about half of the associated city welfare gains, despite rent increases from population inflows and income growth. In contrast, banning existing buildings above 55 meters would reduce worker welfare by 0.9%. That is, existing land use and height regulations mean that only about one-fifth of potential welfare gains from heights have been realized.

Fully relaxing existing height constraints would reduce aggregate land values by 3.9% in developing economies, as higher central densities allow peripheral land to be taken out of urban use. Reducing height regulation redistributes welfare from land to labor. Landlords lose with the lower rents associated with the supply expansion that comes with new heights but workers gain more due to higher real wages and enhanced access to preferred locations. As in Ortalo-Magné and Prat (2014) and Duranton and Puga (2023), this result highlights incumbent landlords' incentives to enact land use restrictions to impede development, thereby restricting densification and associated welfare gains. Because land use restrictions are more stringent in developed economies, their corresponding consequences of eliminating height restrictions are even greater.

Impacts of height constraints are also increasing in city size and declining in the cost of height. Relatedly, given expected global urban population growth of 1.5% per year till 2050 (United Nations, 2018) and an annual rate of technological progress in the tall building sector of ∼2% (Ahlfeldt and Barr, 2022), the global cost of height restrictions will only increase in the future.

For identification of elasticities of population and built land area with respect to heights, we use an instrumental variables strategy that leverages both cross-sectional and time series variation in the cost of building tall. In the cross-section, we use variation in city mean bedrock depth as a key source of identifying variation. Descriptive analysis and building cost function estimates indicate that the elasticity of construction cost to height per building floor area is U-shaped in bedrock depth, which is consistent with engineering standards for foundation depth and the narrative in Barr et al. (2011). Bedrock that is too close to the surface must be blasted away at high cost to make room for building foundations. Foundations built above bedrock that is beyond the optimal depth must be reached with the costly installation of deep wide piles, placed on a costly raft, or engineered to be underpinned by many very long deeply bored piles.

As favorable bedrock depth acts as a cost shifter, cities with more favorable bedrock depths experienced more construction of tall buildings conditional on their levels of real estate demand. However, a sufficiently high level of demand, proxied for with 1975 city population, is needed for bedrock depth to matter for tall building construction. As a result, the elasticity of tall building construction with respect to 1975 city population is greater at more favorable bedrock depths. Differencing over the 1975-2015 period additionally leverages secular reductions in the cost of height for identification. Particularly in the developing world, costs were sufficiently prohibitive in 1975 to preclude the existence of many tall buildings. Put together, our identification strategy amounts to triple difference comparisons of historically (pre-1975) large versus small cities on more versus less favorable bedrock depths over time (between 1975 and 2015).

To implement the empirical strategy, we compile a unique data set of all 12,877 urban agglomerations with populations over 50,000 worldwide (in 182 countries), covering about 90% of the world's total urban population. For these cities, we organize census-based population and satellite-based area estimates going back to 1975, allowing us to measure population and land use in and around these cities over time. To capture the vertical size of cities, we use a data set of 300 thousand tall buildings from *Emporis*. This data set has comprehensive information on the location, use, and construction year of almost all buildings over 55 meters tall worldwide.

A large literature assesses the extent to which various types of infrastructure construction drive urban change. However, this is the first paper to comprehensively study how declines in the costs of building tall have contributed to economic development around the world. Like highways and accessibility (Faber, 2014; Chiovelli et al., 2018; Balboni, 2019; Morten and Oliveira, 2024), railroads/subways (Gonzalez-Navarro and Turner, 2018; Heblich et al., 2020; Balboni et al., 2021), airports/ports (Campante and Yanagizawa-Drott, 2018; Ducruet et al., 2020), and sewers (Coury et al., 2022), tall buildings form a central component of the global capital stock.

Our estimates are of similar or greater magnitudes to those in the literature for impacts of other components of urban capital stocks. For example, Duranton and Turner (2012) estimates an elasticity of urban population growth with respect to urban highway stocks of 0.15 for the US, similar to our tall building elasticity estimate of 0.13 for the developing world. However, our estimated population density elasticity for tall buildings of 0.31 is about three times as large

as those found for urban radial highways in the US and China (Baum-Snow, 2007; Baum-Snow et al., 2017) and much larger than for other types of infrastructure. These investigations of how infrastructure drives urban growth are grounded in the classic empirical literature going back to Glaeser et al. (1992), Henderson et al. (1995), and Ades and Glaeser (1995) that study the determinants of urban TFP growth and variation across locations in equilibrium city sizes.

Understanding how the skyscraper revolution fits into the process of urban development is all the more important as cities that do not develop vertically tend to sprawl (Brueckner and Fansler, 1983; Burchfield et al., 2006; Civelli et al., 2023) and/or become inefficiently spatially configured. Odd urban spatial structures impede growth (Harari, 2020), and associated sprawl typically occupies land that is particularly valuable in non-urban uses. According to World Bank (2022), urban areas occupied 3.6 million sq km in 2011, whereas 48.0 million sq km of land was in agriculture. As cities are more likely to be sited on agriculturally productive land (Henderson et al., 2018), land savings through increased urban compactness frees up more space for agriculture and tree canopy. Taller cities make us "greener" (Glaeser, 2012) by accommodating more people on less land. In that, the skyscraper revolution has parallels with the Green Revolution, whose goal was to use rural land more intensively in order to use less land globally (Gollin et al., 2021).

Our model incorporates insights from the land use and housing production literatures to accommodate height restrictions and linkages across labor and housing markets within and between residential and commercial sectors. As in Albouy et al. (2020), we employ the classical land use theory of Alonso (1964), Mills (1967), and Muth (1969), with additional elements from quantitative spatial models (Redding and Rossi-Hansberg, 2017; Sturm et al., 2022; Rosenthal-Kay, 2024). Qualitative conclusions mirror those from the more targeted modeling frameworks in Bertaud and Brueckner (2005) and Henderson et al. (2021), though we emphasize variation across cities in the cost of height. The use of the simple monocentric city structure allows our model to reasonably characterize cities of many different sizes and shapes, in part as captured by differences in fundamental productivities and amenities. While the flow of tall buildings reflects economic activity at the time they are built (Ahlfeldt and Barr, 2020; Harari and Wong, 2019), in our model skyscrapers also increase densities and productivities (Curci, 2020; Liu et al., 2020).

Research on the existence and implications of housing market regulation for developed economies demonstrates how such regulation promotes lower densities, sprawl, and higher housing costs (Saiz, 2010; Gyourko and Molloy, 2015; Jedwab et al., 2022; D'Amico et al., 2024). Work for the developing world also comes to the conclusion that binding height regulations have negative welfare consequences (Brueckner and Sridhar, 2012; Brueckner et al., 2017). Another literature emphasizes the role of height regulations on crowding and slums if formal housing supply is constrained (Lall et al., 2007; Henderson et al., 2021; Jedwab et al., 2021). We provide a comprehensive quantitative evaluation of the extent to which reductions in the cost of building tall have influenced urbanized land expansion (including as slums), urban compactness, affordability, rural-urban migration, productivity, and welfare globally. Moreover, we quantify the prospects for further gains through relaxation of existing height regulations. Contrary to the literature, our quantitative analysis emphasizes that agglomeration effects associated with lifting height limits boosts housing demand enough to increase average rents, with these rent increases more than counteracted with higher wages and reduced commuting costs (or higher localized amenities) to generate welfare gains. Additionally, allowing vertical expansion benefits workers over landowners and may thus inhibit widespread support for such deregulation.

## 2 Data and Descriptive Evidence

Here we explain the data assembly for the 11,257 cities in our main sample. We then describe the evolution of skyscraper technology, demonstrating how variation in bedrock depth is useful for identification. This leads to estimates of the relationship between bedrock depth and the cost of height. Finally, we build up to the first stage estimation equation and present these results.

### 2.1 Data Sources

**City-Level Outcomes:** Using the *Global Human Settlements-Urban Centre Database* (GHS-UCDB) (Florczyk et al., 2019, v1.2), we obtain the GIS boundaries of all 12,877 2015 vintage agglomerations worldwide. The GHS-UCDB reports the built-up area and population of each city circa 1975, 1990, 2000 and 2015 within 2015 definition city geographies. It also reports land area, which is calculated separately for each year using common density thresholds. As built-up area is consistently measured over time, this is our main measure of urbanized land.[3] The 12,877 cities account for ∼90% of the world's urban population in 2015 (United Nations, 2018). We focus on 11,257 cities in the 125 developing economies as defined by the World Bank in 2015.

As an alternative measure of growth, we use the radiance calibrated (not top-coded) version of night lights data (NGDC, 2015), which is available for select years 1996-2011. We calculate the total sum of lights at night across ≈1 km resolution pixels for each city in each year. Lastly, historical population data (Bairoch, 1988; Buringh and Hub, 2013) is used to study pre-trends.

Figure 1: Global Evolution of Aggregate Tall Building Heights (km), 1895-2021

(a) All Tall Buildings

(b) Residential vs. Office Towers, World

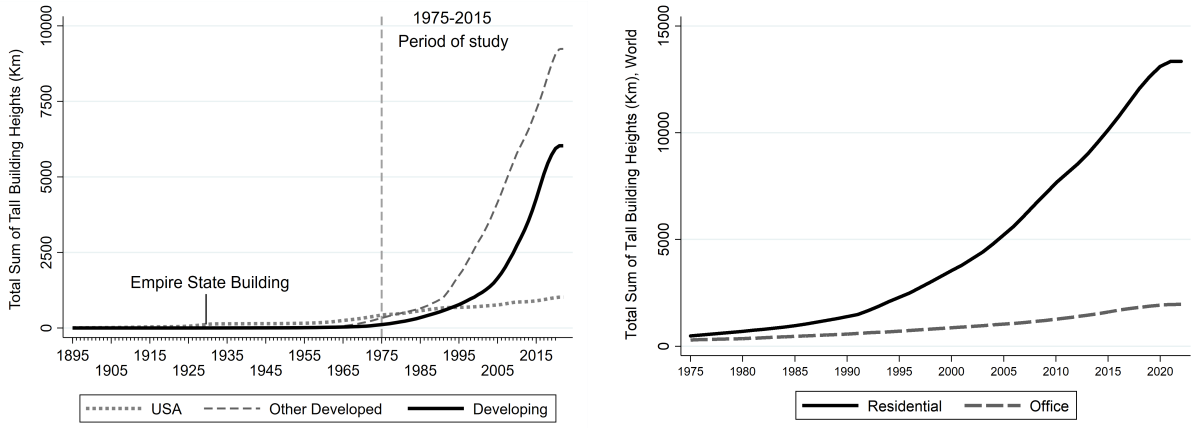


*Notes:* The left panel shows the evolution of the total stock of tall building heights (km) for cities in the U.S., other developed ("high-income") economies, and developing economies, all defined circa 2015. The right panel shows the evolution of the total world stock of tall building heights (km) separately for residential buildings and office buildings 1975-2021 (mixed use buildings are rare). Only tall buildings above 55 meters (≈ 180 feet or 13-14 floors) are included in the calculations.

**Building Data:** Emporis (2022) was a provider of global high-rise building data. Emporis collected information about the life-cycle of each building over 55 meters tall worldwide, and many shorter buildings. The database contains information for about 700,000 "existing" buildings. We observe geographic coordinates or locality, allowing us to assign each building to a GHS-UCDB city. For a select set of 1,033 buildings, Emporis also reports the construction

[3] Agglomeration, which we refer to as cities, are defined as clusters of contiguous 1 km$^2$ grid cells, each with densities of at least 1,500 inhabitants or with at least 50% built-up surface area, and a minimum total population of 50,000. 1975 and 2015 built area is the sum of building area within the 2015 city's boundary (measured using satellites). 1975 total area is based on the city's boundary in 1975. Population is taken from censuses.

cost, which excludes land acquisition costs. As "soft" legal, regulatory and engineering costs tend to scale with building height, we consider our cost data to cover variable costs only.

Inspection of the kernel density of 2015 building heights reveals a mode and large spike at 55 meters. Since cities are likely to have more buildings below than above 55 m and the observed distribution of building heights is relatively smooth above it, following Barr and Jedwab (2023) we infer that Emporis likely only captures the universe of buildings above this height (N ≈ 300,000). Using the year of construction (and demolition if demolished), we obtain the *sum of heights* (m) of all buildings of at least 55 meters for each city-year from the 19th century to date.

Figure 2: Sum of Tall Building Heights (km), World Cities, 1975 and 2015

(a) 1975

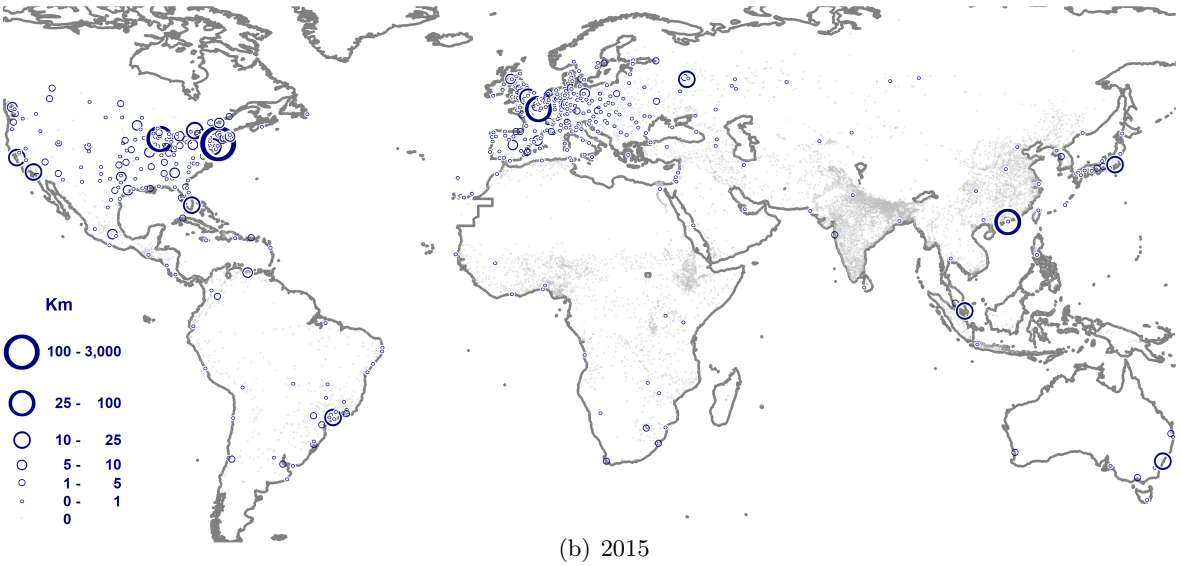


(b) 2015

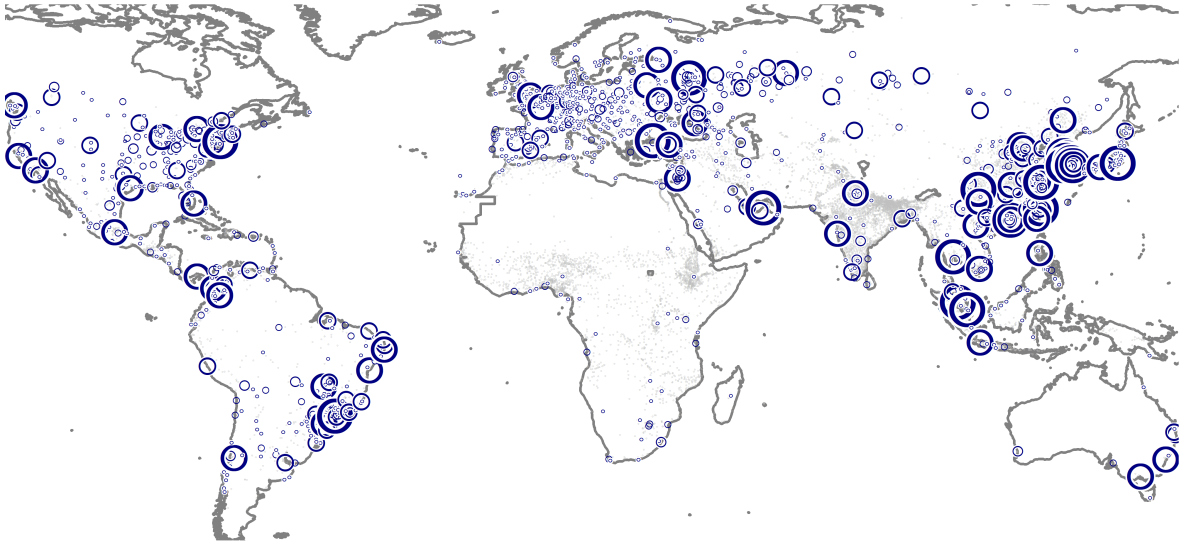

*Notes:* Bubble sizes indicate the total stock of tall building heights (km) for all 12,877 world cities of at least 50,000 residents circa 2015. The same legend applies to both panels, with tiny grey dots indicating cities with no tall buildings. Only buildings above 55 meters (≈ 180 feet or 13-14 floors) are included in the calculations.

As seen in Figure 1, until the 1960s, the vast majority of the world's tall buildings housed offices in large cities of high income countries. Starting in the 1970s, the construction of tall buildings spread through many middle income countries. Most such construction was for residential use. During our primary study period of 1975-2015, the total stock of heights increased from a clean slate of near 0, with only 1% of cities having any heights, to over 6,000

km in developing economies.[4] While tall buildings were concentrated in a few developed regions in 1975, one can observe the growth of tall buildings in the developing world by 2015 (Figure 2). Using cities in developing economies only for the analysis contributes to cleaner identification and allows us to focus conceptualization on the process of urbanization in economic development.

To account for the fact that many cities have no buildings above 55 m in some years, we use $\ln(\text{Heights} + 1)$ to measure the sum of heights in each city. While this is not the only way to aggregate intensive and extensive margin comparisons across cities, we show below that it provides results that are consistent with examination of extensive margin comparisons and can be interpreted in the context of the model. Various such robustness checks are described below.

**Bedrock Depth:** Shangguan et al. (2017) reports bedrock depth at ≈1 km resolution for the world. To avoid introducing selection on construction decisions within cities, we use *mean bedrock depth* (MBD) for each city within its 2015 boundary as our main bedrock measure. The data is "extracted from a global compilation of soil profile data (about 1.3 million locations) and borehole data (about 1.6 million locations)." Looking across all pixels within our city boundaries, 80% of the variance in bedrock depth is between rather than within cities.

Bedrock depths were determined through geological processes, including movements of glaciers during past ice ages and of tectonic plates. The main glaciation periods occurred millions of years ago; the last episode of the Last Glacial Period ended ∼10,000 years ago. Plate tectonics in the past 4 billion years have also shaped the earth's terrain. Weathering and erosion contribute to exposing or decomposing bedrock, thereby making it shallower or deeper. The role of past ice ages and the ambiguous effects of weathering and erosion may explain the weak correlations that we find between bedrock depth and geographical features such as elevation, ruggedness, proximity to coasts and lakes, earthquake risk, soil quality, and wind speed, whether for all cities or large (million-plus) cities where tall buildings are mostly found (Table A1 Cols. (1) and (2)). Appendix A.1 provides details on these controls. Table A2 presents summary statistics.

## 2.2 The Data Generating Process for Heights

Two attributes of the tall building cost function are central for our analysis. First, the cost of height has declined over time. Second, by 2015, construction costs of tall buildings were lower in cities with intermediate bedrock depths. Here we describe the history and engineering principles that generate these facts. The model in Section 4 formalizes these ideas.

Until the mid-1950s, almost all tall buildings were constructed using steel frame technology. Over the following decades, concrete technology matured enough such that it was used to frame about half of new US tall buildings by 1975. Steel technology is capital and expertise intensive, whereas concrete construction uses lower cost labor and materials. The advent of standardized computer aided design and engineering, which expanded greatly into the 1970s and 1980s, complemented the move to concrete based construction. By automating the calculations determining building specifications required to withstand collateral wind loads, this technology further reduced the cost of height. By 2005, over 80% of new construction tall buildings over 80 meters in the US were reinforced concrete (CTBUH, 2022). Crane technology also improved, with tower cranes from the 1950s giving way to mobile cranes in the 1960s and climbing tower cranes in the 1970s. Based on our cost data, this technical progress came with at least a 25%

[4] In 1975, 40% of developing economy heights are in Brazilian cities; Johannesburg, Mexico City, and Caracas each had an additional 10%. Our main results hold when excluding the few cities with heights in 1975 (unreported).

decline in the cost of height in the US over the 1975-2015 period (Appendix Figure A1).

While construction practices in the US transitioned slowly from steel to concrete, concrete construction dominated *from the beginning* in the developing world. Lower labor costs and higher shipping and production costs for steel than cement, which is mixed into concrete, justifies this choice. Even today, there are almost no steel-framed tall buildings in the developing world, though steel reinforced concrete is a common building type (CTBUH, 2022). US firms were in charge of most tall building construction projects in the developing world through the 1970s. Diffusion of technologies over time meant that local builders managed most new construction by the 1990s. Moreover, the rise of tall building construction contributed to a 1975-1980 tripling of cement imports into developing economies (USGS, 2020; UN COMTRADE, 2020).

The relationship between the cost of height and bedrock depth is determined by the minimum building foundation depth required for stability. Rankine's Theory lays out a proportional relationship between building weight (which is roughly proportional to height conditional on construction materials) and required foundation depth, with the constant of proportionality differing as a function of soil conditions. According to this rule, optimal foundation depth is ∼10% of a building's height. In order for a building to be stable, the bottom of the foundation must either be anchored to bedrock, have a sufficiently wide base ("raft"), or incorporate many deeply bored piles. As rafts and piles are costly to install, builders prefer to anchor to bedrock. However, if bedrock is within only a few meters of the surface, expensive blasting is required to install the foundation. Figure A2 provides a visualization. Figure A3 provides descriptive evidence showing that unit construction cost is minimized at intermediate bedrock depths.[5]

This engineering evidence suggests that a reasonable approximation of the cost function for developing a building of height $S$ on bedrock depth $B_{ac}$ in city $a$ of country $c$ at time $t$ is

$$C_{act}(S) = c_{act} S^{1+\theta_t(B_{ac})}, \tag{1}$$

where $\theta$ is the height elasticity of cost per square meter, a measure of the cost of height. Consistent with our evidence of reductions in the cost of height conditional on bedrock depth, we allow $\theta$ to change over time. As the cost of height is greater at low and high bedrock depths, $\theta$ is U-shaped in $B_{ac}$.[6] As $c_{act}$ is non-parameterically indexed by city and time, it incorporates differences in bedrock depth in addition to labor and materials costs that change over time.

To corroborate the descriptive evidence that cost of height $\theta$ is U-shaped in bedrock $B$, we recover rough non-parametric estimates of the $\theta$ function with our limited cost data. We regress log construction cost per floor area on log building height for each bedrock depth using a locally weighted regression approach.[7] The result, depicted in Figure A4, supports the engineering-based hypothesis that bedrock at intermediate depths is associated with lower costs of height. $\theta$ ranges from 0.2 at intermediate depths to 0.8 at depth 0 and more than 1.0 at high depths.

As construction cost differs by bedrock depth, the profit maximizing level of height differs by bedrock depth conditional on demand conditions. The model in Section 4 shows how developers' choices of height depend on the interaction between bedrock depth and real estate demand, as measured by 1975 city population. That is, not only do developers build taller in locations with

[5] Our construction cost data is dominated by steel construction buildings in the US. Due to their extra weight, concrete buildings would typically have greater optimal bedrock depths conditional on height.

[6] It is straightforward to show that $\theta$ is the inverse of the intensive margin supply elasticity of floorspace with respect to price if developers make 0 profits (Baum-Snow and Duranton, 2025).

[7] See Appendix A.4 for details. Distance to the central business district (CBD) instruments for building height, conditional on included controls for city and country-decade fixed effects.

higher demand, the elasticity of profit-maximizing height with respect to price is greater in cities with better bedrock depths. The model also accommodates regulatory height limits.

The logic for our triple difference empirical strategy comes out of this narrative. The first two differences are over time and for intermediate relative to shallow bedrock depths. The third difference is the amplification that comes in higher demand locations, as measured by 1975 city population. The secular decline in the cost of height over time has facilitated more tall building construction in high demand locations, *and particularly so in cities with favorable bedrock*. In 1975, building tall was prohibitively costly throughout the developing world. As the cost of height subsequently declined for all cities, it is the locations with strong (pre-1975) demand conditions *and* favorable bedrock depths that are predicted to increase their heights the most (post-1975). In the data, the gap in log heights growth in initially "large" (one-million-plus) developing economy cities in 1975 on intermediate (15-40 m) relative to shallow (0-14.99 m) bedrock is 1.19** (se=0.52). For initially "small" cities, an insignificant difference of -0.02 (se=0.02) is observed between intermediate and shallow bedrock depth cities.

We formalize the triple difference relationship discussed above in the following regression, which additionally includes adjustments for 125 developing country fixed effects.

$$\begin{aligned} y_{ac} = \gamma_{DiD} \mathbb{1}(15m \leq \text{MBD}_{ac} < 40m) \times \mathbb{1}(\text{Pop}_{ac75} > 1 \text{ million}) \\ + \tilde{\phi} \mathbb{1}(15m \leq \text{MBD}_{ac} < 40m) + \tilde{\rho} \mathbb{1}(\text{Pop}_{ac75} > 1 \text{ million}) + \tilde{\kappa_c} + \tilde{\varepsilon}_{ac} \end{aligned} \tag{2}$$

Depending on the empirical goal, the outcome $y_{ac}$ is the 1975-2015 growth rate in heights in city $a$ of country $c$ (first stage), the 1975-2015 growth rate in city population (reduced form), or 1975 city characteristics (identification checks). $\text{MBD}_{ac}$ denotes mean bedrock depth for city $ac$. Excluding the few deep bedrock cities, $\hat{\gamma}_{DiD}$=1.14** (se=0.53) for heights. The corresponding estimate for population growth is 0.30** (se=0.12). Together these imply a simple Wald estimate of the bedrock depth-induced effect of heights on population growth of 0.26** (se=0.13). As these estimates only use some available identifying variation, masking within population-bedrock category heterogeneity, they are noisier than their more refined counterparts discussed below.

One identification concern may be that city geographic or economic characteristics correlated with the interaction between bedrock depth and city size are driving differential trends in both heights and outcomes of interest. While we also show results controlling for them below, we also evaluate this possibility by putting such characteristics (measured in 1975) as dependent variables in Eq. (2). Consistent with their low correlations with bedrock depth discussed above, none of these DiD coefficients are significant when accounting for multiple testing (Table A1).

### 2.3 Predicting City Level Height Growth

We add flexibility to Eq. (2) by replacing the binary measure of bedrock depth $\mathbb{1}(15 \leq \text{MBD}_{ac} < 40)$ with a quadratic function. Results in Table 1 Panel A Column (1) show the expected concave relationship between heights growth and bedrock depth in large relative to small cities. Panel B shows the same pattern for city population growth. These results are driven by the combinations of concave relationships in large cities and no significant relationships in small cities (unreported). The corresponding IV estimate of the impact of heights on population growth is 0.14** (se=0.06). However, the first stage remains somewhat under-powered with an F-statistic of 9.6.

For statistical power, our primary first stage specification further increases flexibility by replacing the binary function of 1975 city population used in Table 1 Column (1) with log

1975 population. The result is an aggregate heights supply, first stage, or reduced form equation that isolates comparisons of 1975-2015 heights or population growth rates in initially large versus small cities with favorable relative to unfavorable depth bedrock, while using continuous variation across the joint distribution of bedrock depth and 1975 log population for identification.

$$\begin{aligned} y_{ac} = {} & \gamma_1[\text{MBD}_{ac} \times \ln \text{Pop}_{ac75}] + \gamma_2[\text{MBD}_{ac}^2 \times \ln \text{Pop}_{ac75}] \\ & + k_1 \text{MBD}_{ac} + k_2 \text{MBD}_{ac}^2 + \delta \ln \text{Pop}_{ac75} \\ & + X_{ac75}\xi_1 + [X_{ac75} \times \ln \text{Pop}_{ac75}]\xi_2 + X_{ac75}^2\xi_3 + [X_{ac75}^2 \times \ln \text{Pop}_{ac75}]\xi_4 + \kappa_c + \epsilon_{ac} \end{aligned} \tag{3}$$

Key components are the population-bedrock depth interactions with coefficients $\gamma_1$ and $\gamma_2$. These terms capture how the relationships between tall building construction or population growth and bedrock depth differ by pre-Skyscraper Revolution 1975 city population. To verify that bedrock depths and not correlates drive identification, in robustness checks explored below we include a vector of control variables $X_{ac75}$ and its interaction with ln $\text{Pop}_{ac75}$.

Table 1: First Stage Estimates and Identification

| Period for Dep. Var.: | 1975-2015 | | 1975 | 2015 |
|---|---|---|---|---|
| | (1) | (2) | (3) | (4) |
| Interaction Variable = | 1975 Large City Dummy | ln 1975 CityPop | ln 1975 CityPop | ln 1975 CityPop |
| **Panel A: First Stage** | Dep Var: Δln (H+1) | | Dep Var: ln(H+1) | |
| MBD*Interaction Variable | 0.052* | 0.026*** | 0.003 | 0.029*** |
| | [0.030] | [0.006] | [0.003] | [0.006] |
| MBD$^2$*Interaction Variable | -0.0001 | -0.0002** | -0.0000* | -0.0002** |
| | [0.0002] | [0.0001] | [0.0000] | [0.0001] |
| (Partial) First Stage F | 9.61 | 22.84 | 1.71 | 22.84 |
| **Panel B: Reduced Form** | Dep Var: Δln Pop | | Dep Var: ln Pop | |
| MBD*Interaction Variable | 0.012** | 0.004*** | - | 0.004*** |
| | [0.006] | [0.001] | - | [0.001] |
| MBD$^2$*Interaction Variable | -0.0001* | -0.0000*** | - | -0.0000*** |
| | [0.0000] | [0.0000] | - | [0.0000] |
| 1975 Large City Dummy | Yes | No | No | No |
| ln 1975 City Population | No | Yes | Yes | Yes |
| Bedrock, Bedrock$^2$ | Yes | Yes | Yes | Yes |
| Country Fixed Effects | Yes | Yes | Yes | Yes |

*Notes: Notes:* "1975 Large City" is a dummy variable for the city being over 1 million in 1975. "MBD" refers to mean bedrock depth in meters. Specification (1) focuses on the 1975 large city-bedrock depth quadratic interaction. Specification (2) is our primary specification which uses the ln Pop 1975-bedrock depth quadratic interaction instead. Specifications (3) and (4) are cross-sectional regressions for 1975 and 2015, respectively. Remaining coefficients are reported in Appendix Table A3. Robust standard errors in brackets. Each regression has 11,258 observations.

Table 1 Specification (2) reports estimates of $\gamma_1$ and $\gamma_2$ in Eq. (3). These first stage coefficients in Panel A and reduced form coefficients in Panel B are significant and maintain the concave relationship shown in Specification (1). However, t-statistics are much larger than in Column (1) and the first stage F-statistic rises to 22.8. These estimates continue to show that bedrock

depth had greater impacts on heights and population growth in larger than in smaller cities. The implied IV estimate hardly changes to 0.13*** (se=0.03), but is estimated more precisely.[8]

To demonstrate that the quadratic form for bedrock depth fits the data well, Figure 3 displays graphs of estimated coefficients $\gamma_b$ from the following descriptive regression:

$$y_{ac} = \sum_b \gamma_b \left[\ln \text{Pop}_{ac75} \times \mathbb{1}(b \leq \text{MBD}_{ac} < b+5)\right] + \delta \ln \text{Pop}_{ac75} + \kappa_c + \phi_{b(ac)} + \varepsilon_{ac}, \qquad (4)$$

where b = {0,5,...} meters. The $\gamma_b$ coefficients describe elasticities of height or population growth with respect to 1975 population for each bedrock bin $b$, conditional on bin and country fixed effects. As the regression controls for log 1975 population, all $\gamma_b$ coefficients are of the bin-specific relationship between 1975 log population and 1975-2015 growth relative to that for the the "0" (0-4.99 m) bin. Bubble sizes are proportional to the number of observations. Quadratic lines of fit are indicated.

Figure 3: Relationships Between 1975-2015 Heights or Population Growth and log 1975 Population by Bedrock Depth Bin

(a) Heights Growth, 1975-2015 (b) Population Growth, 1975-2015

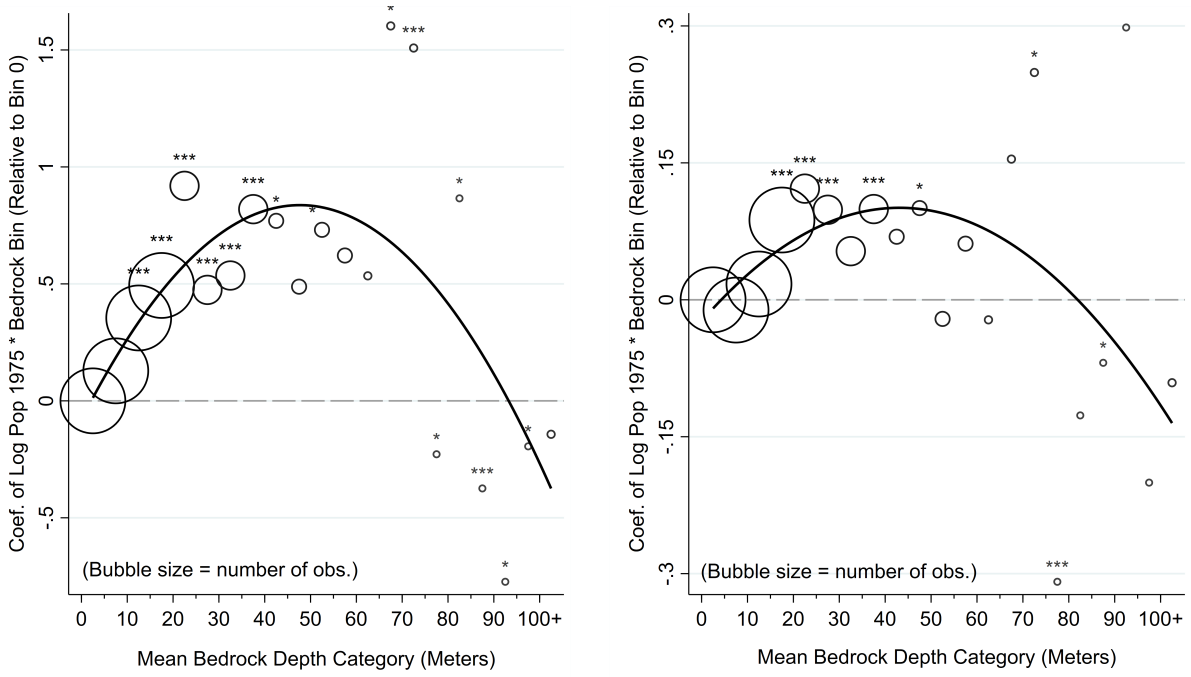


*Notes:* Panel A graphs coefficients on ln 1975 city population for each 5 meter bin of city-level mean bedrock depth in which the dependent variable is the 1975-2015 change in the log sum of heights plus one. Panel B is analogous but with the dependent variable the 1975-2015 change in log population. The size of the bubbles indicates the relative number of city observations in each mean bedrock depth bin. Stars indicate the statistical significance of each bin-specific coefficient on log 1975 city population (we use robust SE). The quadratic fit is shown, weighting by the number of observations in each bin.

Figure 3 Panel (a) shows the inverse U shaped impact of bedrock depth on the (residualized) 1975-2015 growth rate in aggregate heights in strong relative to weak demand cities. Such height elasticities are greater by up to 0.8 in cities at intermediate bedrock depths than in cities with bedrock at the surface. As seen in Panel (b), the elasticity of (residualized) population growth with respect to 1975 population is about 0.1 greater for cities in the same intermediate range of

[8]Using estimates reported in Tables 1 and A3 Column (2) and Figure A4, the implied partial elasticity of heights with respect to the cost of height $\theta$ (as determined through differences in bedrock depths) is -0.9 for cities of 500 thousand, -1.3 for cities of 1 million, and -2.3 for cities of 5 million. That is, reductions in the cost of height result in larger real estate supply shocks in higher population cities.

bedrock depth than the low or high ranges. Implied Wald statistics for population elasticities of aggregate heights are thus in the 0.10-0.15 range. As the quadratic function does a reasonable job of fitting coefficient patterns, most of the empirical work uses this parameterization.

Results in the final two columns of Table 1 put 1975 or 2015 levels of dependent variables on the left hand side of regressions that have the same form as our primary specification. Evident is no predictive power of the bedrock depth-population interaction in 1975 and strong predictive power in 2015. 1975 is indeed approximately a "clean slate" for cities in the developing world. It is thus almost the same to estimate regressions using 2015 levels or 1975-2015 changes.

We carry out three "placebo" checks that lend additional support to our identification strategy. First, putting the city 1950-1975 population growth rate as the dependent variable in the reduced form regression described in Eq. (3) yields no evidence of differential pre-1975 population trends. This analysis is of 560 cities from the Clio-Infra database on settlement size in the 42 developing economies with available population data on at least two-thirds of our sample cities (Buringh and Hub, 2013). These cities exhibit the same post-1975 population growth patterns as in our full sample. Second, favorable bedrock depths near city centers predict heights growth only in these areas. Peripheral bedrock depths, which are more likely to be correlated with factors outside cities, do not predict construction anywhere. Finally, cities which we infer to be in the 47 most height constrained countries exhibit no relationship between bedrock depth and population growth. If intermediate bedrock depth interacted with 1975 population either had a direct impact on population growth or were correlated with unobservables with a direct impact, thereby not satisfying the exclusion restriction, significant coefficients would also appear for this sample of countries with few tall buildings.[9] Table A4 presents these results.

## 3 Estimation of Central Elasticities

Our central empirical interest is in estimating the effects of technology-induced changes in aggregate heights in tall buildings on city population and built area. As is clarified in the model in Section 4 below, we conceptualize these labor and land market responses to operate through the following causal chain. Identifying variation in heights is through cost of height ($\theta$) induced variation in real estate supply. Holding local productivities and amenities constant, a positive real estate supply shock leads to lower real estate prices. The associated aggregate real estate demand response comes from a combination of greater floorspace use by existing residents and firms and in-migrants to the city from the hinterland. The lower cost of height disproportionately grows real estate supply near the center, where the demand response is greatest because of local agglomeration forces. This increases urban compactness, which enhances the average city productivity and real wage. Demand for urban living shifts out, representing an additional in-migration force. With a finite migration elasticity from idiosyncratic location preferences, urban utility grows. An increase in equilibrium floorspace near the center comes with depressed land demand near the urban fringe, manifesting as a negative built area response.

The following decomposition incorporates these relationships, where $Y$ indicates city population or built area, $H$ is the quantity of real estate services in tall buildings, and MBD indicates city mean bedrock depth.

[9] We defer discussion of how we define height constrained countries to Section 3.5.

$$\frac{d\ln Y}{d\ln H} \equiv \beta = \frac{d\ln Y}{d\text{ MBD}} \Big/ \frac{d\ln H}{d\text{ MBD}} = \frac{d\ln Y}{d\theta} \Big/ \frac{d\ln H}{d\theta}$$

As seen from the estimates in Table 1 Column (2), $\frac{d\ln H}{d\text{ MBD}}$ and $\frac{d\ln Y}{d\text{ MBD}}$ both follow the same pattern of increasing in log 1975 population at intermediate bedrock depths. While the model in Section 4 formally describes $\frac{d\ln Y}{d\theta}$ following the logic discussed above, with conversions from $\frac{d\ln Y}{d\text{ MBD}}$ to $\frac{d\ln Y}{d\theta}$ possible using estimates of $\frac{d\text{ MBD}}{d\theta}$ calculated from Figure A4, here we intentionally remain agnostic about the exact mechanisms behind the observed city population and built area responses and instead focus directly on using variation in bedrock depth to identify $\beta$.

We will use reduced form estimates of $\beta$ to discipline the model. Height elasticity estimates for a sample of cities we infer to have lax development restrictions are used to fit the parameter governing the disamenity value of urban density. The smaller are the population and built area responses to tall building supply shocks, the more negative we infer this parameter to be.

Long difference regressions of the form in Eq. (5) make up the heart of our empirical analysis. Our primary dependent variables of interest $\Delta \ln Y_{ac}$ are the 1975-2015 growth rates of population or built-up area in agglomeration $a$ of country $c$. Consistent with the first stage specification in Eq. (3), our baseline specification includes controls for a quadratic in mean city bedrock depth, log 1975 city population, and country fixed effects. Robustness checks additionally include controls for quadratics in potential confounders $X_{ac}$ interacted with log 1975 population.

$$\begin{aligned}\Delta\ln \text{Y}_{ac} = \beta\Delta\ln\left(\text{Heights}_{ac}+1\right) + \alpha_1\text{Bedrock}_{ac} + \alpha_2\text{Bedrock}_{ac}^2 + \alpha_3\ln\text{Pop}_{ac75} \\ + X_{ac75}\eta_1 + [X_{ac75}\times\ln\text{Pop}_{ac75}]\eta_2 + X_{ac75}^2\eta_3 + [X_{ac75}^2\times\ln\text{Pop}_{ac75}]\eta_4 + k_c + e_{ac}\end{aligned} \tag{5}$$

We primarily examine IV versions of Eq. (5), in which log population in 1975 interacted with a quadratic in city mean bedrock depth enters as instruments for $\Delta\ln(\text{Heights}_{ac}+1)$.

### 3.1 Main Empirical Results

Panel A Column (1) of Table 2 shows that a 100 log point increase in tall building heights leads to about a 13 percent increase in city population. This magnitude of height increase is the average for cities worldwide in the top tercile of 1975 population, while the average city in the developing world had 1975-2015 height growth of 27 log points. Column 2 shows that a 100 log point increase in heights caused the built-up land area of a city to decline by about 16 percent, which is similar to the 18 percent response for total city area (Column 3). Putting the results in Columns 1 and 3 together, it is clear that height growth has substantially increased population density. When it is put as a dependent variable, the coefficient is 0.31 (Column 4). The final column shows results for the growth rate in the total sum of lights at night 1996-2011.[10]

A potential concern is that trends in city demand factors are differentially correlated with bedrock depth in initially large versus small cities. These differential trends may be predicted by natural features or 1975 economic characteristics of cities. Relatedly, cities with bedrock depths favorable to the construction of tall buildings may have been more likely to build other types of infrastructure that drove their growth or have lower cost access to natural resources. Figure 4 provides evidence against these threats to identification. It shows robustness of estimated

[10]Spatial dependence in error terms extend to 600 km for population and 800 km for built area outcomes. Clustering at the administrative level or correcting for spatial autocorrelation to these distances using triangular spatial kernels increases standard errors for these two outcomes to 0.05 and 0.09-0.10, respectively (Table A6).

population and built area elasticities to a large number of controls for physical and economic geographic factors. Row 1 graphs coefficients and 95% confidence intervals from the first two columns of Table 2 as benchmarks. Rows 2-11 report corresponding coefficients when additionally controlling for the indicated $X_{ac75}$ variables along with their squares and their interactions with log 1975 city population, mimicking the way bedrock depth is included. Rows 12-16 evaluate robustness of Table 2 coefficients to dropping portions of the sample.[11]

Table 2: Main Empirical Results

| Dep. Var.: | (1) Δ ln Pop. 1975-2015 | (2) Δ ln Built Area 1975-2015 | (3) Δ ln Urban Area 1975-2015 | (4) Δ ln Pop Dens 1975-2015 | (5) Δ ln Lights 1996-2011 |
|---|---|---|---|---|---|
| | | | Panel A: IV Estimates | | |
| Δ ln(Heights+1) | 0.13*** | -0.16*** | -0.18** | 0.31*** | 0.17*** |
| | [0.03] | [0.04] | [0.08] | [0.08] | [0.06] |
| First Stage F | 22.84 | 22.84 | 22.84 | 22.84 | 16.32 |
| | | | Panel B: OLS Estimates | | |
| Δ ln(Heights+1) | 0.08*** | -0.02*** | 0.10*** | -0.02** | 0.05*** |
| | [0.00] | [0.01] | [0.01] | [0.01] | [0.01] |

*Notes:* The sample consists of 11,257 cities in developing economies. Eq. (5) shows the specification used. Country fixed effects and controls for ln 1975 city population and a quadratic in city mean bedrock depth are included. (5) uses $\Delta \ln(\text{Heights} + 1)$ for 1990-2015 and ln 1990 city population to construct the instruments. Appendix Table A5 reports coefficients on control variables. Population density is defined using urban area. Robust standard errors in brackets.

Controls for physical geography include mean altitude and ruggedness within the city boundary, dummies for being a coastal city, a lake shore city, and being crossed by a major river, mean earthquake risk, agricultural suitability, and wind speed within the city boundary (rows 2-4).[12] Similarly, excluding cities in the top quartile of the altitude distribution or that are on a coast, lake or major river has no significant effect on coefficient estimates. Nor does excluding cities within 25 km of mines or oil and gas fields (Figure A6). As subway construction costs are influenced by bedrock depth, we either include dummies for whether the city had a subway in 1975 and 2015 and the number of subway stations in 1975 and 2015 (row 6) or exclude subway cities from the sample (row 15). We alternatively include dummies for whether the city has a deep port and non-deep port, the number of deep and non-deep ports, and the maximum channel depth in the city, all defined in 2020 (row 7), or exclude port cities (row 16).[13] We also include dummies for whether the city has a reservoir and river barrier, the number of reservoir and river barriers, and the total storage capacity of reservoirs, all defined in 2025 (row 8).[14] We can also exclude dam cities from the sample (Figure A6). Finally, we control for the log of market potential, measured as the sum of the 1975 population of other cities $j$ in the same country weighted by the inverse Euclidean distance between cities $i$ and $j$ (row 9). Individually or simultaneously adding these sets controls may increase or decrease magnitudes of estimates, and these responses sometimes go in opposite directions for the population and built area outcomes.[15] Excluding cities with bedrock depths below 5 m, the bottom quartile of the

[11] Corresponding results for urban area, population density, and night lights outcomes are in Figure A5.

[12] Coastal and lake shore cities are those within 10 km of a coast and a large lake, respectively. Results hold with other distance cutoffs (not shown).

[13] We use ports located in 10 km buffers from city boundaries. Results hold with other cutoffs (not shown).

[14] We use dams located in 25 km buffers from city boundaries. Results hold with other cutoffs (not shown).

[15] The R-squared of the population regression increases by 18% when including all the controls, confirming

depth distribution, has no effect (row 12), nor does additionally excluding top quartile bedrock depth cities (Figure A6; details in figure notes). This addresses the potential worry that shallow bedrock may interfere with utilities or roads or may be related to agricultural productivity.

Figure 4: Robustness Checks

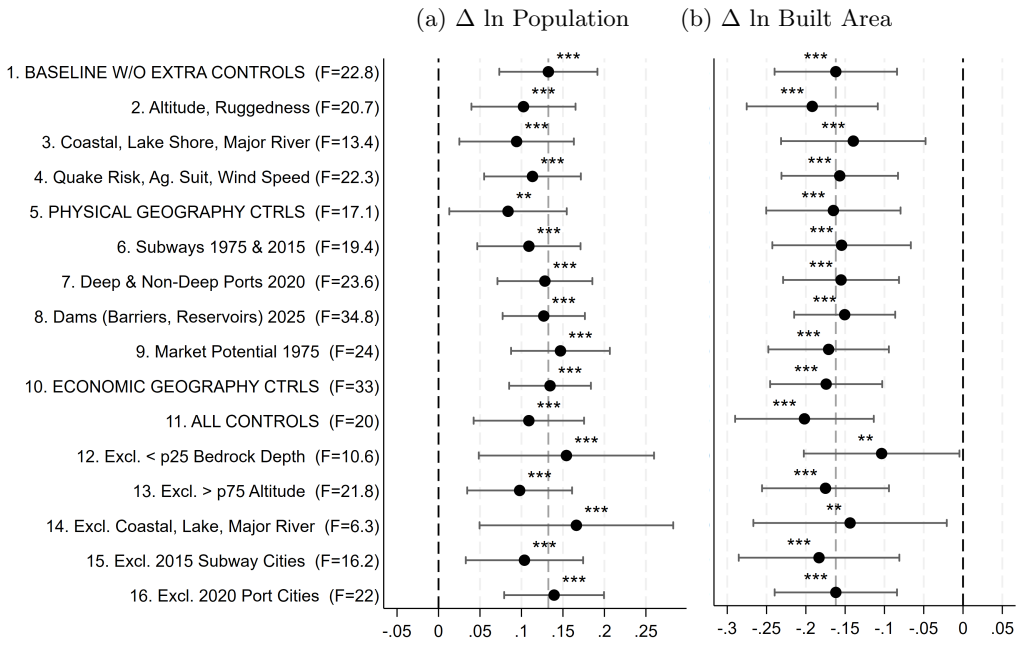


*Notes:* Rows 2-11: Each row graphs estimated IV coefficients on Δ ln (Heights+1) and 95% confidence intervals in regressions with the same specification as in Table 2 with the addition of a quadratic in the control(s) indicated in the row header and interactions of this quadratic with 1975 log city population. Inclusion of these 4 additional variables per control mimics the functional form used for bedrock depth. Rows 12-16: Cities with indicated attributes are excluded from the sample. First stage F-statistics are in parentheses. Details about data sources are in Appendix A.

Next, we carry out analyses using alternative predictors or outcomes in the 2015 cross-section. Results in the final column of Table 1 show the equivalence of 1975-2015 growth and 2015 cross-sectional regressions because tall building height stocks were close to 0 in 1975.

As an alternative predictor to the stock of heights measured with Emporis, we show robustness to using the stock of building volumes in 80X80 m pixels with average building heights above 40 m circa 2015 (Esch et al., 2023). We choose this height threshold as buildings over 55 m tall often share pixels with shorter buildings. The elasticity of the sum of volumes in pixels with average heights of at least 40 m to the 2015 Emporis measured sum of heights is 0.93*** (se=0.24). Estimated elasticities of population and built area to the sum of building volumes in these tall pixels returns identical elasticities to those in Table 2.[16] More tall building heights predicts both more tall building volumes and *lower* total building volumes, meaning that favorable bedrock depth induces a more than 1 for 1 substitution away from floorspace in short buildings to that in tall buildings, thereby confirming that lower costs of height lead to more compact cities. Finally, controlling for short building volume does not affect estimated impacts of tall buildings. The construction cost of short buildings should not be influenced by bedrock depth, especially beyond 5 m, to which our results are robust. These results are in Table A7.

Inspired by Campante and Yanagizawa-Drott (2018), Table A8 provides additional evidence that cities with lower costs of building tall experienced greater amounts of economic activity

they have a significant impact on population growth. We can also control for the stock of bridges (2025), tunnels (2025), or wastewater treatment plants (2020; proxying for the size of sewer networks) (Figure A6).

[16]The first-stage F statistic is 8.3. A cut-off of 55 m yields an F of 51.5 but lower magnitude estimated population and built area elasticities because the elasticity of volume with respect to heights over 55 m increases.

in the cross-section. It shows strong effects of heights on (i) the number of flights departing the city's airports, (ii) the number and economic size of headquarters of major world companies located in the city, (iii) the number of leading service firm establishments in the city, and (iv) the number of events related to business or multinational corporations.

### 3.2 Implied Aggregate Impacts of Tall Buildings

While model-based counterfactuals reported in Section 4 are best suited for determining magnitudes by which reductions in the cost of height have influenced urbanization and land savings, here we provide a rough sense of the magnitudes implied by reduced form estimates. Taking observed 1975-2015 construction as given, IV estimates imply that 18% of 2015 urban population in developing economies is accommodated and 15% of 2015 urban built up land (and 10% of urbanized land) remains as open space or rural because of this construction. As cities over 1 million residents in 1975 constructed ∼80% of developing world heights post-1975, large cities account for the majority of these changes. In these cities, 47% of the 2015 population is accommodated because of tall buildings, absent which 2015 built area would be 28% greater.

Because tall buildings promote urban compactness, they make for more environmentally friendly cities. For each city with 1975-2015 height growth, we allocate predicted land savings to a buffer around each city boundary obtained from the predicted change in city area. Aggregating circa 1982 land uses within these buffers, we find that 12% of land saved is tree canopy and 73% is non-tree vegetation (including cropland).[17] Regressions similar to those in Table 2 but with changes in various land use measures *within* urbanized areas as dependent variables reveals that a one unit growth in log heights increased urbanization of 2015 UC land by 21% on a base average of 21 percent between 1982 and 2015, or by 4.4 percentage points (Table A9). The associated reduction in tree cover of 24 percent and short vegetation of 3 percent within urbanized areas amount to similar land areas given initial fractions of land in each of these uses. Comparing the urban area coefficient of -0.18 in Table 2 to the 4.4 percentage point increase in within-city urbanized land indicates that total amounts of short vegetation and forested land at the edges of cities saved by tall building construction are about four times the total amount of vegetated land lost inside urbanized regions.

### 3.3 Additional Identification Checks

**IV vs. OLS:** OLS estimates, reported in Table 2 Panel B above, are muted relative to IV estimates. As demand side threats to identification should bias both OLS coefficients in the same direction, we conclude that these smaller magnitudes reflect some combination of measurement error in heights and endogenous supply side forces. If unobserved demand factors, like productivity or amenity shocks correlated with intermediate bedrock depth conditional on 1975 population, were a central endogeneity concern, the OLS population and built area elasticities would both be biased upwards. IV estimates that correct this endogeneity problem would thus be smaller (or more negative) than OLS estimates for both population and built area. Instead, we have attenuation bias. Greater restrictions on tall building construction in growing cities, as has been found China (Brueckner et al., 2017) and India (Brueckner and Sridhar, 2012), can explain our results. Moreover, local officials in many lagging Chinese cities offer discounted

[17] This analysis uses the satellite-based 1982-2015 ≈5X5 km pixel resolution *Global Land Change Database* (Hansen and Song, 2018).

land to commercial skyscraper developers (Wang et al., 2023). IV estimates for built and urban area outcomes are very similar, whereas OLS estimates are not and have opposite signs.[18]

**Measurement Error (ME):** Any classical ME in heights within countries is accounted for by the IV estimator with country fixed effects. Non-classical ME could occur if Emporis systematically misses buildings of certain heights. Administrative data for Chicago, Hong Kong, New York and Sao Paulo suggests that Emporis misses some buildings between 55 and 80 m. However, results hold if the stock of tall buildings is restricted to those above 80, 100, 200, or 300 m (Table A10). Emporis stocks have correlations of ≈0.90 with height stocks calculated using data from the Council on Tall Buildings and Urban Habitat across all city income levels (source: Jedwab et al. (2021)). This is also true using satellite-based building volume data from the WSF3D, GHS-Volume, or the Global Building Atlas (see notes to Table A7). Using the cross-sectional IV, the (standardized) effects of total built volume are similar to our baseline results (columns 1 and 6-7 of Table A7). For bedrock depths, our source relies on soil profile and borehole data plus pseudo-observations based on expert knowledge, with this last source perhaps least reliable. Results hold if we only use cities with soil profile or borehole sources for bedrock depth data, or if we give more weight to cities whose central business district is closer to soil profile/borehole observations (Table A11).[19]

**Functional Forms:** Our estimates combine treatments at the extensive margin with those at the intensive margin. Estimated extensive margin treatment effects, which measure heights growth as a dummy variable for any 1975-2015 tall building construction, are 1.16*** for population (se=0.32) and -1.43*** for built area (se=0.42). It is complicated to separate out intensive margin effects because doing so introduces selection challenges, reduces statistical power over the lower part of the support of the 1975 population distribution, and requires an additional source of identifying variation.[20] Table A12 shows robustness of baseline results to alternative implicit weighting between intensive and extensive margins by i) using a building height cutoff of 100 m rather than 55 m, ii) excluding cities with 1975 populations of less than 150,000, iii) using $\Delta \ln(\text{Heights}+55)$, asinh(Heights), or asinh(Heights/1000) as the treatment, and v) using a negative binomial regression with a dispersion parameter of 3-8 in the first stage. Intensive margin comparisons that are closer to base heights of 55 m grow coefficient magnitudes and reduce first stage power. Focusing on larger cities only (increasing weighting of intensive margin comparisons) reduces estimated treatment effects, though they remain highly significant.

Next, Table A13 shows that our IV strategy respects the monotonicity conditions needed for a local average treatment effect interpretation. We replace the bedrock depth polynomial with a piecewise linear spline function, in which one kink captures the "optimal" bedrock depth and a second kink captures the point beyond which bedrock depth no longer affects the cost of height. The first-stage F-statistic is maximized with the first kink at a bedrock depth of 20 m and the second kink at the maximum observed depth of 158 m, with results insensitive to using 80-158 m. This specification allows us to demonstrate that variation in bedrock depth on both sides of the optimal depth each contributes to identification. When including the spline as two separate

[18] About one-third of the gaps between OLS and IV estimates can be explained by the fact that they capture different local average treatment effects. In developing countries with at least 5 cities and a Gini index of the distribution of mean bedrock depth across cities above the 75th percentile, IV-OLS gaps are one-third smaller.

[19] To avoid using their potentially lower quality data, we verify that results in Table 2 hold dropping cities in the 34 "low income" countries in 2015 as defined by the World Bank (not shown).

[20] Chen and Roth (2024) highlights the difficulty of interpreting treatment effect estimates that combine extensive and intensive margin responses and the perils of arbitrary scaling.

instruments, first stage coefficients on the spline terms are 0.043*** (se=0.006) on the deep bedrock side of 20 m and 0.033*** (se=0.008) on its shallow bedrock side, yielding population and built area elasticities of 0.16*** (se=0.03) and -0.22*** (se=0.04), respectively (F=26.6). Only using variation within shallow or deep bedrock depths and controlling for 1975 log city population interacted with bedrock depth on the other side of the kink yields estimates that are not significantly different. The deeper bedrock comparisons allay potential concerns that shallow bedrock depths are correlated with above-ground factors driving outcomes of interest.[21]

**Potential Displacement Effects:** Our estimated elasticities primarily capture migration of people from rural areas to cities rather than displacement between cities. Borusyak et al. (2022) demonstrates the econometric challenges associated with endogenous migration flows between regions in the empirical setting in which local outcomes are regressed on exogenous location-specific shocks. As our data does not include rural units, our analysis is not subject to these biases provided that city growth in response to exogenous heights draws from the hinterland rather than from other cities. With an average UN measured urban share of ∼25% and very few tall buildings in 1975, our context is one of primarily rural-to-urban migration. This setting matches that of developed economies in history and our finding, discussed below, of similar population elasticities in the developed world for periods starting in 1850 as those for developing economies in 1975-2015. Robustness of results to various levels of subnational fixed effects, a sub-sample of low urbanization rate countries, and controls for market potential all support this conclusion (Tables A15 and A16). Appendix B.1 provides further details.

### 3.4 Treatment Effect Heterogeneity

**Regional:** Column 1 of Table 3 presents population and built area growth coefficients for all developing economy cities in Asia except the Middle East of 0.17 and -0.20, respectively. Other cities in the developing world generate similar estimates of 0.15 and -0.26, though these are slightly underpowered (F-stat. = 7.9; (2)). (3) presents results for developing economies that have relatively lax building restrictions. We defer the discussion of these results to Section 3.6.

Estimates for developed economies (4) are subject to more complicated interpretation, as large cities in developed economies had significant heights in 1975 and these countries had largely completed their rural-to-urban transitions by 1975. There is potential concern about differential pre-trends that are correlated with bedrock depths interacted with 1975 city size. Nonetheless, the null results for developed economies are driven by cities in former communist countries. Estimates are similar in magnitudes to those reported in Table 2 for both old world and new world cities in other developed economies, though they are underpowered (unreported).

**Historical:** To further understand why estimates differ for developing and developed economies, we look back in time to 1850-1975 for two samples of developed economy cities. During this period, they experienced similar phases of development as in many developing economies in 1975-2015. Their Skyscraper Revolution started earlier, as the Industrial Revolution allowed them to use steel frame technology for their tall buildings. So, while historic cities in *developing* countries serve as a placebo test in Section 2.3, those in *developed* countries provide validation. The

[21] In our main specification, log 1975 population appears in the dependent variable, as a component of the IV, and as a control variable. Table A14 shows results are robust to various alternative strategies for controlling for base year urban demand conditions. In particular, we (i) also include log built area in 1975 as a control, (ii) carry out the analysis for 1990-2015 while continuing to use log city population in 1975 to construct the instruments and as a control, and (iii) use log population 2015 as the outcome and log heights 2015 as the IV.

specifications are the same as above except for the different base year. Population elasticities are 0.14** for the world (5) and 0.20** for Europe (6), though the Europe estimate is underpowered.

Table 3: IV Results by World Region and Time Period

| | (1)-(3) Developing Economies (1975-2015) | | | (4)-(6) Developed Economies | | |
|---|---|---|---|---|---|---|
| | Asia (no Middle-East) | Other Countries | Unconstrained Countries | 1975-2015 All | 1850-1975 (Historical) 55 Developed | 39 European |
| | | | Panel A: Δ ln Population | | | |
| Δ ln(Heights+1) | 0.17*** | 0.15** | 0.21*** | -0.02 | 0.14** | 0.20** |
| | [0.03] | [0.07] | [0.04] | [0.03] | [0.06] | [0.10] |
| | | | Panel B: Δ ln Built Area | | | |
| Δ ln(Heights+1) | -0.20*** | -0.26*** | -0.39*** | -0.04 | - | - |
| | [0.04] | [0.09] | [0.09] | [0.03] | - | - |
| First Stage F | 20.92 | 7.88 | 11.36 | 14.28 | 10.94 | 5.51 |
| Observations | 6,990 | 4,267 | 5,315 | 1,592 | 918 | 1,095 |

*Notes:* Each entry is from a separate IV regression using data from cities in world regions indicated in column headers over the indicated time period. "Asia (no Middle-East)" refers to developing economies in Asia except the Middle East (as of 2015). "Unconstrained" refers to 38 countries with no history of communism and with below median regulatory environments. Section 3.6 explains in more detail how this sample is selected. "55 Developed" refers to 918 cities in 55 developed countries (as of 2015) during the period 1850-1975 (source: Buringh and Hub (2013)). "39 European" refers to 1,095 cities in 39 European countries from Portugal to Russia (source: Bairoch (1988)). (5)-(6) The instrumental variables are the interactions of ln 1850 city population with bedrock and bedrock$^2$. We control for country fixed effects, ln 1850 city population, and a quadratic in city mean bedrock depth. As we do not have historical data on built area before 1975, Panel B columns (5)-(6) are empty. Robust SEs in brackets. Results for urban area are similar to those in Panel B, though less precise, as 1975 and 2015 urban area are inconsistently measured in the GHS data.

**Building Use:** While we observe building use in the Emporis data, we do not have separate instruments for commercial and residential heights. Instead, we exploit the fact that country-specific industrial structure and land use planning regimes influence the extent to which tall buildings host residential or commercial tenants. For example, Egypt and Pakistan have ∼50% of their tall buildings dedicated to commercial uses whereas Brazil and India have >90% of tall buildings in residential use. Because the residential share of tall buildings is in part driven by country-specific factors, we can learn about use-specific impacts by restricting the sample to countries with at least some baseline share of tall buildings in residential use. Figure 5 shows estimates by country residential share. Cities in countries that built more residential heights accommodated more population and saved more land. Population elasticities rise from 0.13 to 0.21 when moving from the sample of developing countries with at least 50% of tall buildings residential to those with at least 90% residential. The residential impact is even greater for built area as built area elasticities decline from -0.13 to -0.50. As residential real estate is much more space intensive than offices per-capita, it is not surprising that residential buildings have bigger effects. The model in the following section is parameterized to respect this observation.

### 3.5 City Height Gaps

One aim of the model is to quantify the implications of allowing unrestricted heights in cities worldwide. This calculation requires measures of the extent to which each city constrains tall building construction. To this end, our "height gap" measure is the fraction of potential heights in each city justified by fundamental supply and demand conditions that has not been realized,

most likely due to regulatory supply constraints.

Figure 5: Effects of Heights by Country Tall Building Residential Share

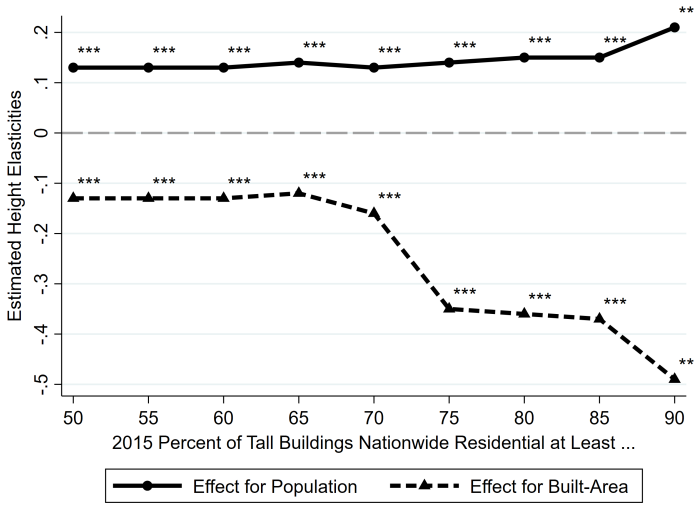


*Notes*: This figure shows two sets of estimated coefficients on the change in log heights in IV regressions of the form in (5). The top portion of the graph indicates coefficients for which the 1975-2015 change in log population is the outcome ("Effect for Population"). The outcome in the bottom half of the graph is 1975-2015 change in log city built area ("Effect for Built-Area"). Moving from left to right, the sample becomes increasingly constrained to include only developing economies with at least the fraction of tall buildings nationwide in 2015 residential use indicated on the horizontal axis.

We follow Barr and Jedwab (2023) to determine each city's potential heights under no constraints. Their regression model predicts city log heights using fundamental demand and supply factors across cities. They consider 12,755 GHS-UCDB cities worldwide for the years 1995, 2000, 2005, 2010, 2015, and 2020. Predictors in this regression are measures of city lights at night and city population category interacted with quadratics in national per-capita GDP, as well as city population category interacted with quadratics in bedrock depth, earthquake risk, elevation and ruggedness, country population and area, all additionally interacted with year fixed effects. The R-squared is 0.64. Resulting 2015 predicted heights are measures of the heights justified by each city's fundamental demand and cost factors absent local regulation.

After ordering cities by their *predicted* log heights in 2015, we calculate the 95$^{\text{th}}$ percentile (3rd ranked city) of *actual* log height in 2015 for the moving window of 51 cities centered on each city in the data. This accommodates the possibility that one or two cities in each group of 51 has built particularly tall for idiosyncratic reasons. We smooth this 95$^{\text{th}}$ percentile function using local polynomial regression. The resulting function of predicted log heights, $h^{95}(\cdot)$, describes our inferred "unconstrained" heights. The height gap measure for city $ac$ follows as

$$\text{Gap}_{ac} = \max\left(1 - \frac{\text{Heights}_{ac2015}}{H^{95}(\widehat{\text{LHEIGHTS}}_{ac2015})}, 0\right), \tag{6}$$

where $H^{95}(\cdot) = \exp\left[h^{95}(\cdot)\right]$ and $\widehat{\text{LHEIGHTS}}_{ac2015}$ is predicted log heights for city $ac$ in 2015. $\text{Gap}_{ac}$ is between 0% and 100%. We emphasize that while this measure is reasonable on average and is plausible for most cities, it will not accurately measure building constraints in every city.[22]

[22]Height gaps are 0% for Chicago, Kuala Lumpur, Sao Paulo, Seoul and Shanghai, 11% for Guangzhou, 26% for NYC, 45% for Miami, 51% for Jakarta, 66% for London and Mexico City, 68% for Bogota, 70% for Boston, 75% for Houston, 80% for Buenos Aires, 82% for L.A., 86% for Washington DC, 91% for Karachi, and 93% for Cairo. We find a correlation of 0.74 between these height gaps and Brueckner et al.'s (2017) land use regulation stringency measures for 200 Chinese cities and 0.46 with the 2008 Wharton Land Use Regulation Index (Gyourko

The population weighted height gaps are larger in developed economies in Oceania (90%), Europe (85%), and North America (77%), and smaller in developing economies in Asia (41%), Africa (48%), and Latin America (63%). We therefore infer greater land use regulation limiting tall buildings in developed economies. The fact that our 1975-based instrument is not correlated with 1995 or 1995-2015 changes in height gaps is further evidence that identification of our elasticity estimates is driven by exogenous tall building supply factors rather than endogenous regulatory changes (not shown). Appendix B.2 has further details about the height gaps.

### 3.6 Model-Relevant Estimates

Under its baseline parameterization, the model developed in the next section describes an environment in which fundamental supply and demand forces determine a city's equilibrium heights, population, and area. As such, we estimate the model under a baseline parameterization without height limits. Model quantification thus requires elasticity estimates for a sub-sample of cities that are unregulated. In order to maintain the same specification and identification assumptions as for the empirical analysis on the broader sample, we select this unconstrained city sample to include all cities in the most unregulated countries (with the lowest height gaps).

We aggregate the 2015 city-level residuals from Section 3.5 to the country level with 2015 city population weights. We then select developing countries without a history of Communism with an aggregated residual above 0, yielding a sample of 5,315 cities in 38 economies. The elasticity estimates for this sample, reported in Column (3) of Table 3, are larger than our broader average estimates reported in Table 2. We find an unconstrained population elasticity of 0.21*** (se=0.04) and an unconstrained built area elasticity of -0.39*** (se=0.09).

## 4 Theoretical Analysis and Quantification

Here we develop a theory that facilitates conceptual and quantitative analyses of the role of tall buildings in economic development. The model follows in the tradition of Muth's (1969) monocentric city land use model with endogenous housing supply. This setup draws from Ahlfeldt and Barr (2022) and formalizes the logic of the relationship between bedrock depth and real estate development discussed in Section 2.2. This "representative city" model is intended to be flexible enough to capture forces that link tall building construction to urban growth and change that are common to cities of different shapes, sizes, and stages of development.

We expand on the standard urban model with endogenous heights (Duranton and Puga, 2015; Albouy et al., 2020) by allowing rural residents the discrete choice of entering the city, following Ahlfeldt et al. (2022)'s approach to modeling labor market entry. By incorporating preference heterogeneity in this way, the model generates the finite height elasticities of city population and area estimated in Section 3. A city level population density disamenity parameter is estimated by indirect inference to match the reduced-form estimates presented in Section 3.6. Using the parameterized model, we evaluate the global consequences for welfare and aggregate land values of lifting existing height caps.

et al., 2008) for the 25 metro areas with at least 10 sampled municipalities. Other data sets either do not measure stringency or they over-represent suburban areas with few tall buildings.

### 4.1 Model Setup

**Environment:** We consider a circular city of endogenous radius. The city is embedded in a region of $\bar{N}$ workers, which also has a rural hinterland. $\mathcal{L}(x) = 2\ell\pi x$ units of land are available for development at each distance $x$ from an exogenously located historic city center, where $\ell = [0, 1]$ is the fraction of land that is developable. The area beyond the endogenous city margin at $x = x_1$ is the rural hinterland.

**Workers:** All workers are ex-ante identical and choose to either live inside the city or outside in the hinterland. Our approach follows the dual-sector model of Lewis et al. (1954) whereby surplus rural labor is absorbed by the urban sector. The utility of worker $\nu$ is described by:

$$U(\nu) = \max_{o}[U^o \exp(a^o(\nu))], \tag{7}$$

where $o \in \{inside, outside\}$ and $a^o(\nu)$ is an idiosyncratic taste shock for living in location $o$. These shocks $a^o(\nu)$ are drawn from the same Gumbel distribution with distribution function

$$G(a^o(\nu)) = \exp[-\exp(-\zeta a^o(\nu) - \Gamma)]. \tag{8}$$

Workers living in the rural hinterland receive an exogenous subsistence utility $U^{o=outside} = \widetilde{U}^{1/\zeta}$. All workers choosing to live in the city enjoy the same endogenous utility $U^{o=inside} = \bar{U}$. The central parameter $\zeta > 0$ summarizes the degree of taste dispersion across locations and therefore governs the extent to which workers respond to city-hinterland utility differences. If $\zeta$=0, it is a *closed* city and as $\zeta \to \infty$ the city becomes perfectly *open* with $\bar{U} = \widetilde{U}^{1/\zeta}$. $\Gamma$ is the Euler-Mascheroni constant, included so that the Gumbel shocks are mean zero.

Utility maximization delivers the urban population $N$ as share $\mu$ of region population $\bar{N}$.

$$N = \mu\overline{N} = \frac{\overline{U}^{\zeta}}{\overline{U}^{\zeta} + \widetilde{U}}\overline{N} \tag{9}$$

The elasticity of urban population with respect to urban utility (the migration elasticity) is $\zeta(1-\mu)$, with $1-\mu$ reflecting the stock of available rural residents at risk of moving to the city.

City utility depends on a local amenity $A$, tradeable goods consumption $g$, and residential floor space $f^R$. Each worker's choice of residential location, on floor $s$ in a building located at CBD distance $x$, must deliver the same utility level $U(x, s) = \bar{U}$ in equilibrium. Utility is Cobb-Douglas with a floor space expenditure share of $0 < (1 - \alpha^R) < 1$. Put together,

$$U(x, s) = A^R(x, s)\Big(\frac{g}{\alpha^R}\Big)^{\alpha^R}\Big(\frac{f^R(x, s)}{1 - \alpha^R}\Big)^{1-\alpha^R}. \tag{10}$$

The local amenity decays with distance from the center and rises with height:

$$A^R(x, s) = \mathcal{D}^{\beta^R}\bar{a}^R e^{-(\tau^R \max(0, x-\underline{x}^R))}s^{\tilde{\omega}^R}, \tag{11}$$

where $\mathcal{D} = \frac{N}{\ell\pi(x_1)^2}$ is the population density of the city (with $x_1$ the endogenous radius of the urban area) and $\beta^R < 0$ is the density elasticity of urban amenities (quality of life). This is the parameter we will estimate by indirect inference.

$\tilde{\omega}^R > 0$ is the height elasticity of the residential amenity (from better views or less exposure to noise). $\tau^R > 0$ determines the rate at which the amenity component of utility declines in distance from the edge of a central district located at $x = \underline{x}^R$, with $\bar{a}^R$ the amenity within this

district. $\tau^R > 0$ generates the centripetal force of rising residential demand nearer to the center and can be interpreted as the utility cost of commuting an additional unit distance. Relative to observed equilibrium allocations, we will separately report contributions of changes in the density disamenity $\mathcal{D}^{\beta^R}$, spatially varying local amenity or commuting cost $e^{-(\tau^R \max(0, x - \underline{x}^R))}$, and height amenity $s^{\tilde{\omega}^R}$ to welfare changes under various counterfactual scenarios.

Workers face the budget constraint

$$y = p^R(x,s) f^R(x,s) + g, \tag{12}$$

in which the endogenous wage $y$ can be spent on housing, with endogenous unit price $p^R(x,s)$, and the numeraire tradeable good.

Utility maximization and imposing $U(x,s) = \bar{U}$ yields the residential floorspace bid rent at location $(x,s)$

$$p^R(x,s) = A^R(x,s)^{\frac{1}{1-\alpha^R}} y^{\frac{1}{1-\alpha^R}} \bar{U}^{-\frac{1}{1-\alpha^R}}. \tag{13}$$

Averaging across all floors of a residential building of height $S^R(x)$ by integrating over $s$ at every location delivers the horizontal residential bid rent

$$\bar{p}^R(x) = \frac{1}{1+\omega^R} \left[ \frac{\mathcal{D}^{\beta^R} \bar{a}^R y}{\bar{U}} e^{-(\tau^R \max(0, x - \underline{x}^R))} \right]^{\frac{1}{1-\alpha^R}} S^R(x)^{\omega^R}, \tag{14}$$

where $\omega^R = \frac{\tilde{\omega}^R}{1-\alpha^R}$ is the height elasticity of residential rent. $\bar{p}^R(x)$ is declining in distance to the center $x$ both because of declining amenities, as captured by $\tau^R > 0$, and declining equilibrium building heights $S^R(x)$.

The mass of residents at each location in the residential zone, in which residential use outbids commercial and agricultural use, is

$$n(x) = \frac{\mathcal{L}(x) S^R(x)}{y} \frac{\bar{p}^R(x)}{1-\alpha^R}. \tag{15}$$

In this expression, higher housing costs are associated with higher population densities.

**Firms:** Atomistic perfectly competitive firms produce the tradeable good using labor $l$ and commercial floor space $f^C$ with the Cobb-Douglas production function

$$g(x,s) = A^C(x,s) \Big( \frac{l}{\alpha^C} \Big)^{\alpha^C} \Big( \frac{f^C(x,s)}{1-\alpha^C} \Big)^{1-\alpha^C}. \tag{16}$$

Productivity at each location is shifted by

$$A^C(x,s) = \bar{a}^C N^{\beta^C} e^{-(\tau^C \max(0, x - \underline{x}^C))} s^{\tilde{\omega}^C}. \tag{17}$$

$\tilde{\omega}^C > 0$ is the height elasticity of productivity, capturing benefits such as signaling and workplace amenity effects. The agglomeration elasticity $\beta^C > 0$ describes how productivity increases in city employment $N$. $\tau^C > 0$ determines the rate at which productivity declines in distance from the edge of a central urban core at $\underline{x}^C$, with $\bar{a}^C$ the exogenous productivity within this core.[23] Profit maximization and zero profits delivers the commercial bid rent, where $y$ is the wage

$$p^C(x,s) = A^C(x,s)^{\frac{1}{1-\alpha^C}} y^{\frac{\alpha^C}{\alpha^C - 1}}. \tag{18}$$

[23] By flattening the amenity and productivity functions in the central urban core, we avoid the peaking of bid-rents and profit-maximizing heights at unrealistically high levels at the most central point in the city.

Averaging across all floors of a commercial building with height $S^C(x)$ at each location $x$ delivers the horizontal commercial bid rent

$$\bar{p}^C(x) = \frac{1}{1+\omega^C}\left[\bar{a}^C N^{\beta^C} e^{-(\tau^C \max(0, x-\underline{x}^C))}\right]^{\frac{1}{1-\alpha^C}} y^{\frac{\alpha^C}{\alpha^C-1}} S^C(x)^{\omega^C}, \tag{19}$$

where $\omega^C = \frac{\tilde{\omega}^C}{1-\alpha^C}$ is the height elasticity of commercial rent. This form resembles Eq. (14). Labor demand at each location in the central commercial zone is

$$L(x) = \frac{\alpha^C}{1-\alpha^C}\frac{\bar{p}^C(x)}{y}\mathcal{L}(x)S^C(x). \tag{20}$$

This expression reflects the unitary elasticity of substitution between labor and floor space embodied in the Cobb-Douglas production technology.

**Developers:** We specify the construction cost function of building type $U \in \{R, C\}$ and height $S$ as

$$C^U(S^U(x)) = c^U S^U(x)^{1+\theta_t^U(B)}. \tag{21}$$

$\theta_t^U(B)$ denotes the unit "cost of height" above city bedrock depth $B$.[24] Following the engineering discussion in Section 2.2, $\theta$ is U-shaped in $B$ and declining over time conditional on $B$.

Unconstrained competitive building type $U$ developers have the following profit function per unit of land associated with building to height $S^U(x)$.

$$\pi^U(S^U(x)) = S^U(x)\bar{p}^U(x) - C(S^U(x)) - r(x) \tag{22}$$

$\bar{p}^U(x)$ is from (14) and (19) and $r(x)$ denotes the fixed cost component of development, which includes both the land price and any regulatory development costs at location $x$.

Profit maximization delivers each location's equilibrium height by building use[25]

$$\ln S^{*U}(x) = \frac{1}{\theta_t^U(B) - \omega^U}\left(\ln\frac{\tilde{p}^U(x)}{c^U} + \ln\frac{1+\omega^U}{1+\theta_t^U(B)}\right), \tag{23}$$

where $\bar{p}^U(x) \equiv \tilde{p}^U(x)[S^U(x)]^{\omega^U}$, with $\tilde{p}^U(x)$ the height-invariant demand shifter in the horizontal bid-rent schedule. Analysis of Eq. (23) demonstrates how the model generates the greater growth rates in aggregate building heights in large cities with intermediate bedrock depths than those with shallow or deep bedrock depths, and the smaller corresponding differences for small cities. Differentiation of $\ln S^{*U}(x)$ with respect to $t$, $B$ and $\ln N$ yields positive height effects of time, better bedrock depth and the strength of local real estate demand at each location $x$.[26]

Developers may be subject to a height limit $\bar{S}^U$ imposed by the planning system. Conditional on building type $U$, the developer's resulting choice of height is thus

$$\tilde{S}^U(x) = \min(S^{*U}(x), \bar{S}^U). \tag{24}$$

Inserting into Eq. (22) and imposing zero profits delivers the use-specific bid rent for land

[24] For Cobb-Douglas production with capital share $\alpha$ and fixed lot size, $\theta = \frac{1-\alpha}{\alpha}$.

[25] An interior solution requires that $\theta > \omega$ and $\tilde{p}^U(x) > \frac{c^U(1+\theta^U(B))}{1+\omega^U}$.

[26] This third derivative is $\frac{2}{(\theta-\omega)^3}\frac{\mathrm{d}\theta}{\mathrm{d}t}\frac{\mathrm{d}\theta}{\mathrm{d}B}\frac{\mathrm{d}\ln\tilde{p}^U(x)}{\mathrm{d}\ln N} > 0$.

$$r^U(x) = \tilde{p}^U(x)\left[\tilde{S}^U(x)\right]^{1+\omega^U} - c^U\left[\tilde{S}^U(x)\right]^{1+\theta^U}. \tag{25}$$

If planning restrictions do not bind, this function is declining in distance from the center $x$. Stronger demand for location $x$, as summarized in $\tilde{p}^U(x)$, gets capitalized into higher land rents.

**Spatial Equilibrium:** For given values of the city-wide endogenous objects $\{y, N, \bar{U}\}$, all location-specific endogenous variables are uniquely determined. We obtain floorspace rents from Eqs. (14) and (19), heights from Eq. (24), and use-specific land rents from Eq. (25). Land use then goes to the highest bid use at each location $x$, given agricultural bid-rent $r^A$. Under the restriction that the commercial rent gradient is steeper than the residential rent gradient, which is consistent with plausible parameter values and empirical evidence, there is a distance $x_0$ at which commercial and residential land rents equate: $r^C(x_0) = r^R(x_0)$. At shorter distances, commercial developers outbid residential developers when competing for land; thus $x_0$ defines the boundary of the central business district (CBD).[27] Similarly, there is a distance $x_1$ at which residential and agricultural land rents intersect, $r^R(x_1) = r^A$, and the city ends.

**General Equilibrium:** Aggregating labor supply in Eq. (15) and labor demand in Eq. (20) across the city, the labor market must clear at the city population $N$.

$$N = \int_{x_0}^{x_1} n(x)dx = \int_0^{x_0} L(x)dx \tag{26}$$

This implies an equilibrium wage of

$$y = \frac{\alpha^C}{1-\alpha^C}\frac{\int_0^{x_0} \bar{p}^C(x)\mathcal{L}(x)S^C(x)dx}{N}. \tag{27}$$

Aggregate housing market clearing is then

$$(1-\alpha^R)yN = \int_{x_0}^{x_1} \bar{p}^R(x)\mathcal{L}(x)S^R(x)dx. \tag{28}$$

Inserting Eq. (14) into Eq. (28) delivers equilibrium urban utility

$$\bar{U} = \left[\frac{\frac{1}{1+\omega^R}[y\bar{a}^R\mathcal{D}^{\beta^R}]^{\frac{1}{1-\alpha^R}}\int_{x_0}^{x_1} e^{-\frac{\tau^R}{1-\alpha^R}\max(0,x-\underline{x}^R)}S^R(x)^{1+\omega^R}\mathcal{L}(x)d(x)}{(1-\alpha^R)yN}\right]^{1-\alpha^R}. \tag{29}$$

Eqs. (9), (27), and (29) constitute the exactly identified system of equations that determines the general-equilibrium constants $\{y\,(\text{wage}), \bar{U}\,(\text{reservation utility}), N\,(\text{urban population})\}$.

**Welfare:** Following Ahlfeldt et al. (2022), expected utility across all workers is

$$\mathcal{V} = \left(\widetilde{U} + \overline{U}^{\zeta}\right)^{\frac{1}{\zeta}}. \tag{30}$$

The aggregate land rent is

$$\mathcal{R} = \int_0^{x_0} r^C(x)\mathcal{L}(x)dx + \int_{x_0}^{x_1} r^R(x)\mathcal{L}(x)dx + \int_{x_1}^{\bar{x}} r^A\mathcal{L}(x)dx. \tag{31}$$

These rents are paid by urban firms, urban resident-workers, and rural resident-workers, respectively, to absentee landlords.

[27] In our quantification, $\frac{\tau^C}{1-\alpha^C} > \frac{\tau^R}{1-\alpha^R}$ ensures a commercial center surrounded by a residential area.

### 4.2 Quantification and Estimation by Indirect Inference

For illustration and parameter estimation, we first quantify the model to one baseline city. In Section 4.4, we will quantify it to each 2015 city in our data to perform welfare counterfactuals.

Given parameters $\{\alpha^U, \beta^U, \omega^U, \theta^U, \tau^U, \underline{x}^U, \bar{a}^U, c^U, \bar{S}^U, r^A, \zeta, \ell, \tilde{U}\}$ and endowments $\{\bar{N}, \bar{x}\}$, we solve for $\{y, N, \bar{U}, x_0, x_1\}$ and $\{L(x), n(x), \bar{p}^U(x), r^U(x), \tilde{S}^U(x)\}$ using the numerical procedure described in Appendix C.1. Table 4 lists parameter values associated with our baseline analysis with brief rationales below. While values for $\{\alpha^U, \beta^C, \theta^U, \omega^U\}$ can be taken from the literature, remaining parameters involving the spatial organization of the city and its interaction with the rural hinterland apply more specifically to our inquiry or merit additional discussion. We set the radius of the urban core $\underline{x}^C = \underline{x}^R$ to 1 km. We set the share of built-up land $\ell$ to 0.5, which is approximately the observed mean ratio of built-up area over total land area across all cities in our data. Targeting a city of 3 million, we set the total city plus rural population to $\bar{N} = 6$ million and thus an urban fraction $\mu$ of 0.5. We choose a large city as a baseline so that heights above a sufficiently high threshold $\mathcal{T}$ are generated by the model.

Table 4: Baseline Parameterization

| Parameter | | Value | Source |
|---|---|---|---|
| $1-\alpha^C$ | Share of floor space in production | 0.15 | Lucas and Rossi-Hansberg (2002) |
| $1-\alpha^R$ | Share of floor space in consumption | 0.33 | Combes et al. (2019) |
| $\beta^C$ | Agglomeration elasticity in production | 0.03 | Combes and Gobillon (2015) |
| $\hat{\beta}^R$ | Density elasticity in urban amenity | -0.11 | Estimated: see text and Section C.2 |
| $\theta^C$ | Commercial height elasticity of construction cost | 0.5 | Ahlfeldt and McMillen (2018) |
| $\theta^R$ | Residential height elasticity of construction cost | 0.55 | Ahlfeldt and McMillen (2018) |
| $\omega^C$ | Commercial height elasticity of rent | 0.03 | Liu et al. (2018) |
| $\omega^R$ | Residential height elasticity of rent | 0.07 | Danton and Himbert (2018) |
| $\tau^C$ | Production amenity decay | 0.014 | See text and Section C.2 |
| $\tau^R$ | Residential amenity decay | 0.016 | See text and Section C.2 |
| $\zeta$ | Preference heterogeneity | 6.4 | Bryan and Morten (2019) |

Notes: We set the scale parameters to $\bar{a}^C = \bar{a}^R = 2, c^C = c^R = 150$, $r^A = 50$, $\bar{N} = 6$ million, $\ell = 0.5$, $\bar{x} = 100$ km and invert $\tilde{U}$ so that $\mu = 0.5$. In the baseline parameterization, height limits are not binding ($\bar{S}^C = \bar{S}^R = \infty$). With the exception of $\beta^R$ and $\zeta$, related literature is discussed in Ahlfeldt and Barr (2022). Reduced form population and built area elasticities for unconstrained cities both deliver an identical $\hat{\beta}^R$, while the use of corresponding OLS or full sample IV elasticities yield conflicting estimates. The standard error is 0.057 based on 100 bootstrap replications, drawing from estimated distributions of population and built area elasticities reported in Table 3 Column (3). Taking $\beta^R = -0.09$ as given and instead estimating $\zeta$ by indirect inference yields $\hat{\zeta} = 5.7$ (Figure A8). $\beta^R$ and $\zeta$ are not easily separately identified and so cannot be jointly estimated (Appendix C.2.4).

We set the preference heterogeneity parameter $\zeta$ to 6.4 based on Bryan and Morten's (2019) migration elasticity estimate $\zeta(1-\mu)$ of 3.2 for Indonesia.[28] The amenity decay parameters $\tau^U$ must rationalize urban height, population, and rent gradients. We set $\tau^R$ to reflect estimated log residential height CBD distance gradients of near -0.10 for both both Chicago and São Paulo. We set $\tau^C$ to -0.20 to match Chicago only, as São Paulo's estimated non-residential gradient of -0.15 includes government and other non-commercial structures. Chicago and São Paulo are in the middle of estimated overall gradients using volumes data for all types of buildings in 50 large unconstrained world cities (Appendix Section C.2.1).

[28] 3.2 is very close to the mean value of estimates from Indonesia (Ibid.), Brazil (Morten and Oliveira, 2024), China (Imbert et al., 2022), India (Imbert and Papp, 2020), and West Africa (Jedwab et al., 2025).

Finally, $\beta^R$ governs how much heights affect urban utility via density disamenities. While the popularity of height restrictions in cities around the world implies that many planners take $\beta^R$ to be negative, empirical evidence on it is thin. We estimate $\beta^R$ using indirect inference. In particular, we fit the value of $\beta^R$ for which the model generates values of the height elasticities of population and built area that match our reduced-form estimates for unconstrained cities reported in Section 3.6. To this end, we simulate variation in tall buildings, population, and area that arise from varying $\theta$ to obtain the model analogs to our instrumental variable estimates, regressing model-generated log population or log area on model-generated log heights above some height threshold $\mathcal{T}$ (details in Appendix C.2.3). A more negative $\beta^R$ implies that the attractiveness of the city increases less in response to a height supply shock, due to disamenity effects (e.g. travel congestion, crowding, shadowing), matching smaller population and more negative area responses. Holding other parameters constant, population and area elasticities monotonically increase in $\beta^R$, making the estimation of $\beta^R$ straightforward (Figure A7).

Logic for how the model generates variation in population and built area as a function of $\theta$-induced heights supply shocks is as follows. Imposed variation in $\theta$ generates variation in heights at each location as described by Eq. (23). Aggregation across locations within the city and only counting heights of at least $\mathcal{T}$ delivers the same pattern of aggregate tall building height growth across cities of different bedrock depths and 1975 populations over time as seen in the data. Expansion of floorspace supply from lower $\theta$ reduces residential rents conditional on $N$ and increases urban utility via Eqs. (28) and (29). Higher $\bar{U}$ attracts migrants according to Eq. (9), generating the positive second stage reduced form population response given migration elasticity $\zeta(1-\mu) > 0$. With more residential heights $S^R(x)$, a smaller residential area from $x_0$ to $x_1$ is needed to satisfy Eq. (28). Labor market clearing in Eq. (26) limits commercial floorspace demand growth, implying that vertical expansion leads to a horizontally smaller CBD via Eq. (27). Together, these residential and commercial land use contractions correspond to the negative second-stage reduced-form finding for city built area. These tight mappings between the first and second stage empirical results and the model's quantitative predictions are what allows us to use the model for structural estimation of $\beta^R$.

Differences in land use and building patterns between the data and the model require attention when matching moments. As our building heights data is bottom-coded at 55 m, model generated heights must also be bottom-coded. However, unlike in the model, the data exhibit variation in building heights at each CBD distance and buildings that tend to taper toward the top. Moreover, about half of land near CBDs in the data is not built up. For these reasons, the threshold above which to measure heights (per unit of land) in the model should be well below 55 m ($\approx$ 13 stories). As it is unclear which height threshold $\mathcal{T}$ to use in the model, we treat $\mathcal{T}$ as an additional parameter to be estimated through indirect inference, thereby rendering model parameters just identified. In the counterfactual exercises below, $\mathcal{T}$ also serves as our minimum tall building height per unit land, corresponding to 55 m per building in the data. Under $\mathcal{T} = 3$ and $\beta^R = -0.11$, we exactly match estimated population and area elasticities reported in Section 3.6.[29] As long as $\mathcal{T} \geq 2$, we obtain a $\beta^R$ value around -0.11.

[29]Using CoreLogic property assessment data from Chicago, the CBD distance ring of 750 to 1000 meters has total residential and office building floorspace that is 3.7 times the land area and average building heights of 12.8 stories, or about 55 m. If floorspace in these buildings was reallocated to cover all of this land area at an equal height, the building height would be 12.8/3.7 = 3.5 stories, close to our $\mathcal{T}$ estimate of 3.

### 4.3 Comparative Statics

The model facilitates conceptualization and quantification of two phenomena of central interest. First is to study the impacts of reducing the cost of height $\theta$, which can come through more favorable bedrock depths or technical progress, on city spatial structure, worker welfare and land values. Second is to explore the normative consequences of imposing stricter height limits $\bar{S}^U$.

To visualize these two comparative statics, we first depict equilibrium building height, floorspace rent, and land rent under the baseline parameterization in the first row of Figure 6. Slopes of use-specific floorspace bid-rent functions are co-determined with height gradients and bid-rent functions for land. A central commercial district is surrounded by a residential district and then rural land. The small discontinuities in floor space rents and heights at the commercial-residential boundary $x_0$ arise endogenously as a result of a net-cost of height $\theta^U - \omega^U$ that is smaller for commercial than residential developments.

Figure 6: Urban Spatial Structure, Cost of Height, and Regulation

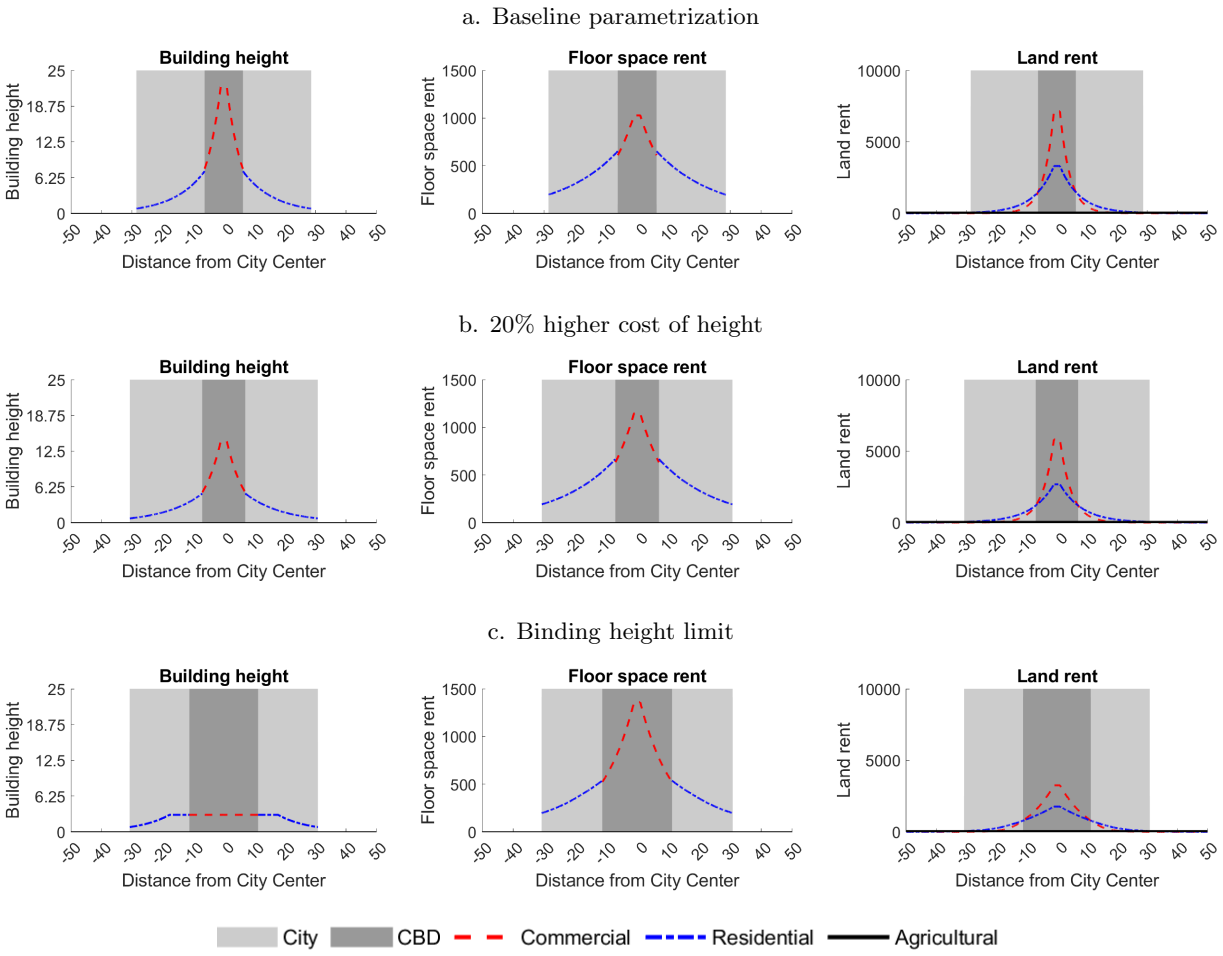


*Note:* Figure illustrates the model solutions under Table 4 parameter values (upper panels), higher costs of height $\theta^C = 0.6, \theta^R = 0.65$ (middle panels), or a height limit of $\bar{S}^C = \bar{S}^R = \mathcal{T} = 3$, meaning 3 floors per unit land or 55 m per empirical building, instead (lower panels). Table A17 reports corresponding impacts on aggregate outcomes.

In the second row of Figure 6, we raise the costs of height by 20%. Heights fall and area expands by 16%. The relocation of firms and residents to peripheral locations increases commuting costs (or, equivalently, reduces residential amenities) by 2.6% and lowers productivity (commercial amenities) by 0.9%. Due to the reduction in floorspace supply, average commercial rents increase by 8%. Lower productivity and higher commute costs make the city less attractive,

thereby reducing housing demand and leading to lower average residential rents, despite the reduction in residential floor space. Lower productivity and higher commercial rents reduce labor demand; reduced accessibility to the center reduces labor supply. The result is a reduction of 2.5% in the equilibrium wage. Due to the lower wage and greater commuting costs, city utility $\bar{U}$ falls by 5.3%. Since living in the city has become less attractive, the population falls by 8.7%. Expected utility across all workers inside and outside the city, $\mathcal{V}$, falls by 2.6%. Aggregate land values fall by 0.7%. Owners of land in the center are worse off, as this is where the intensity of land use falls. Owners of peripheral land are better off, as this land is now more urbanized.

In the third row, we instead impose height caps such that there are no tall buildings, implying a "height gap" of 100%. This results in a substantial horizontal expansion of the CBD. Although we have imposed a tighter constraint on vertical growth, the horizontal area of the city increases only slightly more (at 18%) than in the cost counterfactual, rationalized through a larger population decline of 18%. The more pronounced horizontal expansion of the CBD results in an 8% increased average commuting cost and 5% reduction in average productivity. With a 7% decline, the wage falls more than in the cost counterfactual. The result is a reduction in housing demand that is so large that, despite the negative shock to residential supply, residential rents fall substantially by 14%. The increase in commuting costs and the lower wage, however, dominate the effect of rents on indirect utility in the city, which decreases by 10%, leading to a decline in expected utility $\mathcal{V}$ of 5%. Driven by the conversion of rural into residential and residential into commercial land use, aggregate land values increase by 11%, though land values fall markedly near the center. The height limit redistributes income from the mobile labor factor to the immobile land factor. A major cost of height limits arises from the induced spatial misallocation of firms away from central locations, at which they are most productive.

The size of positive supply shocks from lifting height limits determines the magnitudes of associated welfare consequences. Height limits in cities with high costs of height $\theta$ and/or low populations $N$ bind less strongly. Therefore, the greatest gains from reducing height gaps are in the largest cities with the lowest costs of height. Eliminating them in a city of three million triples the gain if $\theta$ is 0.3 rather than 0.6. As vertical compression leads to horizontal expansion, binding height limits increase aggregate land values if there is large enough horizontal city expansion as a result, even as CBD area land values fall. Figure A9 illustrates how the welfare and land value capitalization effects of height limits depend on population and the cost of height.

By revealed preference, positive city population responses to reductions in $\theta$ must reflect increased urban utility $\bar{U}$, expected utility, and welfare. The logic for welfare gains associated with relaxing building height limits is similar to that from reductions in the cost of height $\theta$, as both feature positive shocks to tall building supply. Differentiating the indirect utility function derived from Eq. (10) facilitates a full accounting of the mechanisms driving these welfare gains.

Urban utility changes through equilibrium adjustments to wages $y$, housing rents $\bar{p}^R$, the combination of variable commuting costs and local amenities $e^{-\tau^R x}$, height amenities $s^{\tilde{\omega}^R}$, and the density dismaneity $\mathcal{D}$ according to the following decomposition:

$$\mathrm{d}\ln\bar{U} = \mathrm{d}\ln y + (\alpha^R - 1)\mathrm{d}\ln\bar{p}^R - \tau^R \mathrm{d}x + \tilde{\omega}^R \mathrm{d}\ln s + \beta^R \mathrm{d}\ln\mathcal{D}. \tag{32}$$

In simulations reported in Table 5 below, we quantify the importance of each of these five forces, measuring the residential rent, residential height amenity, and commuting cost components as population-weighted averages across all locations in each city in our data.

### 4.4 The Welfare Costs of Limiting Heights

We use the model to evaluate the welfare consequences of height caps in each of the 12,877 cities in the full GHS-UCDB sample. We invert the model to rationalize observed populations and height gaps conditional on the observed construction cost of height for each city in our data (Algorithm 4). We set the population of the region, including the rural population, to the city population scaled by the inverse of its 2015 country-specific urbanization rate.[30] We obtain city-specific estimates of the cost of height using mean bedrock depths and the non-parametric estimated relationship between bedrock depth and the cost of height illustrated in Figure A4.

Table 5 considers two counterfactuals. Relative to current height-constrained equilibria, we first calculate losses associated with banning all equilibrium buildings with heights above $\mathcal{T}$ ("no tall building"), capturing the economic benefits of the tall building technology as it is currently used in each city. Second, we calculate the benefits associated with fully relaxing existing height gaps ("no height limit"). We include all rural potential migrants in our welfare calculations.

Table 5: Welfare Costs of Limiting Tall Building Construction

| **Panel A:** | City characteristics | | | Expected utility $\mathcal{V}$ | | Agg land rent $\mathcal{R}$ | |
|---|---|---|---|---|---|---|---|
| World region | In cities >1 mill. | Cost of height $\theta$ (bedrock) | Est. height gap | No tall building | No height limit | No tall building | No height limit |
| Developing Economies | 43% | 0.53 | 45% | –0.9% | 3.7% | –0.8% | –3.9% |
| Developed Economies | 60% | 0.37 | 78% | –1.4% | 7.0% | –2.1% | –8.1% |
| All Economies | 46% | 0.50 | 51% | –1.0% | 4.3% | –1.0% | –4.6% |

| **Panel B:** | Components of city welfare changes from Eq. (32) | | | | | | |
|---|---|---|---|---|---|---|---|
| Region & Experiment | Wages $\Delta \ln y$ | Rents $(\alpha^R - 1)\Delta \ln \bar{p}^R$ | Commutes $-\tau^R \Delta x$ | Views $\tilde{\omega}^R \Delta \ln s$ | Density $\beta^R \Delta \ln \mathcal{D}$ | Total $\Delta \ln \bar{U}$ | Frac adj rent |
| Developing, No Tall | –0.024 | 0.010 | –0.029 | –0.006 | 0.025 | –2.1% | 0.78 |
| Developed, No Tall | –0.025 | 0.005 | –0.030 | –0.006 | 0.024 | –2.9% | 0.77 |
| Developing, No Limit | 0.052 | –0.023 | 0.047 | 0.010 | –0.032 | 6.0% | 0.48 |
| Developed, No Limit | 0.096 | –0.043 | 0.089 | 0.020 | –0.064 | 10.9% | 0.52 |

*Notes:* Entries are population-weighted averages across cities and hinterlands in each indicated region. Welfare effects are from counterfactual analysis within the model parameterized to match all cities' urban population, rural population, cost of height, and height gap. City height gaps are estimated as described in Section 3.5. To compute hinterland populations, we combine the city population with the country-specific 2015 urbanization rate. Results in "No tall building" and "No height limit" columns report average changes in expected utilities and aggregate land rents relative to city constrained equilibria under *existing* height gaps. "No tall building" imposes a height limit of model defined $\mathcal{T}$ floors. "No height limit" sets each city height gap to 0. Panel B shows associated population-weighted changes in indicated urban utility components as calculated using Eq. (32), along with average urban utility responses and the fraction from changes in rents plus commuting costs. Components of urban utility changes $\Delta \ln \bar{U}$ do not add up exactly due to the local linearization.

For developing economies, capping buildings at 55 m reduces worker welfare by 0.9%. As fully relaxing current height constraints increases worker welfare by 3.7%, only (0.9/(0.9+3.7) =) 20% of the potential welfare gains from building tall have been realized. Because of the associated horizontal compression of the city, eliminating existing height limits decreases aggregate land rents by 3.9%. Imposing an even more binding height cap *also* reduces aggregate land rents, by 0.8% because associated CBD area rent declines dominate peripheral rent growth.

The mechanisms are indicated in Panel B. Each component is listed in the same order as in

[30] This implicit partitioning of rural areas into multiple city-specific hinterlands is empirically justified with our evidence in Tables A15 and A16 of minimal heights-driven growth spillovers across cities.

Eq. (32). Positive signs indicate contributions to higher city utility. Results in the final two rows show that relaxing existing height restrictions leads to higher wages, higher average property rents, lower commuting costs (or equivalently, higher localized amenities), higher view amenities, and lower citywide density amenities. The large positive utility contributions of higher wages and lower commuting costs (of 0.052 and 0.047, respectively, for developing economies) and the small view amenity improvement (0.010) outweigh the negative utility contributions from higher rents and lower density amenities (–0.023 and –0.032). Combining the commuting cost/amenity and rent components, the resulting "adjusted rent" (cost of living) component accounts for ∼80% of utility declines from banning heights and ∼50% of utility gains from eliminating height limits. Altogether, average urban utility in developing economy cities falls by 2.1% absent any tall buildings and rises by 6.0% if current height limits are relaxed. As the overall losses reported in the first row of Table 5 include rural residents, they are smaller than urban utility responses.

City population, the cost of height, and the height gap all influence the magnitude of welfare benefits associated with relaxing height limits. With gaps larger in the developed world, and its greater share of population in large cities and lower costs of height due to better bedrock depths, welfare costs of height limits are greater than that for the developing world, at –1.4% for imposing a height ban and 7.0% for relaxing all height restrictions. Aggregating across developing and developed economies, worldwide welfare costs associated with no tall buildings and benefits of relaxing existing height limits are 1.0% and 4.3% of current welfare, respectively.[31]

Departures from current height restrictions reduce land values. Further constraining heights reduces central land values through lower densities in city centers whereas relaxing current height limits decreases peripheral land values by making cities more compact. These positive aggregate land value responses to moderate height constraints rationalize the political economy of height and density restrictions seen in many countries, as articulated in Duranton and Puga (2023). They also confirm that height limits redistribute income from the mobile labor factor to the immobile land factor. As such, relaxing height limits could reduce aggregate inequality.

### 4.5 Additional Results and Sensitivity Analyses

Except for a few cases detailed below, reasonable parameter changes yield worldwide welfare benefits of lifting height limits that are within 0.3 percentage points of our headline 4.3% estimate, though variation in land value responses is more dispersed (Table A19).

Magnitudes of the congestion disamenity and preference heterogeneity parameters $\beta^R$ and $\zeta$ are central for welfare conclusions. Calibrating $\beta^R$ to -0.09 (justified in Appendix C.2.4) and estimating $\zeta$ instead, we get $\hat{\zeta} = 5.7$, below our baseline parameterization of 6.4. Associated gains from relaxing height limits rise from 4.3% to 4.7%, as the congestion amenity rises less with the associated population growth. Constraining $\beta^R$ all the way to 0 leads to a much lower $\zeta$ estimate of 3.4. Without this congestion externality, the model needs a lower migration elasticity to justify observed population responses to heights supply shocks. Since vertical expansion no longer reduces density amenities under this parameterization, removing height limits increases the welfare gain to 7.2%. Welfare and land value implications of manipulating height limits grow the smaller is $\beta^R$. The higher is $\zeta$, the larger the population inflow in response to height supply

[31] As cities in developed areas of Asia are large, this region's opportunities for welfare gains from eliminating existing height limits are large at 13.7% (Table A18). North America and Europe are at 6.4% and 4.6%, respectively. In the developing world, Africa and Latin America have the most to gain from relaxing height limits, at 5.6% and 5.5%, as their cities' average costs of height are low. We obtain 3.0% in developing Asia.

shocks and the more any affordability gains are congested away through migration. Bookending calibrations of $\zeta$ between 4.8 and 9 yields a range of gains from 5.4% for low $\zeta$ to 3.4% for high $\zeta$, given that estimates of $\beta^R$ adjust to match reduced form elasticity estimates.

The only other component of model quantification that has a large effect on welfare conclusions is in how we calculate city height gaps. If we use actual heights relative to the 75th percentile rather than 95th percentile of heights in similar cities, the welfare gain from eliminating height limits declines from 4.3% to 2.3%. This decline comes as associated positive city building supply shocks are mechanically reduced in most cities and eliminated in some cities.

Changing the floorspace share in production, the agglomeration elasticity, the rate of amenity decay, the specification of $\theta$ as a function of bedrock depth, or the housing expenditure share has a minor impact on the results (Table A19). Note that we re-estimate the congestion disamenity $\beta^R$ each time a parameter is changed. $\beta^R$ adjusts to rationalize the empirical moments, thereby mostly reallocating components of welfare changes across channels.

We finish by examining two types of counterfactuals. First, the cost-of-height parameter $\theta$ has declined by ∼2% per year over the past 50 years (Ahlfeldt and Barr, 2022) suggesting continued innovation in construction. The implicit costs of height limits are thus likely to further grow over time. For example, a 20% reduction in the cost of height will come with a welfare cost that increases by about one-quarter, from 4.3% to 5.3%, assuming no world population growth.

Second, we consider the consequences of lifting height limits on commercial or residential buildings only. Lifting commercial height limits has a large effect on city size through the associated boost in labor demand and productivity. However, as residential supply remains constrained, rents are bid up while commuting costs cannot be reduced through increased compactness. This results in a smaller welfare gain of 2.3% and an *increase* of 3.5% in aggregate land value (Table A19). In contrast, lifting only the residential height limit leads to a very small welfare gain of 0.1%. The residential zone becomes more compact, with higher rents capitalizing reduced commuting costs. However, a larger density disamenity almost entirely congests away any residual benefits. Wages hardly change as employers are inhibited from expanding much. Complementarities across residential and commercial land uses means that relaxing both types of height limits together results in a larger welfare gain than the sum of gains associated with relaxing each limit separately. Relaxing residential limits results in a larger reduction in land values of 5.2% than in the baseline scenario in which both height limits are lifted. It is thus perhaps no surprise that policy makers tend to impose laxer height constraints on commercial buildings than their residential counterparts.

## 5 Conclusion

The Skyscraper Revolution has allowed cities around the world to accommodate greater populations on less land. Using bedrock depth induced variation across cities in 1975-2015 reductions in the cost of building tall, estimated elasticities of city population and built land area with respect to aggregate city building heights are 0.13 and -0.16, respectively. As heights respond more to variation in the cost of height in higher demand locations, aggregate responses to reductions in the cost of building taller appear disproportionately in the world's largest cities.

By revealed preference, there are benefits associated with the heights that result from lower construction costs. Quantification using a land use model reveals that the enhanced urban compactness facilitated by the lower costs of building tall results in both productivity gains and

reduced urban travel costs. Migration responses mute potential housing affordability benefits. Given the gap between actual and potential building heights for each city, we find that only about one-fifth of the potential welfare gains from heights have been realized. Gains of 7.0% and 3.7% are available by eliminating existing height regulations in developed and developing economies, respectively. As the cost of building tall declines with technical progress, and as the global population keeps growing, such potential for welfare gains will increase into the future.

With the losses in land values that would come with relaxing height limits, it is perhaps not surprising that so many cities restrict tall building construction. The political economy of such deregulation is fraught. Even though aggregate gains associated with allowing more tall building are to be found, in many areas these gains are distributed disproportionately to potential urban residents that do not own property in the city. Given the potential negative amenity and productivity responses from the congestion associated with increased density, tall building construction may also be regressive and costly in the short run, even if it expands real estate supply to the benefit of all renters in the long run. Tall buildings are also often seen as environmentally wasteful and can destroy historical character. A priority for future research should be to develop a better understanding of the extent to which each of these reasons for the opposition to densification hold up empirically, and to devise viable policy remedies. Lastly, research studying the conditions under which localized densification benefits local residents, such as through transit-oriented development for example, would be fruitful. More generally, by making cities more compact, tall building construction could reduce the needs for public investments in roads and the share of urban land that must be devoted to them.

## References


**Ades, Alberto F and Edward L Glaeser**, "Trade and circuses: explaining urban giants," *The Quarterly Journal of Economics*, 1995, *110* (1), 195–227.

**Ahlfeldt, Gabriel M. and Daniel P. McMillen**, "Tall buildings and land values: Height and construction cost elasticities in Chicago, 1870-2010," *Review of Economics and Statistics*, 2018, *100* (5), 861–875.

**_ and Jason Barr**, "Viewing urban spatial history from tall buildings," *Regional Science and Urban Economics*, 11 2020, p. 103618.

**_ and _** , "The economics of skyscrapers: A synthesis," *Journal of Urban Economics*, 5 2022, *129*, 103419.

**_ , Duncan Roth, and Tobias Seidel**, "Optimal minimum wages," *CEPR Discussion Paper 17026*, 2022.

**Albouy, David, Mauricio Arango, and Minchul Shin**, "Crowning the metropolis: skylines, land values, and urban population," *Working paper*, 2020.

**Alonso, William**, *Location and Land Use*, Cambridge, MA: Harvard Univ. Press, 1964.

**Anagol, Santosh, Fernando Vendramel Ferreira, and Jonah M Rexer**, "Estimating the economic value of zoning reform," Technical Report, mimeo 2024.

**Bairoch, Paul**, *Cities and economic development: from the dawn of history to the present*, University of Chicago Press, 1988.

**Balboni, Clare**, "In harm's way? infrastructure investments and the persistence of coastal cities." PhD dissertation, London School of Economics and Political Science 2019.

_ , **Gharad Bryan, Melanie Morten, and Bilal Siddiqi**, "Could Gentrification Stop the Poor from Benefiting from Urban Improvements?," in "AEA Papers and Proceedings," Vol. 111 American Economic Association 2014 Broadway, Suite 305, Nashville, TN 37203 2021, pp. 532–537.

**Barr, Jason and Remi Jedwab**, "Exciting, boring, and nonexistent skylines: Vertical building gaps in global perspective," *Real Estate Economics*, 2023.

_ , **Troy Tassier, and Rossen Trendafilov**, "Depth to Bedrock and the Formation of the Manhattan Skyline, 1890–1915," *The Journal of Economic History*, 2011, *71* (4), 1060–1077.

**Baum-Snow, Nathaniel**, "Did Highways Cause Suburbanization?," *Quarterly Journal of Economics*, 2007, *122* (2), 775–805.

_ **and Gilles Duranton**, "Housing supply and housing affordability," in "Handbook of regional and urban economics," Vol. 6, Elsevier, 2025, pp. 353–461.

_ , **Loren Brandt, J Vernon Henderson, Matthew A Turner, and Qinghua Zhang**, "Roads, Railroads, and Decentralization of Chinese Cities," *The Review of Economics and Statistics*, 1 2017, *99* (3), 435–448.

**Bertaud, Alain and Jan Brueckner**, "Analyzing building-height restrictions: predicted impacts and welfare costs," *Regional Science and Urban Economics*, 2005, *35* (2), 109–125.

**Borusyak, Kirill, Rafael Dix-Carneiro, and Brian Kovak**, "Understanding migration responses to local shocks," *Available at SSRN 4086847*, 2022.

**Brueckner, Jan and Kala Seetharam Sridhar**, "Measuring welfare gains from relaxation of land-use restrictions: The case of India's building-height limits," *Regional Science and Urban Economics*, 2012, *42* (6), 1061–1067.

**Brueckner, Jan K.**, "The structure of urban equilibria: A unified treatment of the muth-mills model," *Handbook of Regional and Urban Economics*, 1987, *2*, 821–845.

**Brueckner, Jan K and David A Fansler**, "The economics of urban sprawl: Theory and evidence on the spatial sizes of cities," *The review of Economics and Statistics*, 1983, pp. 479–482.

**Brueckner, Jan, Shihe Fu, Yizhen Gu, and Junfu Zhang**, "Measuring the stringency of land use regulation: The case of China's building height limits," *Review of Economics and Statistics*, 2017, *99* (4), 663–677.

**Bryan, Gharad and Melanie Morten**, "The aggregate productivity effects of internal migration: Evidence from Indonesia," *Journal of Political Economy*, 2019, *127* (5), 2229–2268.

_ , **Edward Glaeser, and Nick Tsivanidis**, "Cities in the developing world," *Annual Review of Economics*, 2020, *12* (1), 273–297.

**Burchfield, Marcy, Henry G Overman, Diego Puga, and Matthew A Turner**, "Causes of sprawl: A portrait from space," *The Quarterly Journal of Economics*, 2006, *121* (2), 587–633.

**Buringh, Eltjo and Urbanization Hub**, "The Clio-infra database on urban settlement sizes: 1500–2000," 2013.

**Campante, Filipe and David Yanagizawa-Drott**, "Long-range growth: economic development in the global network of air links," *The Quarterly Journal of Economics*, 2018, *133* (3), 1395–1458.

**Chen, Jiafeng and Jonathan Roth**, "Logs with zeros? Some problems and solutions," *The Quarterly Journal of Economics*, 2024, *139* (2), 891–936.

**Chiovelli, Giorgio, Stelios Michalopoulos, and Elias Papaioannou**, "Landmines and spatial development," Technical Report, National Bureau of Economic Research 2018.

**Civelli, Andrea, Arya Gaduh, Alexander D Rothenberg, and Yao Wang**, "Urban sprawl and social capital: Evidence from Indonesian cities," *The Economic Journal*, 2023, *133* (654), 2110–2146.

**Combes, Pierre-Philippe and Laurent Gobillon**, "The Empirics of Agglomeration Economies," in Gilles Duranton, J Vernon Henderson, William C B T Handbook of Regional Strange, and Urban Economics, eds., *Handbook of Regional and Urban Economics*, Vol. 5, Elsevier, 2015, pp. 247–348.

_ , **Gilles Duranton, and Laurent Gobillon**, "The Costs of Agglomeration: House and Land Prices in French Cities," *The Review of Economic Studies*, 10 2019, *86* (4), 1556–1589.

**Coury, Michael, Toru Kitagawa, Allison Shertzer, and Matthew Turner**, "The value of piped water and sewers: Evidence from 19th century chicago," Technical Report, National Bureau of Economic Research 2022.

**CTBUH**, "Council on Tall Buildings and Urban Habitat Database," Technical Report 2022.

**Curci, Federico**, "The taller the better? Agglomeration determinants and urban structure," *Working paper*, 2020.

**D'Amico, Leonardo, Edward L Glaeser, Joseph Gyourko, William R Kerr, and Giacomo AM Ponzetto**, "Why Has Construction Productivity Stagnated? The Role of Land-Use Regulation," Technical Report, National Bureau of Economic Research 2024.

**Danton, Jayson and Alexander Himbert**, "Residential vertical rent curves," *Journal of Urban Economics*, 2018, *107*, 89–100.

**Ducruet, César, Réka Juhász, Dávid Krisztián Nagy, and Claudia Steinwender**, "All aboard: The effects of port development," Technical Report, National Bureau of Economic Research 2020.

**Duranton, Gilles and Diego Puga**, "Urban Land Use," in Gilles Duranton, J. Vernon Henderson, and William C. Strange, eds., *Handbook of Regional and Urban Economics*, Vol. 5, Elsevier, 2015, chapter 8, pp. 467–560.

_ **and** _ , "Urban growth and its aggregate implications," *Econometrica*, 2023, *91* (6), 2219–2259.

_ **and Matthew A. Turner**, "Urban Growth and Transportation," *The Review of Economic Studies*, 2012, *79* (4), 1407–1440.

**Emporis**, *Emporis* 2022.

**Esch, Thomas, Klaus Deininger, Remi Jedwab, and Daniela Palacios-Lopez**, "Outward and Upward Construction: A 3D Analysis of the Global Building Stock," Working Papers 2023-09, The George Washington University, Institute for International Economic Policy September 2023.

**Faber, Benjamin**, "Trade Integration, Market Size, and Industrialization: Evidence from China's National Trunk Highway System," *The Review of Economic Studies*, 7 2014, *81* (3), 1046–1070.

**Florczyk, A., M. Melchiorri, C. Corban, M. Schiavina, L. Maffenini, M. Pesaresi, P. Politis, F. Sabo, S. Carneiro Freire, D. Ehrlich, T. Kemper, P. Tommasi, D. Airaghi, and L. Zanchetta**, "Description of the GHS Urban Centre Database 2015," *Publications Office of the European Union*, 2019.

**Gechter, Michael and Nick Tsivanidis**, "Spatial spillovers from high-rise developments: Evidence from the Mumbai Mills," *Unpublished manuscript*, 2023.

**Glaeser, Edward**, *Triumph of the City: How Our Greatest Invention Makes Us Richer, Smarter, Greener, Healthier, and Happier* 2012.

_ **and Joseph Gyourko**, "The economic implications of housing supply," *Journal of economic perspectives*, 2018, *32* (1), 3–30.

**Glaeser, Edward L, Hedi D Kallal, Jose A Scheinkman, and Andrei Shleifer**, "Growth in Cities," *Journal of Political Economy*, 5 1992, *100* (6), 1126–1152.

**Gollin, Douglas, Casper Worm Hansen, and Asger Mose Wingender**, "Two Blades of Grass: The Impact of the Green Revolution," *Journal of Political Economy*, 2021, *129* (8), 2344–2384.

**Gonzalez-Navarro, Marco and Matthew A. Turner**, "Subways and urban growth: Evidence from earth," *Journal of Urban Economics*, 11 2018, *108*, 85–106.

**Gyourko, Joseph, Albert Saiz, and Anita Summers**, "A new measure of the local regulatory environment for housing markets: The Wharton Residential Land Use Regulatory Index," *Urban studies*, 2008, *45* (3), 693–729.

_ **and Raven Molloy**, "Regulation and housing supply," in "Handbook of regional and urban economics," Vol. 5, Elsevier, 2015, pp. 1289–1337.

**Hansen, M. and X. Song**, *Vegetation Continuous Fields (VCF) Yearly Global 0.05 Deg.* 2018.

**Harari, Mariaflavia**, "Cities in bad shape: Urban geometry in India," *American Economic Review*, 2020, *110* (8), 2377–2421.

_ **and Maisy Wong**, "Slum upgrading and long-run urban development: Evidence from Indonesia," *Working paper*, 2019.

**Heblich, Stephan, Stephen J Redding, and Daniel M Sturm**, "The Making of the Modern Metropolis: Evidence from London," *The Quarterly Journal of Economics*, 11 2020, *135* (4), 2059–2133.

**Henderson, J Vernon, Tanner Regan, and Anthony Venables**, "Building the city: from slums to a modern metropolis," *The Review of Economic Studies*, 2021, *88* (3), 1157–1192.

_ **, Tim Squires, Adam Storeygard, and David Weil**, "The global distribution of economic activity: nature, history, and the role of trade," *The Quarterly Journal of Economics*, 2018, *133* (1), 357–406.

**Henderson, Vernon, Ari Kuncoro, and Matt Turner**, "Industrial Development in Cities," *Journal of Political Economy*, 5 1995, *103* (5), 1067–1090.

**Hsieh, Chang-Tai and Enrico Moretti**, "Housing Constraints and Spatial Misallocation," *American Economic Journal: Macroeconomics*, 2019, *11* (2), 1–39.

**Imbert, Clément and John Papp**, "Short-term migration, rural public works, and urban labor markets: Evidence from India," *Journal of the European Economic Association*, 2020, *18* (2), 927–963.

**Imbert, Clement, Marlon Seror, Yifan Zhang, and Yanos Zylberberg**, "Migrants and firms: Evidence from china," *American Economic Review*, 2022, *112* (6), 1885–1914.

**Jedwab, Remi, Federico Haslop, Roman Zarate, and Carlos Rodriguez Castelan**, "Lakes and Economic Development: Evidence from the Permanent Shrinking of Lake Chad," Technical Report 2025.

_ **, Jason Barr, and Jan K. Brueckner**, "Cities Without Skylines: Worldwide Building-Height Gaps and their Possible Determinants and Implications," *Journal of Urban Economics*, 2022, *132*, 103507.

_ **, Prakash Loungani, and Anthony Yezer**, "Comparing cities in developed and developing countries: Population, land area, building height and crowding," *Regional Science and Urban Economics*, None 2021, *86* (C), None.

**Knoll, Katharina, Moritz Schularick, and Thomas Steger**, "No price like home: Global house prices, 1870–2012," *American Economic Review*, 2017, *107* (2), 331–353.

**Lall, Somik V, Hyoung Gun Wang, Daniel Da Mata et al.**, "Do urban land regulations influence slum formation? Evidence from Brazilian cities," *Brazilian Association of Graduate Programs in Economics*, 2007.

**Lewis, William Arthur et al.**, "Economic development with unlimited supplies of labour," 1954.

**Liu, Crocker, Stuart S Rosenthal, and William C Strange**, "The Vertical City: Rent Gradients and Spatial Structure," *Journal of Urban Economics*, 2018, *106*, 101–122.

_ **,** _ **, and** _ , "Employment Density and Agglomeration Economies in Tall Buildings," *Regional Science and Urban Economics*, 2020, *84*.

**Lucas, Robert E Jr. and Esteban Rossi-Hansberg**, "On the Internal Structure of Cities Author," *Econometrica*, 2002, *70* (4), 1445–1476.

**Mills, Edwin S**, "An Aggregative Model of Resource Allocation in a Metropolitan Area," *The American Economic Review*, 1967, *57* (2), 197–210.

**Morten, Melanie and Jaqueline Oliveira**, "The effects of roads on trade and migration: Evidence from a planned capital city," *American Economic Journal: Applied Economics*, 2024, *16* (2), 389–421.

**Muth, R**, *Cities and Housing*, Chicago: Chicago University Press, 1969.

**NGDC**, *Global Radiance Calibrated Nighttime Lights* 2015.

**Ortalo-Magné, François and Andrea Prat**, "On the political economy of urban growth: Homeownership versus affordability," *American Economic Journal: Microeconomics*, 2014, *6* (1), 154–181.

**Redding, Stephen J. and Esteban Rossi-Hansberg**, "Quantitative Spatial Economics," *Annual Review of Economics*, 2017, *9* (1), 21–58.

**Rosenthal-Kay, Jordan**, "Urban costs around the world," Technical Report, Working paper 2024.

**Saiz, Albert**, "The geographic determinants of housing supply," *The Quarterly Journal of Economics*, 2010, *125*, 1253–1296.

**Schleier, Merill**, *The Skyscraper in American Art, 1890–1931* 1986.

**Shangguan, Wei, Tomislav Hengl, Jorge Mendes de Jesus, Hua Yuan, and Yongjiu Dai**, "Mapping the global depth to bedrock for land surface modeling," *Journal of Advances in Modeling Earth Systems*, 2017, *9* (1), 65–88.

**Sturm, Daniel M., Kohei Takeda, and Anthony J. Venables**, "Exploring the Urban Model Employment, Housing, and Infrastructure," *World Bank Policy Research Working Paper*, 2022, *9910*.

**UN COMTRADE**, "UN COMTRADE," 2020.

**United Nations**, *World Urbanization Prospects: The 2018 Revision* 2018.

**USGS**, "Mineral Industry Surveys 1960-2020," 2020.

**Wang, Jin, Ting Chen, Ziyang Chen, and Yatang Lin**, "Building Tall, Falling Short: An Empirical Assessment of Chinese Skyscrapers," *Falling Short: An Empirical Assessment of Chinese Skyscrapers*, 2023.

**World Bank**, *World Development Indicators* 2022.

# WEB APPENDIX NOT FOR PUBLICATION

## A Data and stylized facts

### A.1 Additional Data Sources

The following data sources are used to construct robustness results reported in Figure 4.

Elevation data comes from GMTED (2010) (resolution: 15 arc-seconds, or 500 m close to the equator). We use the mean of elevation ("altitude") and standard deviation of elevation ("ruggedness") within city boundaries (measured in m). Data on the location of coastal and lake shorelines comes from Wessel and Smith (1996). Data on the location of major rivers comes from Natural Earth (2025). Giardini et al. (1999) reports peak ground acceleration (PGA; m per $s^2$) at the 0.0833*0.0833° level (≈ 9 x 9 km). PGA takes into account the probability of strong earthquakes in each pixel as well as the probability of diffusion over space. Since land-use regulations related to earthquake risk tend to be adopted based on fuzzily defined local conditions, we consider buffers of 0.05 decimal degrees (5.55 km) around each city. We then obtain the mean PGA for each city/buffer. Data on agricultural suitability comes from Schneider et al. (2022). We rely on their measure of "historic 1980-2008 suitability with current irrigation patterns" and use mean suitability within the city's boundary. Wind speed data comes from Davis et al. (2023). We obtain mean wind speed within each city's boundary. Data on the location of mines circa 2005 comes from USGS (2023). Data on the location of oil and gas fields circa 2009 comes from Lujala et al. (2007). Data on subway stations and network length comes from Gonzalez-Navarro and Turner (2018) and Gendron-Carrier et al. (2022). Data on ports comes from Maritime Safety Office (2019). Deep water ports are ports whose channel depth must be deep enough to accommodate the draft of very large ships, typically 45 feet. Data on the location of dams comes from Global Dam Watch (2025). It includes data on river barriers as well as data on reservoir polygons with a cumulative storage capacity of 7,405 $km^3$ and an artificial terrestrial surface water area of 302,450 $km^2$. Data on the location of wastewater treatment plants comes from Ehalt Macedo et al. (2022). Data on the location of bridges and tunnels comes from OSM. We select all bridges located over a water body. Knowing their length, we obtain the respective total length of bridges and tunnels within each city's boundary.

### A.2 Construction Cost Index

This index nets out factors that contribute to construction costs but are unrelated to height and bedrock depth (e.g. labor costs, construction materials prices, and exchange rate differences). To build the index, we residualize construction cost $C_{i,a(i),c(i),t}$ per unit of floor area $F_{i,a(i),c(i),t}$ of each building $i$, constructed in city $a$ in country $c$ during decade $t$ using the following regression:

$$\ln C_{i,a(i),c(i),t} - \ln F_{i,a(i),c(i),t} = \mu_{a(i)} + \eta_{c(i),t} + \varepsilon^{C}_{i,a(i),c(i),t},$$

where $\mu_{a(i)}$ is a time-invariant fixed effect controlling for arbitrary demand and supply shifters at the city level and $\eta_{c(i),t}$ is a country by decade effect. We recover the residual, $\varepsilon^{C}_{i,a(i),c(i),t}$, as a relative cost measure that describes log deviations from country-trend-adjusted city averages.

Summary statistics about the Emporis cost data are in the notes to Figures A1 and A3.

## A.3 Temporal and Cross-Sectional Variation in the Cost of Height

To evaluate relationships between the construction cost index, building height, and year or bedrock depth non-parametrically, we employ a locally weighted regressions approach using a bivariate kernel. Using building level data, we grid the two observables $\{s^1, s^2\}$ that determine our construction cost index. These observables are building height and year for Figure A1 or building height and bedrock depth for Figure A3. For each combination of grid values along those dimensions $\tilde{s}^1 \in \tilde{S}^1, \tilde{s}^2 \in \tilde{S}^2$ we run the locally weighted regression

$$\varepsilon_i^C = \bar{\varepsilon}^{\tilde{s}^1,\tilde{s}^2} + \tilde{\varepsilon}_i^{\tilde{s}^1,\tilde{s}^2}$$

using the Gaussian kernel weight

$$\begin{aligned} W_i^{\tilde{s}^1,\tilde{s}^2} &= \frac{w_i^{\tilde{s}^1,\tilde{s}^2}}{\sum_{j=1}^{J} w_j^{\tilde{s}^1,\tilde{s}^2}}, \text{where} \\ w_i^{\tilde{s}^1,\tilde{s}^2} &= \prod_{s=\in\{s^1,s^2\}} \frac{1}{\kappa^s\sqrt{\pi}} \exp\left[-\frac{1}{2}\left(\frac{s_i - \tilde{s}}{\kappa^s}\right)^2\right]. \end{aligned} \tag{33}$$

$\kappa^s$ are bandwidth parameters.

Hence, we run $\tilde{S}^1 \times \tilde{S}^2$ locally weighted regressions to recover $\tilde{S}^1 \times \tilde{S}^2$ parameters $\bar{\varepsilon}^{\tilde{s}^1,\tilde{s}^2}$ which are local means that we plot on the height-year plane in FigureA1 and the height-bedrock plane in Figure A3. This amounts to 112 (years) $\times$ 195 (height values) = 21,840 regressions in FigureA1 and 35 (bedrock depth values) $\times$ 195 (height values) = 6,825 regressions in Figure A3.

Figure A1 provides evidence on reductions in the cost of height over time. Our index of construction cost per floor area is mean 0 (by construction) in each year. Therefore, this figure speaks only to the changes in construction costs in taller relative to shorter buildings. Evident in Figure A1 are steep declines in the cost of height over the past century that continued throughout our study period of 1975-2015. In 1975, buildings of 200 m were on average 3.7% higher cost to build per square m than 125 m tall buildings. By 2015, that gap had fallen to 1.3% greater.

Figure A3 depicts both the non-monotonicity of construction costs in bedrock depth conditional on height and the rate at which construction costs increase in height. The descriptive evidence is that the cost-minimizing bedrock depth for 125 m tall buildings is 18 m (blue lines), while that for 200 m tall buildings is 25 m (red lines). Constructing a 125 m tall building at the optimal bedrock depth saves more than 5% in cost per sq m relative to building on surface level or very deep bedrock. The cost savings are much larger for 200 m tall buildings. Moreover, Figure A3 shows that unit costs increase in building height more rapidly where bedrock is deep.

## A.4 The cost of Height and Bedrock Depth

Eq. (21) defines $\theta$ as the elasticity of per-unit construction cost with respect to height. The engineering literature and stylized evidence discussed in Section 2 suggests that this elasticity should by U-shaped in bedrock depth. To empirically substantiate this notion, we use a instrumental variables locally weighted regression (LWR-IV) approach to estimate how bedrock depth influences unit cost responses to building heights. For implementation, we require a demand-side IV to remove the effect of supply-side factors such as ruggedness that could be correlated with sub-soil geology. We use distance from the CBD as an IV for building heights since it affects building heights via demand side forces and has been shown to be a strong predictor of height (Ahlfeldt and Barr, 2022). If the city has buildings exceeding 100 m in

heights, the city center is defined as the median coordinate of these buildings. Otherwise, the city center is defined to be the location of the tallest building ever built in the city.

Concretely, we estimate the first stage

$$\ln h_{i.a(i),c(i),t} = \alpha^{\tilde{b}} \ln DCBD_{i,a(i)} + \tilde{\mu}^{\tilde{b}}_{a(i)} + \tilde{\eta}^{\tilde{b}}_{c(i),t} + \tilde{\varepsilon}^{\tilde{b}}_{i,a(i),c(i),t} \tag{34}$$

and second stage

$$\ln C_{i,a(i),c(i),t} - \ln F_{i,a(i),c(i),t} = \theta^{\tilde{b}} \widehat{\ln h}_{i,a(i),c(i),t} + \mu^{\tilde{b}}_{a(i)} + \eta^{\tilde{b}}_{c(i),t} + \varepsilon^{\tilde{b}}_{i,a(i),c(i),t} \tag{35}$$

for each LWR $\tilde{b} \in \tilde{B}$ using a weighted 2SLS estimator. $h_{i,a(i),c(i),t}$ is the height of building $i$, constructed in city $a$ in country $c$ during decade $t$, $DCBD_{i,a(i)}$ is building $i$'s distance from the center of city $a(i)$, $\ln C_{i,a(i),c(i),t} - \ln F_{i,a(i),c(i),t}$ is the log cost per unit of floor area, $\{\mu^{\tilde{b}}_{a(i)}, \mu^{\tilde{b}}_{a(i)}\}$ are city fixed effects, and $\{\eta^{\tilde{b}}_{c(i),t}, \eta^{\tilde{b}}_{c(i),t}\}$ are country by decade fixed effects.

In each LWR $\tilde{b} \in \tilde{B}$ we weight observations by the Gaussian kernel weight

$$\begin{aligned} W^{\tilde{b}}_i &= \frac{w^{\tilde{b}}_i}{\sum_{j=i}^{J} w^{\tilde{b}}_j}, \text{where} \\ w^{\tilde{b}}_i &= \frac{1}{\kappa^{\tilde{b}}\sqrt{\pi}} \exp\left[-\frac{1}{2}\left(\frac{b_i - \tilde{b}}{\kappa^{\tilde{b}}}\right)^2\right]. \end{aligned} \tag{36}$$

Eq. (36) uses a univariate version of the same kernel as in Eq. (33), except that we employ a LWR-specific bandwidth. This is because we wish to allow for a more flexible fit via a smaller bandwidth in the more populated part of the bedrock distribution, where we also expect more variation in $\theta$. In the right tail of the bedrock distribution that is more sparsely populated and where we expect less variation in $\theta$, the larger bandwidth reduces standard errors. To this end, we use a variant of Scott's rule of thumb for bandwidth selection and define

$$\kappa^{\tilde{b}} = \mathcal{M} \frac{3.49\hat{\sigma}^{\tilde{b}}}{\left(N^{\tilde{b}}\right)^{\frac{1}{3}}},$$

where the standard deviation $\hat{\sigma}^{\tilde{b}}$ and the number of observations $N^{\tilde{b}}$ are computed for rolling subsamples that satisfy $|b_i - \tilde{b}| \leq \mathcal{B} = 10$. We scale the rule-of-thumb bandwidth by a factor of $\mathcal{M} = 2$ since the non-parametric estimation of derivatives generally requires larger bandwidths than the estimation of levels (Henderson and Parmeter, 2015, Section 5.9).

Figure A4 supports the engineering-based hypothesis that bedrock at intermediate depths reduces the construction cost of tall buildings. Within the sample of buildings for which we observe height, construction cost, and floor area, the elasticity of cost with respect to height is minimized at a bedrock depth of ∼15 m. At depths less than about 5 m or greater than ∼25 m, the cost of height is significantly larger. This range is roughly consistent with the descriptive evidence from Figures A3, given an average building height of 109 m in our sample. Figure A4 supports the idea that as demand for height increases over time, cities with bedrock within an intermediate range will have a greater ease of accommodating that demand.

# B Empirics

## B.1 Assessing Population Displacement Effects

We carry out three types of exercises to evaluate the prevalence of population displacement between cities in our data as a source of migration bias in our estimates. First, we explore

robustness of estimates in Table 2 to different levels of regional and sub-national fixed effects. As migration occurs at higher rates more locally, we expect there to be greater displacement between cities within fixed effects covering smaller regions. If coefficients do not grow with the use of more local fixed effects, that is evidence that our estimates reflect rural-urban migration. Second, we explore robustness to a sub-sample that only includes countries with UN measured urbanization rates below 20% in 1975, in which case the vast majority of migrants to cities must have come from rural areas. Finally, in the spirit of Borusyak et al. (2022), we control for height changes in alternative cities that are likely to be viewed by migrants as substitutes.[32]

Table A15 shows the results of the first two exercises. IV estimates for population grow by at most 0.03 when including finer fixed effects (e.g., regions or districts) and decline by 0.03 when using world sub-region rather than country fixed effects. Table A15 also shows results for the sample restricted to countries that were less than 20% urban in 1975. The population elasticity remains stable at 0.13. Built area elasticities are somewhat more sensitive to the inclusion of various levels of fixed effects and sample. These estimates grow in magnitude to as much as -0.25 with alternative fixed effects. However, the elasticity shrinks to -0.08 for rural countries. None of these estimates are statistically different from our primary built area elasticity of -0.16.

For the third exercise, we calculate market potential (MP) terms that summarize accessibility of each city $a$ in country $c$ to other population centers and their heights in year $t$:

$$\text{MP}^H_{act} = \sum_{a' \in C(a), \neq a} \frac{\text{Heights}_{a'ct}\ \text{Pop}_{a'c75}}{\text{Pop}_{ac75}\ \text{Distance}(a,a')^\alpha}. \tag{37}$$

That is, we sum over heights in all other cities in the country of city $a$, scaling by relative city size and discounting by the distance between city $a$ and $a'$ raised to the power $\alpha$, which we vary between $\frac{1}{3}$ and 3. From these measures in 1975 and 2015, we build the control variable $\Delta \ln \text{MP}^H_{act}$. With this specification, heights in $\text{MP}^H_{act}$ are scaled to be of comparable magnitudes to heights in city $a$ itself. A given percentage increase in heights on a small base will have the potential to redirect fewer migrants as a share of city $a$'s 1975 population than on a large base.

As heights in other cities may be endogenous to trends in demand factors in city $ac$, we build an instrument for $\Delta \ln \text{MP}^H_{act}$ that follows the same logic as our main instruments. These instruments replace $\text{Heights}_{a'c75}$ in Eq. (37) with $\text{Pop}_{a'c75}\text{MBD}_{a'c}$ and $\text{Pop}_{a'c75}\text{MBD}^2_{a'c}$. As in Eq. (5), we also control for three additional terms capturing the discounted sums of 1975 city populations and bedrock depths (MBD) by replacing $\text{Heights}_{a'c75}$ in Eq. (37) with $\text{Pop}_{a'c75}$, $\text{MBD}_{a'c}$, or $\text{MBD}^2_{a'c}$ and taking logs. Lastly, since $\text{MP}^H$ in Eq. (37) also directly includes $\frac{\text{Pop}_{a'c75}}{\text{Pop}_{ac75}}$, we create an additional MP term based on these relative 1975 city populations only.

Table A16 shows the results with these MP controls. Whether instrumenting for $\Delta \ln \text{MP}^H$ or not, estimated population and built area elasticities remain stable (the two cases where the IV F-statistic is below 5 should be ignored). We come to the same conclusion when separately considering the largest 10 cities and the other cities in the country in MP terms (and assuming a lower distance decay parameter for larger cities) or when controlling separately for height growth in each of these cities (unreported). The coefficient on the height MP control is zero or positive when instrumented, which may reflect a growth effect of improved access to markets.

[32] Fully carrying out the proposed fix in Borusyak et al. (2022) requires observing migration flows in a base period; unfortunately, this information is unavailable for most countries in our global data.

## B.2 Details of Height Gap Calculations

We adopt the regression specification to predict city heights used in Barr and Jedwab (2023, eq. (6)). The analysis uses 12,755 GHS-UCDB cities, $a$, in 163 countries, $c$, in the years $t = \{1995, 2000, 2005, 2010, 2015, 2020\}$ (N = 76,530). In each year, these cities are classified into 10 categories, indexed by $p$, as determined by population at time $t$: 0-100K, 100-250K, 250-500K, 500-750K, 750-1,000K, 1,000-2,500K, 2,500-5,000K, 5,000-7,500K, 7,500-10,000K, 10,000K+. Since city population is only available in 1990, 2000, and 2015, population categories are defined using year 2015 population data for 2010-2020 and 2000 data for 1995-2005.

The estimation equation is

$$\begin{aligned} \text{LHEIGHTS}_{act} &= \rho_1 \text{LDMSP}_{act(d)} + \rho_2 \text{LVIIRS}_{act(v)} \\ &+ \Sigma_{p=1}^{10} \gamma_{p,t} \mathbb{1}(\text{CAT}_{act} = p) + \Sigma_{p=1}^{10} \mathbb{1}(\text{CAT}_{act} = p) X_{ct} \beta_{p,t} \\ &+ \Sigma_{p=1}^{10} \mathbb{1}(\text{CAT}_{act} = p) X_{ac} \delta_{p,t} + \nu_{act}. \end{aligned} \tag{38}$$

$\rho_1$, $\rho_2$, and $\gamma_{p,t}$ are scalars. $\beta_{p,t}$ and $\delta_{p,t}$ are vectors to reflect that $X_{ct}$ and $X_{ac}$ are matrices that include the variables described below. $\text{LHEIGHTS}_{act}$ is the log of (total sum of tall building heights + 1) in city $a$, country $c$, and year $t$. Population size dummies ($\text{CAT}_{act}$) are fully interacted with year fixed effects to control for differing levels and trends in real estate demand and construction costs across cities of different sizes. Remaining controls for other demand and supply factors include country-level controls ($X_{ct}$) and time invariant city-level controls ($X_{ac}$), which are interacted with the population size dummies and year fixed effects, allowing their impacts to vary by city size over time. The objective is to estimate residuals $\nu_{ac2015}$, which proxy for land-use regulations and height restrictions in city $ac$ in 2015.

The first two variables in the regression denote city total night lights and proxy for city income in different years. The log of (total sum of DMSP lights + 1) can be calculated for years $t(d)$ 1995, 2000, 2005 and 2010.[33] The log of (total sum of VIIRS lights + 1) can be calculated for years $t(v)$ 2010, 2015 and 2020.[34] Other demand side factors ($X_{ct}$) are accounted for with city population and year interacted with quadratics in national per-capita GDP,[35] national population, and national land area.[36] More populated countries tend to have larger large cities, which naturally have more demand for heights and tall buildings. Likewise, countries with more available (lower cost) land tend to have less vertical cities. Time-invariant city-level controls ($X_{ac}$) (interacted with city size dummies and year fixed effects) account for various demand and supply factors. On the supply side are city mean bedrock depth, earthquake risk, and quadratics in the mean and standard deviation of city elevation. Elevation range also controls for some demand side factors, as cities surrounded by more mountainous land have less scope for horizontal expansion, thereby increasing the demand for heights.

The estimated adjusted R-squared of 0.64 suggests that fundamental demand and supply factors may account for almost two thirds of the international variation in city heights. Assuming

[33] Night lights data corresponding to the DMSP satellites are provided by NGDC (2015). The radiance calibrated version of this data, which is available for select years between 1996 and 2011, is used to avoid top-coding complications. The data are available at a 30 arc second (≈ 1km at the equator) spatial resolution.

[34] Night lights data from VIIRS satellites are provided by Elvidge et al. (2021). The data is not top-coded and are available at a 15 arc second (≈ 500m at the equator) spatial resolution.

[35] Annual per-capita GDP (PPP, constant international 2011 $) is obtained from Maddison (2008) and Bolt and van Zanden (2020) To avoid short-term fluctuations in income, data in year $t$ reflects a 7 year moving-average.

[36] The main sources for land area and total population are United Nations (2018) and World Bank (2022).

the other 0.36 can be attributed to land-use regulation, the residuals $\nu_{act}$ capture the extent to which each city has more or less heights than other cities with similar observable characteristics.

Using estimated parameters in (38), we predict each city's 2015 stock of heights were it to have among the most heights for cities with similar observables. We view this prediction as the amount of heights the city would have were it unconstrained by regulation. Comparisons of actual heights to this prediction of unconstrained heights delivers each city's height gap.

To build up to the determination of each city's counterfactual unconstrained heights, we begin by predicting the log sum of heights in 2015 for each city using parameter estimates in (38). We then select the 25 cities with the most similar predicted heights above and below each city's prediction. For each city's group of 51, we obtain the 95th percentile ("p95"), or 3rd ranked city-level residual. High p95 values indicate that the city's group includes cities that are well above the world's conditional average.[37] By construction, cities that are predicted to have little heights belong to groups where the least constrained cities do not have measurably more heights than the world's conditional average. Cities that are predicted to have a lot of heights also belong to relatively homogeneous groups in terms of heights. Cities with the largest height fundamentals all have similar height stocks, *ceteris paribus*, meaning that their height gaps are relatively low. Larger differences can be observed for cities with intermediate height predictions. Such cities disproportionately belong to developing economies, where more varied patterns of vertical development can be observed within a group of otherwise similar cities.[38]

We calculate the height gap (%) for city *ac* following Eq. (6). A gap of 20% means that the city has built 80% of what the p95 city in the city's group has built despite sharing similar economic conditions. Cities with residuals above the p95 value have their gaps set to 0%. The median gap is 0%, reflecting the many small cities in our data whose fundamentals do not justify tall buildings. However, the distribution has a thick right tail driven by larger cities. The mean and standard deviation are 24% and 41%, respectively. Weighting by city population, the median is 66%, the mean 50%, and the standard deviation 45%.

Among the 100 largest cities in the world, we obtain gaps of 0% for cities including Chicago, Kuala Lumpur, Sao Paulo, Seoul, and Shanghai, and gaps of 11% for Guangzhou, 26% for New York, 37% for Ho Chi Minh City, and 45% for Miami. We obtain larger gaps of 66% for Bangkok, Paris, London, and Mexico City, 73% for Beijing, 80% for Buenos Aires, 91% for Karachi, and 93% for Cairo. Sensible differences are obtained within the US. Lower-gap large cities include Chicago (0%), New York (26%) and Miami (45%). Higher-gap large cities include Boston (70%), Los Angeles (82%), Washington DC (86%) and San Francisco (94%). Lastly, to compute global or regional gaps, we use 2015 city populations as weights. We find a global gap of 50%.

# C Model

## C.1 Equilibrium solver

Values of endogenous objects $\{y, \bar{U}\}$, parameters $\{\alpha^U, \beta^U, \omega^U, \theta^U, \tau^U, \underline{x}^U, \bar{a}^U, \tilde{c}^U, \bar{S}^U, r^a, \zeta, \ell, \tilde{U}\}$, and the endowment $\bar{N}$ deliver a unique mapping to all other endogenous objects. To solve for

[37] We use p95 instead of the max or p99 to allow for the possibility that 2 cities in each group may have a lot of heights due to idiosyncratic city-specific factors rather than laissez-faire planning regulations. For example, they may have a large government sector or developers with interests in marquee skyscrapers that are not justified by city fundamentals.

[38] Similar relationships are obtained when excluding Chinese and Middle Eastern cities (unreported).

these equilibrium values, we implement Algorithm 1.

**Algorithm 1:** Equilibrium solver

**Data:** Given values for primitives $\{\alpha^U, \beta^U, \omega^U, \theta^U, \tau^U, \underline{x}^U, \bar{a}^U, \tilde{c}^U, \bar{S}^U, r^a, \zeta, \ell, \bar{N}, \tilde{U}\}$
Guesses of equilibrium values of $\{\bar{U}, y\}$

**while** $\bar{U} \neq \widehat{\bar{U}}$ *or* $y \neq \hat{y}$ **do**
- Compute $N$ using Eq. (9)
- Compute $\tilde{p}^U(x)$ using Eqs. (14) & (19) (notice $\bar{p}^U(x) \equiv \tilde{p}^U(x)[S^U(x)]^{\omega^U}$)
- Compute $\tilde{S}^U(x)$ using Eq. (24)
- Compute $r^U(x)$ using Eq. (25)
- Allocate land to use with the highest land rent
- Compute market-clearing wage $\hat{y}$ using Eqs. (20) and (26)
- Compute endogenous city-utility $\widehat{\bar{U}}$ using Eq. (29)
- Update guesses to weighted combination of old guesses and $\{\widehat{\bar{U}}, \hat{y}\}$

**Result:** Equilibrium values of $\{\bar{U}, y\}$

## C.2 Quantification

### C.2.1 Amenity decay ($\tau^U$)

In the absence of binding height limits, we can use Eqs (23) and (13) or (18) to obtain the structural equation for building height by use at each location $x > \underline{x}^U$:

$$\ln S^{*U}(x) = k^U - \frac{\tau^U}{(1-\alpha^U)(\theta^U - \omega^U)}\, x, \qquad x > \underline{x}^U. \tag{39}$$

where $k^C$ and $k^R$ summarize parameters and city-specific constants.[39]. This equation motivates the following reduced form building type-specific log-linear regression specification that has been used to estimate various price and density gradients:

$$\ln S^U_{ib} = \mathcal{G}^U_0 + \mathcal{G}^U_1 DIST_{ib} + \mathcal{E}^U_{ib}$$

$DIST_{ib}$ is the distance from building $i$ in distance ring $b$ to the city center and $\mathcal{E}^U_{ib}$ is a residual term that captures deviations in observed height from a smooth gradient. It is straightforward to recover the amenity decay from an estimate of the reduced-form parameters $\mathcal{G}^U_1$:

$$\tau^U = -\mathcal{G}^U_1 (1-\alpha^U)(\theta^U - \omega^U)$$

We separately estimate $\mathcal{G}^U_1$ for Chicago, USA and Sao Paolo, Brazil, adjusting details of the empirical approach to fit the data structure and planning environment for each city. For Chicago, we define $S^U_{ib}$ as the number of stories for all commercial or residential buildings within 10 km of the city center, excluding industrial and government buildings. We define the city center as the average location of the tallest 5 commercial buildings in the city. We use the CoreLogic reported property assessment data from 2021/2022 and weight by the inverse of the number of observations in each 250 m wide distance ring bin $b$, giving each bin equal weight in the

[39] $k^R = \frac{1}{\theta^R - \omega^R}\left[\frac{1}{1-\alpha^R}\ln\left(\frac{\mathcal{D}^{\beta^R}\bar{a}^R y}{\bar{U}}\right) - \ln c^R - \ln(1+\theta^R) + \frac{\tau^R}{1-\alpha^R}\underline{x}^R\right]$,
$k^C = \frac{1}{\theta^C - \omega^C}\left[\frac{1}{1-\alpha^C}\ln\left(\frac{\bar{a}^C N^{\beta^C}}{y^{\alpha^C}}\right) - \ln c^C - \ln(1+\theta^C) + \frac{\tau^C}{1-\alpha^C}\underline{x}^C\right]$

regressions. We choose Chicago as our main case in point because it is arguably the stereotype of an unconstrained, monocentric city that conforms to our land-use model. From the height gradient estimates of -0.2 for commercial and -0.1 for residential buildings, we infer the values of our structural parameters $\tau^C = 0.014$ and $\tau^R = 0.016$.

Sao Paolo is the only large developing economy city with a height gap of 0 for which we could find comprehensive building height data. We use the 2016 property assessment data for the Sao Paolo municipality (Anagol et al., 2024). As Sao Paolo is polycentric, we define each building's CBD distance as that from its block centroid to the nearest of the city's 5 most important CBDs (Historical Center, Avenida Paulista, Faria Lima, Vila Olimpia, Brooklin/Berrini). We then estimate the following spline regression by NLLS.

$$\ln S_{ib}^U = \mathcal{G}_0^U + \mathcal{G}_1^U DIST_{ib} + (\mathcal{G}_2^U - \mathcal{G}_1^U)(DIST_{ib} - \mathcal{K}^U)\mathbb{1}(DIST_{ib} \geq \mathcal{K}^U) + \mathcal{E}_{ib}^U$$

For residential buildings, the estimated kink distance $\mathcal{K}^R$ is 4.6km. As the Sao Paolo planning data defines all non-residential buildings as commercial, this category mixes in government and industrial buildings that we were able to exclude from the Chicago data. As commercial "horizontal" buildings typically comprise multiple connected smaller vertical structures on one combined tax lot, we only use "vertical" commercial buildings in estimation. The estimated commercial kink is at 3.5km with an estimated $\mathcal{G}_1^C = -0.15$, implying $\tau^C = 0.011$. Given the greater difficulties with the Sao Paolo commercial data than that for Chicago, we prefer the Chicago based estimate of $\tau^C$. Whether estimated using all of just vertical residential properties, we estimate $\mathcal{G}_1^R = -0.10$, just as for Chicago.

We are also interested in the degree to which these height gradients generalize more broadly. We thus make use of a global 80X80 m raster data set of remote-sensed building volumes (Esch et al., 2023). We include cities with height gaps below 50% (see Section 3.5 for calculation of height gaps) and with populations of at least 1 million in 2015. This gives us 39 cities in developing economies and 11 cities in developed economies (including Chicago).

Since the volume data does not distinguish between commercial and residential uses, we exploit our model's prediction of a change in the slope of the height gradient at the border between the commercial and the residential zones. Therefore, for each of the 50 selected cities, we estimate the following piece-wise linear spline specification with one endogenous knot:

$$\ln FAR_b = \mathcal{B}_0 + \mathcal{B}_1 DIST_b + (\mathcal{B}_2 - \mathcal{B}_1)(DIST_b - \mathcal{K}_1)\mathbb{1}(DIST_b \geq \mathcal{K}_1) + \mathcal{E}_b$$

$FAR_b$ is the total building volume divided by land area across all 80X80 m pixels in city center distance ring $b$ out to 10 km. Each distance band $DIST_b$ is 250 m wide. Therefore, the outcome measure is close to a floor area ratio ($FAR$) measure of building density, though the denominator includes area of land in all uses (including roads and parks). For each of the 50 cities, we identify the city center location using information on lights at night and the tallest buildings in each city. $\mathcal{K}_1$ gives the distance from the endogenous knot to the city center, $\mathcal{B}_1$ is the height gradient for $DIST_b < \mathcal{K}_1$ and $\mathcal{B}_2$ is the gradient when $DIST_b \geq \mathcal{K}_1$. We use non-linear least squares to estimate $\{\mathcal{B}_0, \mathcal{B}_1, \mathcal{B}_2, \mathcal{K}_1\}$ for each city. Chicago's internal structure is not an outlier. Within the building volume data, Chicago's overall gradient, knot location and location-specific gradients are close to the mean and the mode across these 50 cities (unreported).

### C.2.2 Rural utility

We treat rural utility, $\tilde{U}$, as a fundamental that we can invert for given values of other primitives and an observed or user-specified urban population share, $\mu$, using Algorithm 2.

**Algorithm 2:** $\tilde{U}$ inverter

**Data:** Given values of primitives $\{\alpha^U, \beta^U, \omega^U, \theta^U, \tau^U, \underline{x}^U, \bar{a}^U, \tilde{c}^U, \bar{S}^U, r^a, \zeta, \ell, \bar{N}\}$
Guess of $\tilde{U}$
User-chosen $\mu$

**while** $\tilde{U} \neq \widehat{\tilde{U}}$ **do**
- Compute $\bar{U}$ using Algorithm 1
- Compute rural utility, $\widehat{\tilde{U}}$, using Eq. (9)
- Update guess of $\tilde{U}$ to weighted combination of old guess and $\widehat{\tilde{U}}$

**Result:** $\tilde{U}$ that rationalizes given $\mu$

### C.2.3 Estimating the density elasticity of urban amenity

We need the value of $\beta^R$ under which the model generates our key empirical moments. These are estimates of the height elasticity of population, $\hat{\beta}^N$, and the height elasticity of area, $\hat{\beta}^{\mathcal{L}}$. Our identification strategy exploits subsoil geography to ensure that we identify these parameters from variation in the cost of height, holding demand factors constant. Since we have full control over the data-generating process, it is straightforward to mimic this source of variation in the model.

To this end, we solve the model multiple times for values of $\theta \in \Theta$, where $\theta^C = \theta$ and $\theta^R = \theta + 0.05$ to maintain the same difference between the commercial and residential height elasticity as in the baseline specification in Table 4. We obtain differences in equilibrium outcomes that are solely driven by variations in the cost of height. To operationalize our indirect inference approach, we nest this loop over $\theta \in \Theta$ within a search over a parameter space defined by $\beta^R \in \mathcal{B}$ and $\mathcal{T} \in \mathcal{R}$. We invert $\tilde{U}$ each time we adjust $\beta^R$, setting $\mu = \bar{\mu}$ and all parameters to the values in Table 4 to keep the city population constant. For each combination of $\{\theta, \beta^R, \mathcal{T}\}$, we solve the model and compute (the endogenous outcomes) city area

$$\mathcal{L}_\theta^{\beta^R,\mathcal{T}} = \int_0^{(x_1)^{\theta,\beta^R,\mathcal{T}}} \mathcal{L}(x)\mathrm{d}x,$$

city population

$$N_\theta^{\beta^R,\mathcal{T}} = \int_{(x_0)^{\theta,\beta^R,\mathcal{T}}}^{(x_1)^{\theta,\beta^R,\mathcal{T}}} (n(x))^{\theta,\beta^R}\mathrm{d}x,$$

and city tall building height

$$\begin{aligned} H_\theta^{\beta^R,\mathcal{T}} = &\int_0^{(x_0)^{\theta,\beta^R,\mathcal{T}}} \mathcal{L}(x)\max\left[\left((S^C(x))^{\theta,\beta^R} - \mathcal{T}\right), 0\right]\mathrm{d}x \\ &+ \int_{(x_0)^{\theta,\beta^R,\mathcal{T}}}^{(x_1)^{\theta,\beta^R,\mathcal{T}}} \mathcal{L}(x)\max\left[\left((S^R(x))^{\theta,\beta^R} - \mathcal{T}\right), 0\right]\mathrm{d}x. \end{aligned} \tag{40}$$

For each combination of $\{\beta^R, \mathcal{T}\}$, we run the following regressions on the model-based

outcomes to recover our moments in the model $\{\tilde{\beta}^N, \tilde{\beta}^{\mathcal{L}}\}$:

$$\ln \mathcal{L}_\theta^{\beta^R,\mathcal{T}} = c^{\mathcal{L},\beta^R,\mathcal{T}} + \tilde{\beta}^{\mathcal{L}}_{\beta^R,\mathcal{T}} \ln H_\theta^{\beta^R,\mathcal{T}} + \tilde{\epsilon}_\theta^{\mathcal{L},\beta^R,\mathcal{T}}$$
$$\ln N_\theta^{\beta^R,\mathcal{T}} = c^{N,\beta^R,\mathcal{T}} + \tilde{\beta}^{N}_{\beta^R,\mathcal{T}} \ln H_\theta^{\beta^R,\mathcal{T}} + \tilde{\epsilon}_\theta^{N,\beta^R,\mathcal{T}}$$

To find the combination of $\{\beta^R, \mathcal{T}\}$ that best fits the data, we minimize the value of the residual sum of squares of the moments in the model and the data:

$$\beta^R, \mathcal{T} = \arg \min_{\beta^R \in \mathcal{B}, \mathcal{T} \in \mathcal{R}} \sum_{o \in N, \mathcal{L}} \left(\hat{\beta}^o - \tilde{\beta}^o\right)^2 \tag{41}$$

Algorithm 3 provides a compact summary of the estimation procedure. To solve the minimization problem, we use particle swarm optimization (PSO), a population-based, stochastic optimization algorithm that searches for a global minimum of a nonlinear function within a bounded domain. The algorithm explores the search space using a group of candidate solutions, known as particles, which iteratively update their positions based on both individual experience and the shared knowledge of the swarm. This method is particularly effective for optimizing complex, non-differentiable, or multimodal objective functions, and it supports parallel execution across multiple threads to enhance computational efficiency.

For the data moments, we use $\hat{\beta}^N = 0.21$ and $\hat{\beta}^{\mathcal{L}} = -0.38$ estimated from the subset of cities that are relatively unconstrained by height regulation (col. (3) of Table 3). Under $\beta^R = -0.11$ and $\mathcal{T} = 3$, we almost exactly match the moments. To evaluate whether the particle-swarm algorithm converges to the well-defined global minimum of the objective function, we search over a grid of height costs $\Theta = \{0.2, 0.3, \ldots, 1\}$ and set $\bar{\mu} = 0.5$ and find a clear minimum in the objective function at our identified value of $\beta^R$ (not shown). In contrast, the choice of $\mathcal{T}$ is less consequential. As long as $\mathcal{T} \geq 2.0$, the model generates height elasticities that are close to those estimated from data.

**Algorithm 3:** Calibrating $\{\beta^R, \mathcal{T}\}$

**Data:** Given values of primitives $\{\alpha^U, \beta^C, \omega^U, \theta^U, \tau^U, \underline{x}^U, \bar{a}^U, \tilde{c}^U, \bar{S}^U, r^a, \zeta, \ell, \bar{N}\}$
Moments in data $\{\widehat{\beta}^N, \widehat{\beta}^{\mathcal{L}}\}$
User-chosen $\mu$

**foreach** $\beta^R \in \mathcal{B}$ **do**
  Use Algorithm 2 to invert $\tilde{U}$ so to match $\mu = 0.5 (\Rightarrow) N = \mu \bar{N} = 3M$) under baseline values of $\{\theta^C = 0.5, \theta^R = 0.55\}$
  **foreach** $\mathcal{T} \in \mathcal{R}$ **do**
    **foreach** $\theta \in \Theta$ **do**
      Use Algorithm 1 to solve for equilibrium outcomes of $\{\mathcal{L}_\theta^{\beta^R,\mathcal{T}}, N_\theta^{\beta^R,\mathcal{T}}, H_\theta^{\beta^R,\mathcal{T}}\}$
    **foreach** $o \in N, \mathcal{L}$ **do**
      Regress $\ln o_\theta^{\beta^R,\mathcal{T}}$ against $\ln H_\theta^{\beta^R,\mathcal{T}}$ to obtain model moment $\tilde{\beta}^o$
Use moments in data $\{\widehat{\beta}^N, \widehat{\beta}^{\mathcal{L}}\}$ and model $\{\tilde{\beta}^N, \tilde{\beta}^{\mathcal{L}}\}$ in Eq. (41) to find $\{\beta^R, \mathcal{T}\}$

**Result:** $\{\beta^R, \mathcal{T}\}$ values that match moments in model and data

Our estimated value of $\mathcal{T} = 3$ is a plausible best fit, even if 3 floors corresponds to much less

than 55 meters. To see this, consider that the model generates an average height of 14 floors (55 m). Setting $\mathcal{T}$ to 15 instead would generate no tall buildings in the model ($H = 0$). We should observe a positive value for $H$ because the mean height of 55 m would be generated by a mix of taller and shorter buildings.

#### C.2.4 Estimating preference heterogeneity instead

The density elasticity $\beta^R$ and the preference heterogeneity parameter $\zeta$, which is closely related to the migration elasticity $\zeta(1-\mu)$, are not easily separately identified. In the model, a lower values of either of these parameters leads to lower population and area responses to positive floor space supply shocks. At a more negative $\beta^R$, there is a greater quality of life penalty as the city population grows. At $\zeta$ closer to zero, fewer workers with idiosyncratic tastes for rural life decide to move into the city as $\bar{U}$ increases. We can thus use our empirical elasticity estimates to either indirectly infer $\{\beta^R, \mathcal{T}\}$ for a given value of $\zeta$, or infer $\{\zeta, \mathcal{T}\}$ for a given value of $\beta^R$. Since the evidence base is more developed for $\zeta$, we focus on estimating the cost of densification through tall building construction. As robustness, however, we also implement the latter strategy using a procedure analogous to that developed in the prior sub-section for estimating $\zeta$.

To calibrate $\beta^R$, we use

$$\beta^R = \frac{\partial \ln A^R}{\partial \ln \mathcal{D}} = \frac{\partial \ln A^R}{\partial \ln N} \frac{\partial \ln N}{\partial \ln \mathcal{D}}.$$

We take $\frac{\partial \ln A^R}{\partial \ln N} = -0.04$ from Duranton and Puga (2023). This is their estimate of the elasticity of inverse travel speed with respect to city population using National Household Transportation Survey data for the US. In a monocentric city with fixed lot size, this is also the elasticity of utility with respect to population. We take $\frac{\partial \ln \mathcal{D}}{\partial \ln N} = 0.43$ from the calibrated monocentric model in Ahlfeldt and Pietrostefani (2019). Put together, this gives us $\beta^R = -0.09$. For this value of the density elasticity of amenity, the same indirect inference strategy as described in Section C.2.3 yields an estimate for $\zeta = 5.7$, which implies a migration elasticity of 2.8, which is well within the range of estimates in the literature.

### C.3 Welfare calculations

Algorithm 4 describes the numerical procedure used to compute welfare effects for cities of a given cost of height, population, and height gap.

**Algorithm 4:** Welfare effects

**Data:** Given values of primitives $\{\alpha^U, \beta^U, \omega^U, \tau^U, \underline{x}^U, \bar{a}^U, \tilde{c}^U, \bar{S}^U, r^a, \zeta, \ell, \bar{N}, \mathcal{T}\}$
City population, $Pop_a$, observed in data
Height gap, $HG_a$, observed in data
Bedrock depth, $MBD_a$, observed in data

Use $MBD_a$ and non-linear mapping in Figure A4 to obtain cost of height, $\theta_a^C$
Set $\theta_a^R = \theta_a^C + 0.05$
Set height limit in model to $\bar{S}^U = \mathcal{T}$
**while** *Height gap in model,* $\tilde{HG} > HG_a$ **do**
    Use Algorithm 2 to invert rural utility, $\tilde{U}$, that satisfies $\mu\bar{N} = Pop_a$
    Use Eq. (40) to compute constrained tall building height $H$
    Use Algorithm 1 to solve for counterfactual under no height limit, $\bar{S} = \infty$
    Use Eq. (40) to compute unconstrained tall building height $H^*$
    Compute $\tilde{HG} = 1 - \frac{H}{H^*}$
    Marginally increase height limit in model, $\bar{S}$
Use Algorithm 1 to solve for $\mathcal{W}^{actual}$, where $\mathcal{W} \in \{\mathcal{V}, \mathcal{R}\}$, under calibrated height limit $\bar{S}$
Use Algorithm 1 to solve for welfare $\mathcal{W}^{ban}$ under counterfactual height limit $\bar{S} = \mathcal{T}$
Use Algorithm 1 to solve for welfare $\mathcal{W}^{market}$ under counterfactual height limit $\bar{S} = \infty$
Compute welfare effect of existing tall buildings $\hat{\mathcal{W}}^{actual} = \frac{\mathcal{W}^{actual}}{\mathcal{W}^{ban}} - 1$
Compute welfare potential of tall buildings $\hat{\mathcal{W}}^{potential} = \frac{\mathcal{W}^{market}}{\mathcal{W}^{ban}} - 1$
Compute welfare effect of existing height regulation $\hat{\mathcal{W}}^{regulation} = \frac{\mathcal{W}^{actual}}{\mathcal{W}^{market}} - 1$

**Result:** Effects of existing tall buildings, all potential tall buildings, and height limits on expected utility $\{\hat{\mathcal{V}}_a^{actual}, \hat{\mathcal{V}}_a^{potential}, \hat{\mathcal{V}}_a^{regulation}\}$ and land rent $\{\hat{\mathcal{R}}_a^{actual}, \hat{\mathcal{R}}_a^{potential}, \hat{\mathcal{R}}_a^{regulation}\}$ for city $a$

# Appendix References


**Ahlfeldt, Gabriel M. and Elisabetta Pietrostefani**, "The economic effects of density: A synthesis," *Journal of Urban Economics*, 2019, *111* (February), 93–107.

**_ and Jason Barr**, "The economics of skyscrapers: A synthesis," *Journal of Urban Economics*, 5 2022, *129*, 103419.

**Anagol, Santosh, Fernando Vendramel Ferreira, and Jonah M Rexer**, "Estimating the economic value of zoning reform," Technical Report, mimeo 2024.

**Anderson, Michael L**, "Multiple inference and gender differences in the effects of early intervention: A reevaluation of the Abecedarian, Perry Preschool, and Early Training Projects," *Journal of the American statistical Association*, 2008, *103* (484), 1481–1495.

**Barr, Jason and Remi Jedwab**, "Exciting, boring, and nonexistent skylines: Vertical building gaps in global perspective," *Real Estate Economics*, 2023.

**Bolt, Jutta and Jan Luiten van Zanden**, *Maddison style estimates of the evolution of the world economy. A new 2020 update* 2020.

**Borusyak, Kirill, Rafael Dix-Carneiro, and Brian Kovak**, "Understanding migration responses to local shocks," *Available at SSRN 4086847*, 2022.

**Buringh, Eltjo and Urbanization Hub**, "The Clio-infra database on urban settlement sizes: 1500–2000," 2013.

**Clarke, Damian, Joseph P Romano, and Michael Wolf**, "The Romano–Wolf multiple-hypothesis correction in Stata," *The Stata Journal*, 2020, *20* (4), 812–843.

**Davis, Neil N, Jake Badger, Andrea N Hahmann, Brian O Hansen, Niels G Mortensen, Mark Kelly, Xiaoli G Larsén, Bjarke T Olsen, Rogier Floors, Gil Lizcano et al.**, "The Global Wind Atlas: A high-resolution dataset of climatologies and associated web-based application," *Bulletin of the American Meteorological Society*, 2023, *104* (8), E1507–E1525.

**Duranton, Gilles and Diego Puga**, "Urban growth and its aggregate implications," *Econometrica*, 2023, *91* (6), 2219–2259.

**Elvidge, Christopher D., Mikhail Zhizhin, Tilottama Ghosh, Feng-Chi Hsu, and Jay Taneja**, "Annual Time Series of Global VIIRS Nighttime Lights Derived from Monthly Averages: 2012 to 2019," *Remote Sensing*, 2021, *13* (5).

**Esch, Thomas, Klaus Deininger, Remi Jedwab, and Daniela Palacios-Lopez**, "Outward and Upward Construction: A 3D Analysis of the Global Building Stock," Working Papers 2023-09, The George Washington University, Institute for International Economic Policy September 2023.

**Gendron-Carrier, Nicolas, Marco Gonzalez-Navarro, Stefano Polloni, and Matthew A. Turner**, "Subways and Urban Air Pollution," *American Economic Journal: Applied Economics*, January 2022, *14* (1), 164–196.

**Giardini, D, G Grunthal, KM Shedlock, and Zhang P**, "The GSHAP Global Seismic Hazard Map," *Ann. Geophys.*, 1999, *42* (6).

**Global Dam Watch**, "GDW (v1) Consensus Global Database," Technical Report, GDW (v1) consensus global database, last accessed 11-06-2025 2025.

**GMTED**, *GMTED2010 Global Grids* 2010.

**Gonzalez-Navarro, Marco and Matthew A Turner**, "Subways and urban growth: Evidence from earth," *Journal of Urban Economics*, 2018, *108*, 85–106.

**Henderson, Daniel J. and Christopher F. Parmeter**, *Applied Nonparametric Re- gression* 2015.

**Lujala, Päivi, Jan Ketil R d, and Nadja Thieme**, "Fighting over oil: Introducing a new dataset," *Conflict Management and Peace Science*, 2007, *24* (3), 239–256.

**Macedo, Heloisa Ehalt, Bernhard Lehner, Jim Nicell, Günther Grill, Jing Li, Antonio Limtong, and Ranish Shakya**, "Distribution and characteristics of wastewater treatment plants within the global river network," *Earth System Science Data*, 2022, *14* (2), 559–577.

**Maddison, Angus**, *Statistics on World Population, GDP and Per Capita GDP, 1-2008 AD* 2008.

**Maritime Safety Office**, "World Port Index Database," Technical Report, Springfield, VA, USA: National Geospatial-Intelligence Agency, Maritime Safety Office, last accessed 11-06-2025 2019.

**Natural Earth**, "Rivers and lake centerlines," Technical Report, Natural Earth, 1:10 m Physical Vectors, last accessed 11-06-2025 2025.

**NGDC**, *Global Radiance Calibrated Nighttime Lights* 2015.

**Schneider, Julia M, Florian Zabel, and Wolfram Mauser**, "Global inventory of suitable, cultivable and available cropland under different scenarios and policies," *Scientific Data*, 2022, *9* (1), 527.

**Shangguan, Wei, Tomislav Hengl, Jorge Mendes de Jesus, Hua Yuan, and Yongjiu Dai**, "Mapping the global depth to bedrock for land surface modeling," *Journal of Advances in Modeling Earth Systems*, 2017, *9* (1), 65–88.

**United Nations**, *World Urbanization Prospects: The 2018 Revision* 2018.

**USGS**, "Major mineral deposits of the world," 2023.

**Wessel, Pål and Walter HF Smith**, "A global, self-consistent, hierarchical, high-resolution shoreline database," *Journal of Geophysical Research: Solid Earth*, 1996, *101* (B4), 8741–8743.

**World Bank**, *World Development Indicators* 2022.

**Young, Alwyn**, "Channeling fisher: Randomization tests and the statistical insignificance of seemingly significant experimental results," *The quarterly journal of economics*, 2019, *134* (2), 557–598.

Figure A1: Trends in Construction Costs by Height: U.S.

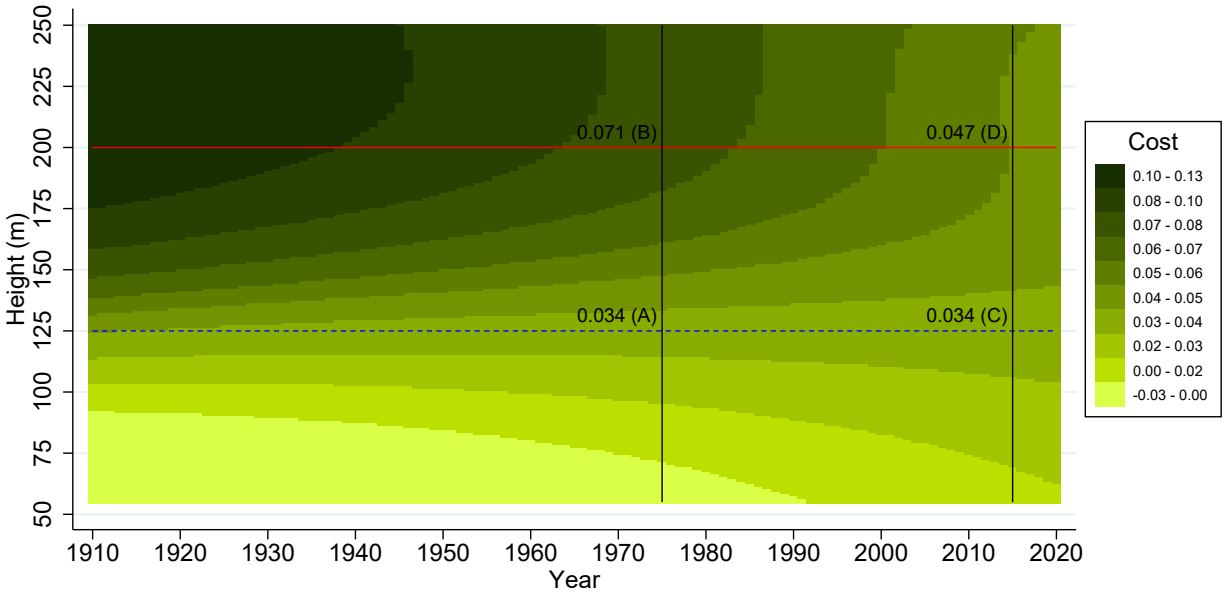


*Notes:* The sample includes 591 tall buildings in 93 U.S. cities built 1902-2021. The mean height is 102 m on a mean bedrock depth of 20 m. "Cost" is the log cost per floor area, residualized for city FE and decade of construction FE. It has a standard deviation of 0.53. Overall log construction cost has a mean of 7.05 and standard deviation of 1.20. We use locally weighted regressions with a bivariate Gaussian kernel to estimate local means of the residualized cost measure within the height-bedrock plane with a bandwidth parameter for both covariates of $\kappa = 50$. Regressing log construction cost per floor area on log height, year, and the interaction yields a coefficient on the interaction of -0.006.

Figure A2: Schematic Diagram of Bedrock Depth and Tall Building Foundations

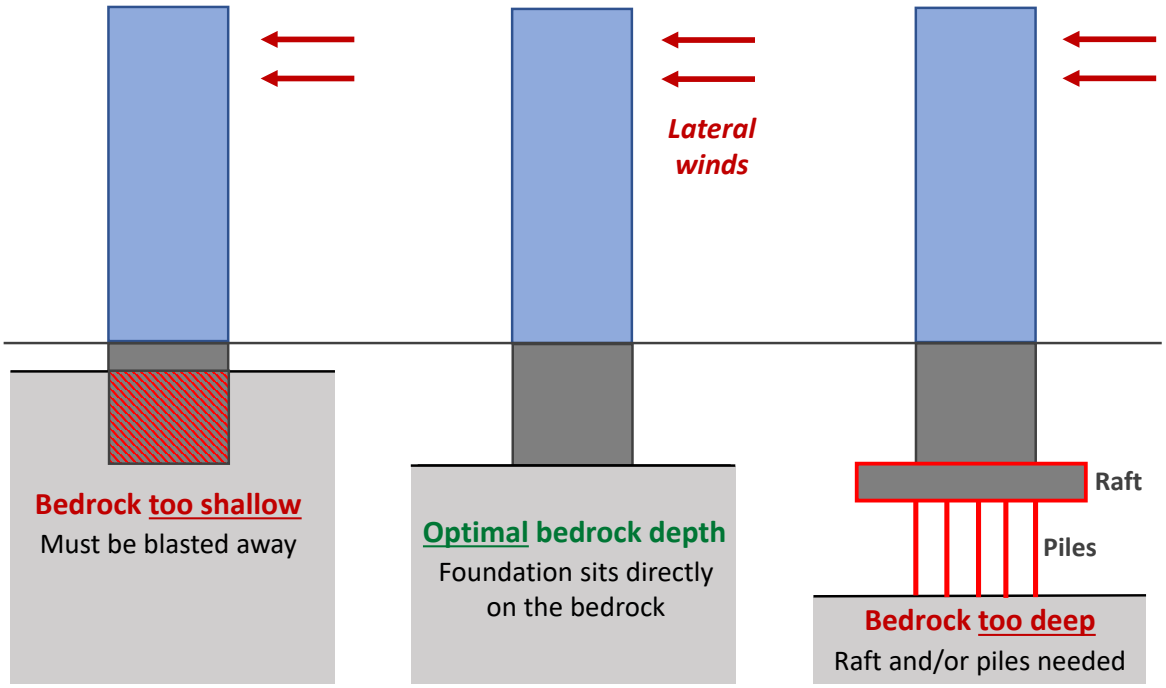

Figure A3: Construction Cost as a Function of Height and Bedrock Depth

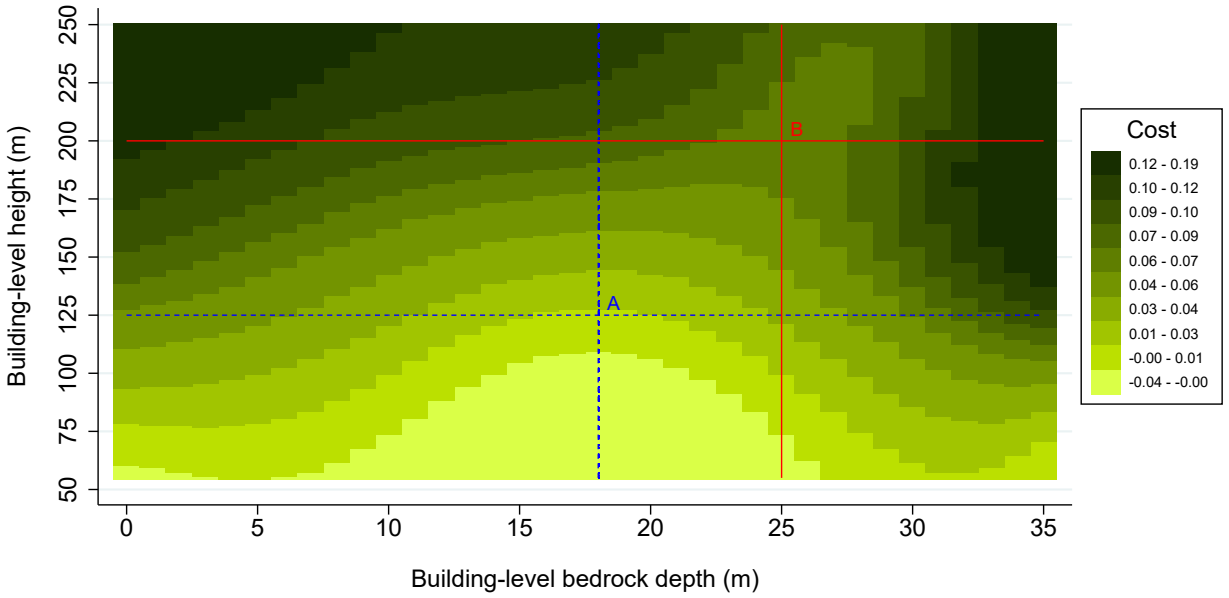


*Notes*: The sample includes 1,033 tall buildings in 206 world cities and 55 countries built through year 2021. The mean construction year is 1995, the mean height is 113 meters, and the mean bedrock depth is 20. Most are concrete buildings. "Cost" is the log cost per floor area residualized for city fixed effects and country-by-decade of construction fixed effects. It has a standard deviation of 0.85. The mean log construction cost is 7.12 with a standard deviation of 1.58. Locally weighted regressions with a bivariate Gaussian kernel are used to estimate local means of the residualized cost measure within the height-bedrock plane. We set the bandwidth parameter for bedrock, $b$, to $\kappa^b = 6$ and for building height, $h$, to $\kappa^h = 40$, which corresponds to about one third of the standard deviation of each respective covariate. We topcode height at the upper limit on the graph, so 250 m includes all buildings of at least 250 m.

Figure A4: Estimated Cost of Height as a Function of Bedrock Depth

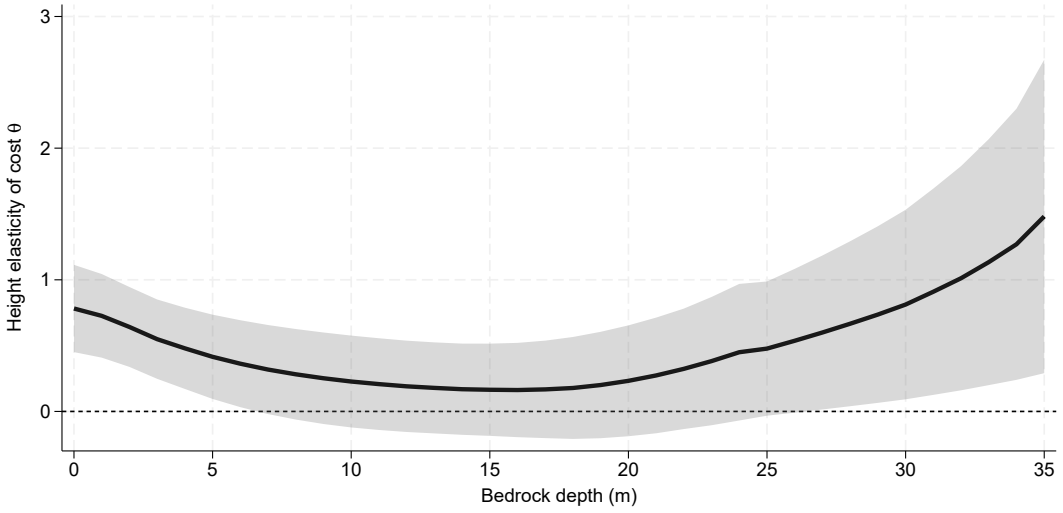


*Notes*: The plot shows non-parametric estimates of the cost of height using the LWR-IV approach explained in Section A.4. In each LWR, we estimate the height elasticity from a regression of the log of construction cost per floor area on building height, controlling for city fixed effects and country by decade of construction effects. The sample consists of 785 tall buildings in 118 cities and 6 countries. We drop countries with fewer than 25 observations to obtain more precise estimates. We use distance from the city center as an instrumental variable for height to remove the effects of unobserved factors that affect construction cost (such as ruggedness) that could be correlated with bedrock depth. The city center is defined as the median coordinate of buildings exceeding 100 meters, or the location of the tallest building if no building exceeds 100 meters. The median first-stage F-statistic is 10.4. We use a Gaussian kernel with a locally varying bandwidth that is inversely related to the density of observations. Confidence bands are at the 95% level.

## Figure A5: Robustness Checks: Other Outcomes

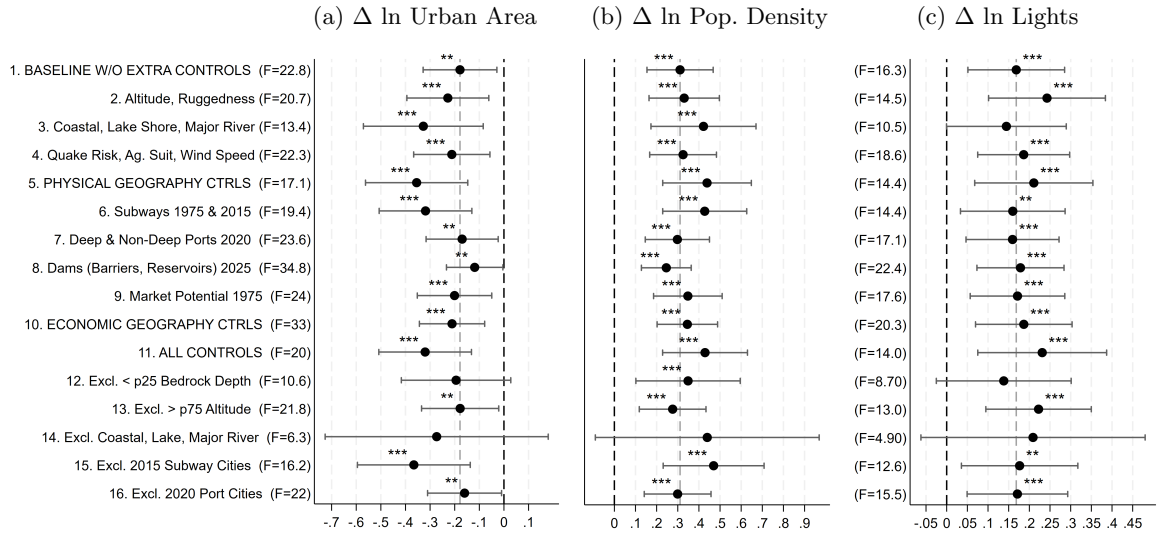


*Notes:* Indicated coefficients and 95% confidence intervals are analogous to those in Figure 4, except using the alternative outcomes indicated in panel headers. Urban Area is total urban area. Population density is based on urban area. For night lights, we consider the period 1990-2015 instead of 1975-2015 and the first-stage F-statistics differ as a result.

## Figure A6: Main Outcomes: Additional Robustness Checks

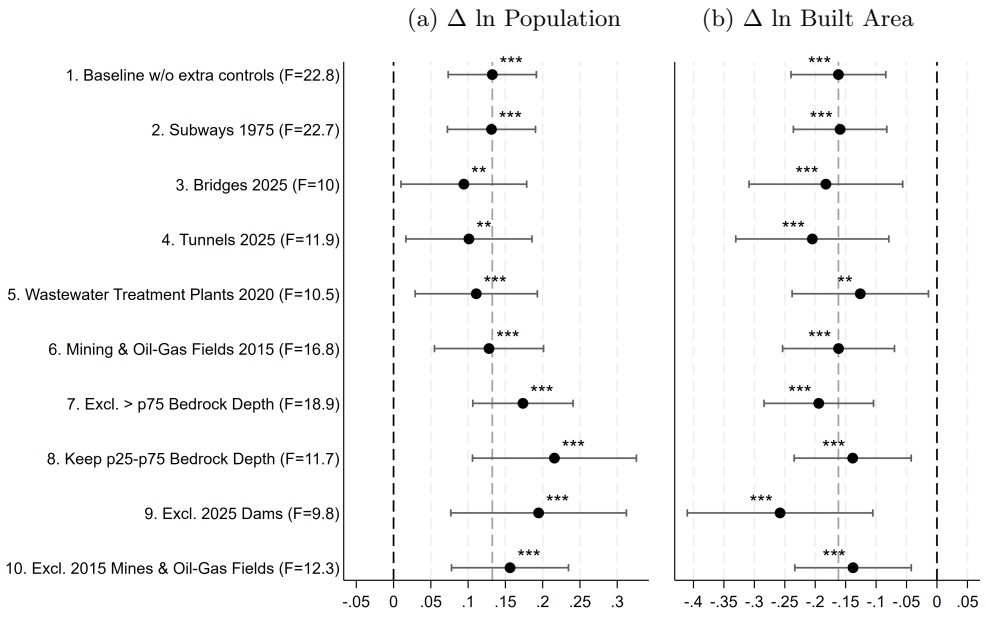


*Notes:* Indicated coefficients and 95% confidence intervals are analogous to those in Figure 4, though for alternative control variables. Row 1 repeats baseline coefficients from Table 2 and rows 2-6 control for indicated variables interacted with bedrock depth and its square. Rows 7-10 exclude indicated cities from the sample. The tests in rows 2, 9 and 10 are described in the main text where we describe Figure 4. For bridges (row 3), we control for the total length (km) of above-water bridges in 2025 and its square, and their interactions with log 1975 city population and its square. For tunnels (row 4), we control for the total length (km) of tunnels in 2025 and its square, and their interactions with log 1975 city population and its square. For wastewater treatment plants (WWTP) in 2020 (row 5), we control for a dummy if there is a WWTP in the city and the number of WWTP and its square, and their interactions with log 1975 city population and its square. For mining and oil-gas fields (row 6), we control for the Euclidean distances to a mine and a gas-field in 2015 and their square, as well as their interactions with log 1975 city population and its square. Appendix A provides details on data sources.

Figure A7: Model Simulated Height Elasticities by Density Disamenity ($\beta^R$)

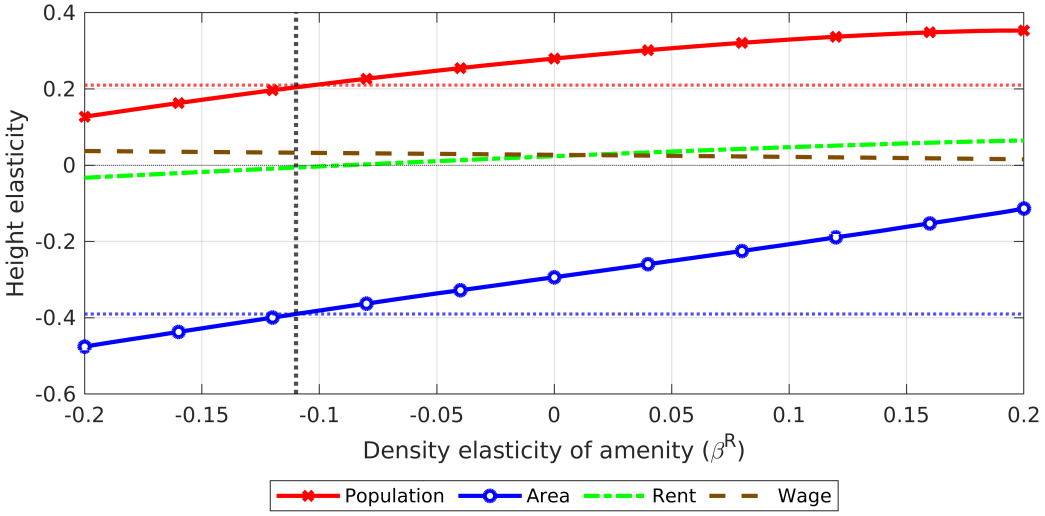


*Note:* Dotted red and blue horizontal lines are our estimates of the height elasticities of population and built-up area for cities located in developing economies unconstrained by height regulation. These are moments matched to model counterparts. To generate model moments, indicated by the four dashed lines, we set one value of $\beta^R$ and then solve the model under varying values of $\theta^U$. We then regress each indicated log outcome on model-generated log heights greater than or equal to $\mathcal{T}$. As such, manipulated variation in heights and the four outcomes originate exclusively from construction supply shocks. We present results for varying values of $\beta^R$ and constant $\mathcal{T} = 3$.

Figure A8: Model Simulated Height Elasticities by Preference Heterogeneity ($\zeta$)

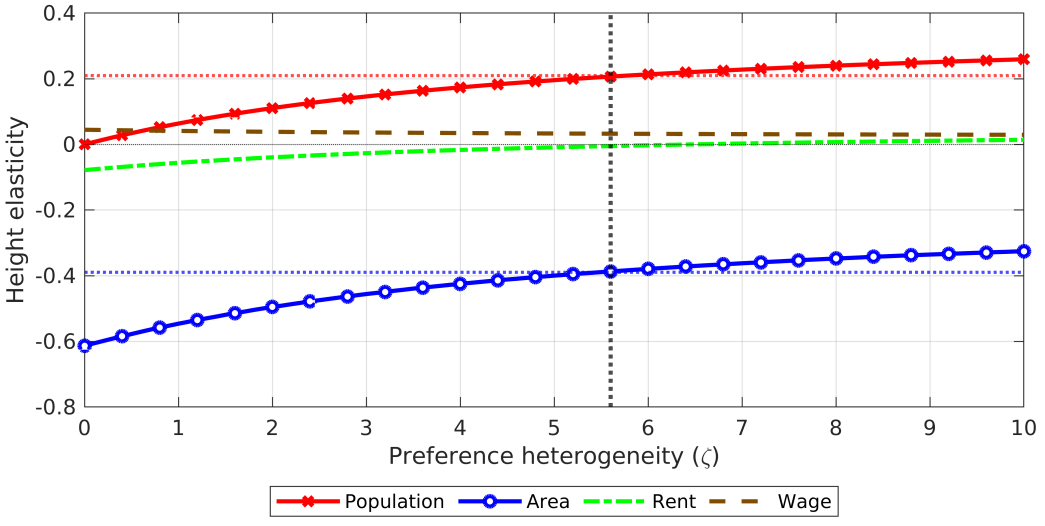


*

*Note:* To generate model moments, we set one value of $\zeta$ and solve the model under varying values of $\theta^U$. We then regress each indicated log outcome on model generated log heights greater than or equal to $\mathcal{T}$. We present results for varying values of $\zeta$ and constant $\mathcal{T} = 2.9$. See the notes to Figure A7 for additional explanationS.

Figure A9: Heterogeneity in Welfare Costs of Height Limits

(a) Utility, small city

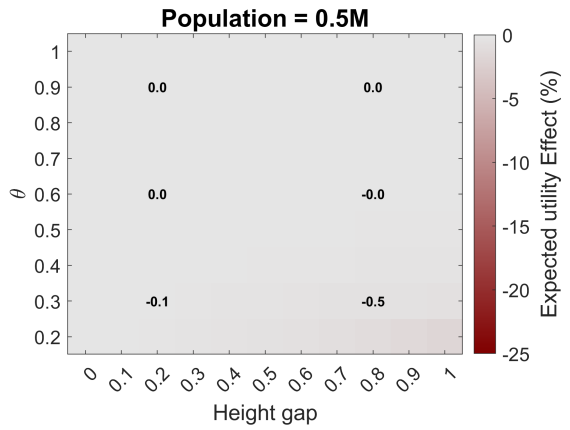


(b) Utility, large city

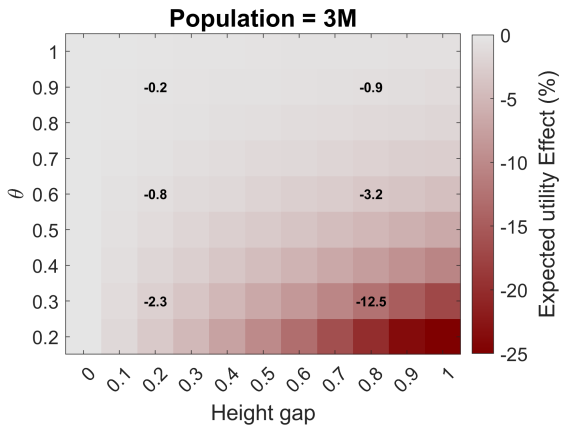


(c) Land value, small city

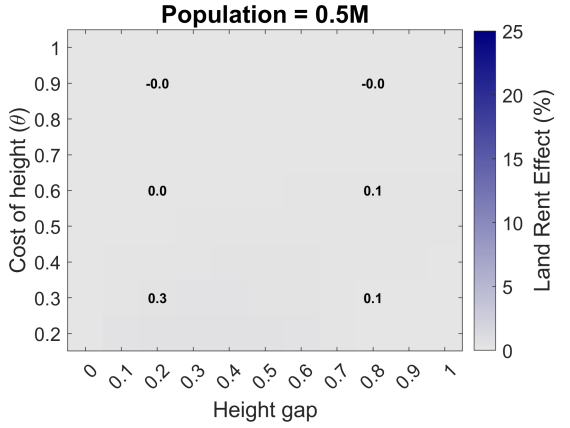


(d) Land value, large city

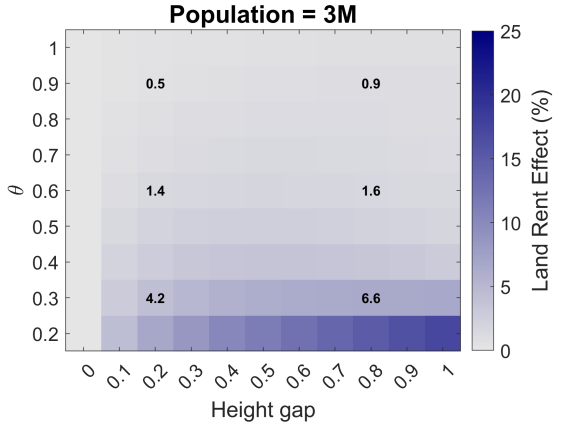


*Note:* We solve the model under different values of $\{\theta^C\}$, setting $\theta^R = \theta^C + 0.05$, finding values of $\{\bar{S}, \tilde{U}\}$ to rationalize a given combination of population and height gap, conditional on each value of $\theta^U$. We adjust the regional population to ensure an urbanization rate of 0.5 and hold all other parameter values constant at the value described in Table 4. The height gap is the fraction of free-market total tall-building height that is not developed due to a height limit.

Table A1: Relationships between Baseline City Attributes and Bedrock Depth

| | Coeff. of Correlation | | (3) Discrete DiD, Excl. Deep Bedrock Cities | | | |
|---|---|---|---|---|---|---|
| Geographic or 1975 Variable: | (1) All Cities | (2) Large Cities 1975 | Coeff. of Large x Intermediate | Romano -Wolf p-values | Sharpened FDR q-values | Sample Mean |
| Altitude: Mean | -0.12 | -0.16 | -114.0 | 0.47 | 0.39 | 528.7 |
| Altitude: Standard Deviation | -0.05 | -0.09 | -59.9 | 0.37 | 0.39 | 265.3 |
| Coastal City (10 km) | 0.09 | -0.06 | -0.06 | 0.92 | 0.44 | 0.1 |
| Lake Shore City (10 km) | 0.08 | -0.02 | 0.07 | 0.90 | 0.44 | 0.1 |
| Major River Crossing the City | 0.10 | 0.16 | 0.15 | 0.37 | 0.39 | 0.1 |
| Mean Earthquake Risk | 0.12 | -0.01 | -0.17 | 0.69 | 0.39 | 1.0 |
| Mean Agricultural Suitability | -0.21 | 0.06 | 2.2 | 0.92 | 0.44 | 57.3 |
| Mean Wind Speed (Definition 1) | 0.14 | 0.04 | 0.06 | 0.92 | 0.57 | 3.7 |
| Mean Wind Speed (Definition 2) | 0.16 | 0.09 | 0.10 | 0.92 | 0.44 | 4.3 |
| Mean Wind Speed (Definition 3) | 0.15 | 0.14 | 0.16 | 0.90 | 0.44 | 4.9 |
| Metro System in 1975 | 0.01 | -0.01 | 0.06 | 0.63 | 0.39 | 0.0 |
| Num. Metro Stations in 1975 | 0.00 | -0.02 | 0.84 | 0.92 | 0.44 | 0.0 |
| Market Potential 1975 ($\alpha$=1) | -0.06 | 0.14 | 0.13 | 0.69 | 0.39 | 11.8 |
| Market Potential 1975 ($\alpha$=2) | -0.08 | 0.01 | 0.04 | 0.92 | 0.81 | 6.9 |
| Observations | 11,269 | 168 | 10,602 [Young Westfall-Young joint test = 0.36] | | | |

*Notes:* Difference in difference coefficients are from regressions of variables at left on the interaction between "large city in 1975" and "intermediate bedrock depth" indicators. Large cities are those above 1 million in 1975 and intermediate bedrock depth is 15-40 meters. In addition to large city and bedrock depth indicator controls, we include country fixed effects. We exclude cities with bedrock depths deeper than 40 m. Romano-Wolf stepdown adjusted p-values control for the familywise error rate and allow for dependence across p-values using 3,000 bootstrap replications (Clarke et al., 2020). Sharpened false discovery rate q-values (Anderson, 2008) does not allow for such dependence. The Young Westfall-Young joint test value (3,000 bootstrap replications) follows Young (2019).

Table A2: Summary Statistics

| | All Developing Countries | | Large Cities Only | |
|---|---|---|---|---|
| | Mean | Std Dev | Mean | Std Dev |
| ln pop 1975 | 11.63 | 0.65 | 14.50 | 0.61 |
| $\Delta$ ln pop, 1975-2015 | 0.50 | 0.39 | 0.58 | 0.69 |
| $\Delta$ ln built area, 1975-2015 | 0.58 | 0.51 | 0.67 | 0.52 |
| Fraction with tall buildings, 1975 | 0.01 | 0.10 | 0.35 | 0.48 |
| $\Delta$ Fraction 1975-2015 | 0.04 | 0.20 | 0.46 | 0.50 |
| ln(Heights+1), 1975 | 0.05 | 0.56 | 2.10 | 3.03 |
| $\Delta$ ln(Heights+1) 1975-2015 | 0.27 | 1.28 | 4.59 | 3.44 |
| Mean Bedrock Depth | 15.73 | 15.81 | 20.86 | 17.37 |

*Notes*: Means and standard deviations are shown for the 11,269 cities in developing countries that make up our primary sample. Also shown in the last two columns are summary statistics for the 168 "large" developing country cities with over 1 million inhabitants in 1975.

Table A3: First Stage Estimates: Remaining Coefficients

| Period for Dep. Var. | 1975-2015 | | 1975 | 2015 |
|---|---|---|---|---|
| | (1) | (2) | (3) | (4) |
| Interaction Variable = | 1975 Large CityDummy | ln 1975 CityPop | ln 1975 CityPop | ln 1975 CityPop |
| Bedrock | 0.0002 | -0.3064*** | -0.0353 | -0.3417*** |
| | [0.0011] | [0.0638] | [0.0323] | [0.0687] |
| Bedrock$^2$ | -0.0000 | 0.0020** | 0.0005* | 0.0025** |
| | [0.0000] | [0.0009] | [0.0003] | [0.0010] |
| Large City Dummy | 3.2449*** | | | |
| | [0.4962] | | | |
| ln 1975 City Pop. | _ | 0.5208*** | 0.2998*** | 0.8206*** |
| | _ | [0.0674] | [0.0477] | [0.0804] |
| 1975 Large City Dummy | Yes | No | No | No |
| ln 1975 City Population | No | Yes | Yes | Yes |
| Bedrock, Bedrock$^2$ | Yes | Yes | Yes | Yes |
| Country Fixed Effects | Yes | Yes | Yes | Yes |

*Notes:* Table reports remaining first stage coefficients associated with each regression in Panel A of Table 1. The dependent variable in columns (1)-(2) is $\Delta$ ln(Heights+1). The dependent variables in the final two columns are ln(Heights+1) in 1975 and 2015, respectively. See the notes to Table 1 for further details about each specification.

Table A4: Temporal and Spatial Placebo Checks

| | (1) | (2) | (3) | | (4) | | (5) |
|---|---|---|---|---|---|---|---|
| Dependent Variable: | $\Delta$ ln Pop (Buringh et al) | | $\Delta$ ln Central Heights | | $\Delta$ ln Periph. Heights | | $\Delta$ ln Pop |
| | 1975-2015 Baseline | 1950-1975 Pre-Trend | Central Bedrock | Periph. Bedrock | Central Bedrock | Periph. Bedrock | Constrained Countries |
| Bedrock*ln 1975 Pop | 0.017*** | 0.004 | 0.035** | -0.015 | 0.022 | -0.003 | -0.001 |
| | [0.006] | [0.014] | [0.017] | [0.018] | [0.022] | [0.023] | [0.002] |
| Bedrock$^2$*ln 1975 Pop | -0.0005*** | 0.0000 | -0.000 | -0.000 | -0.000 | -0.000 | -0.0000 |
| | [0.0001] | [0.0004] | [0.000] | [0.000] | [0.000] | [0.000] | [0.0001] |
| Partial First Stage F | - | - | 7.54 | 2.16 | 1.54 | 0.29 | - |
| Mean | 0.042 | 0.414 | 0.195 | | 0.282 | | 0.602 |
| Observations (Cities) | 560 | 560 | 9,377 | | 9,377 | | 3,315 |

*Notes:* Specifications are similar to those in Table 1 Column (3), with controls for country fixed effects, ln 1975 city population, and a quadratic in city mean bedrock depth. (1) and (2) use all cities belonging to 42 countries that were considered "developing economies" as of 1975 and for which at least two thirds of the cities in our sample have an available historical (pre-1975) population estimate in the Buringh and Hub (2013) database. "Central" in (3) and (4) is defined as the region within 10% of the Euclidean distance to the city center (measured using the center of the brightest 3X3 megapixel in each city). "Peripheral" is the region located between the 10% and 50% of the Euclidean distance to the center. (3) and (4) show the results of one regression each. We lose 1,881 of 11,258 cities from the sample whose area is too small to distinguish central and peripheral areas. In (5), we keep cities belonging to 47 height-constrained countries defined using the height gap methodology discussed in Section 3.5 with an aggregated residual below 0. Robust SEs in brackets.

Table A5: Main IV and OLS Results: Remaining Coefficients

| Period $s$-$t$: | Δ ln Pop 1975-2015 | Δ ln Built Area 1975-2015 | Δ ln Urban. Area 1975-2015 | Δ ln Pop Dens. 1975-2015 | Δ ln Lights 1990-2015 |
|---|---|---|---|---|---|
| | | | Panel A: IV Estimates | | |
| ln Initial Pop $s$ | -0.12*** | 0.24*** | -0.68*** | 0.56*** | -0.15*** |
| | [0.03] | [0.03] | [0.06] | [0.04] | [0.04] |
| Bedrock Depth | 0.00*** | 0.00*** | 0.02*** | -0.02*** | 0.00** |
| | [0.00] | [0.00] | [0.00] | [0.00] | [0.00] |
| Bedrock Depth$^2$ | -0.00 | -0.00** | -0.00*** | 0.00*** | -0.00 |
| | [0.00] | [0.00] | [0.00] | [0.00] | [0.00] |
| | | | Panel B: OLS Estimates | | |
| ln Initial Pop $s$ | -0.10*** | 0.14*** | -0.92*** | 0.82*** | -0.09*** |
| | [0.01] | [0.01] | [0.02] | [0.02] | [0.01] |
| Bedrock Depth | 0.00*** | 0.00*** | 0.02*** | -0.02*** | 0.00** |
| | [0.00] | [0.00] | [0.00] | [0.00] | [0.00] |
| Bedrock Depth$^2$ | -0.00 | -0.00*** | -0.00*** | 0.00*** | -0.00 |
| | [0.00] | [0.00] | [0.00] | [0.00] | [0.00] |
| R-squared | 0.08 | 0.04 | 0.24 | 0.23 | 0.01 |

*Notes:* This table shows coefficients on control variables for regressions in Table 2.

Table A6: IV Results: Alternative Clustering of Standard Errors

| Standard Errors: | | 200 km | 300 Km | 400 km | 600 km | 800 km | Admin 1 |
|---|---|---|---|---|---|---|---|
| Panel A: | | | | Dependent Variable: Δ log Population | | | |
| Δ ln(Heights+1) | 0.13*** | 0.13*** | 0.13*** | 0.13*** | 0.13** | 0.13** | 0.13*** |
| | [0.03] | [0.04] | [0.05] | [0.05] | [0.05] | [0.05] | [0.05] |
| Panel B: | | | | Dependent Variable: Δ log Built Area | | | |
| Δ ln(Heights+1) | -0.16*** | -0.16** | -0.16** | -0.16* | -0.16* | -0.16* | -0.16* |
| | [0.04] | [0.06] | [0.07] | [0.08] | [0.09] | [0.10] | [0.09] |
| F-statistic | 22.84 | 15.34 | 12.88 | 11.46 | 10.72 | 11.54 | 17.00 |

*Notes:* (1) Baseline results. (2)-(6): Conley SE's with a cut-off of 200 km, 300 km, 400 km, 600 km or 800 km (we impose a distance linear decay between observations within the cutoff in the correlation structure). The distance is ≈200 km between Los Angeles and San Diego and ≈300 km between New York and Boston. (7) SE's are clustered at the first administrative level (e.g., "provinces" for China and "states" for India and the U.S.).

Table A7: Analysis of Building Volumes

| Tall B. Volume ≥ ... (m) | 40 | 40 | 55 | 55 | 0 | 40 | 55 |
|---|---|---|---|---|---|---|---|
| Source | (1)-(5) WSF3Dv2 | | | | | (6) GHS-V | (7) GBA |
| | Panel A: ln 2015 City Tall Building Volumes | | | | | | |
| ln(2015 Heights+1) ($\alpha$) | 0.93*** | | 2.87*** | | -0.26*** | 3.35*** | 2.80*** |
| | [0.24] | | [0.32] | | [0.08] | [0.46] | [0.43] |
| First Stage F-Stat | 19.91 | | 19.91 | | 19.91 | 19.91 | 19.99 |
| | Panel B: ln 2015 City Population | | | | | | |
| ln(2015 Tall B. Volumes+1) ($\beta$) | 0.13*** | 0.13*** | 0.04*** | 0.05*** | -0.48** | 0.04*** | 0.05*** |
| | [0.03] | [0.03] | [0.01] | [0.01] | [0.18] | [0.01] | [0.01] |
| ln(2015 Short B. Volumes+1) | | 0.01 | | 0.07*** | | | |
| | | [0.02] | | [0.01] | | | |
| Product of $\alpha$ and $\beta$ | 0.12 | 0.12 | 0.11 | 0.14 | 0.12 | 0.13 | 0.14 |
| First Stage F-Stat | 8.33 | 10.96 | 51.46 | 52.56 | 7.15 | 67.79 | 62.57 |
| | Panel C: ln 2015 City Built Area | | | | | | |
| ln(2015 Tall B. Volumes+1) ($\gamma$) | -0.16*** | -0.12*** | -0.06*** | -0.04*** | 0.61*** | -0.05*** | -0.06*** |
| | [0.05] | [0.03] | [0.01] | [0.01] | [0.16] | [0.01] | [0.01] |
| ln(2015 Short B. Volumes + 1) | | 0.17*** | | 0.12*** | | | |
| | | [0.02] | | [0.01] | | | |
| Product of $\alpha$ and $\gamma$ | -0.15 | -0.10 | -0.17 | -0.11 | -0.16 | -0.17 | -0.17 |
| First Stage F-Stat | 8.33 | 10.96 | 51.46 | 52.56 | 7.15 | 67.79 | 62.57 |

*Notes:* Entries show coefficients and robust standard errors from IV regressions of the variable indicated in the panel header on the variable indicated at left, ln 1975 city population, bedrock depth, bedrock depth squared, and country fixed effects. A quadratic in bedrock depth interacted with ln 1975 city population enters as instruments. Dependent variables in Panel A and predictor variables in Panels B and C are total 2015 city volumes for pixels with heights of at least the threshold indicated in the top row (0, 40 or 55 meters). (1)-(5) use global building volume data from the World Settlement Footprint 3D v2 (WSF3Dv2) database (80X80 meter pixels) (Esch et al., 2023). "Short B. Volumes" indicate the total building volume in remaining pixels in the city. (6) uses global building volume data from the GHS-Volume (GHS-Built-V) database of the Global Human Settlements database (100X100 meter pixels, https://human-settlement.emergency.copernicus.eu/datasets.php). We only include pixels with average heights per built area of at least 40 m in the GHS-Height (GHS-Built-H) database. (7) uses global building volume data from the Global Building Atlas (GBA) database (3X3 meter pixels, https://essd.copernicus.org/articles/17/6647/2025/). Consistent with Emporis, we use building pixels above 55 m.

Table A8: IV Results for Alternative Economic Outcomes

| Dep. Var.: | Log Num. of Flights in June 2014 | | Log ... of GCCC Headquarters c. 2012 | | |
|---|---|---|---|---|---|
| | (1) Within 1 Km | (2) Within 10 Km | (3) Number | (4) Revenue | (5) Employees |
| Log (Height+1) | 0.16** | 0.15** | 0.07** | 0.17*** | 0.57*** |
| | [0.07] | [0.07] | [0.03] | [0.07] | [0.19] |
| F-statistic | 18.77 | 18.77 | 18.63 | 18.63 | 18.63 |

| Dep. Var.: | (6) Log Num of Branches of Top Service Firms 2016 | (7)-(10) Log Num. of ... GDELT Events c. 2000-2005 | | | |
|---|---|---|---|---|---|
| | | Business | | Multinational Corporation | |
| | | All | Material | All | Material |
| Log (Height+1) | 0.62*** | 0.33** | 0.37*** | 0.32** | 0.24** |
| | [0.14] | [0.17] | [0.13] | [0.14] | [0.11] |
| F-statistic | 20.33 | 10.75 | 10.75 | 10.75 | 10.75 |

*Notes:* In (1)-(2) the dependent variable is the log number of originating flights from airports located within 1 km or 10 km from the city's boundary in June 2014 (Open Flights Airports and Airline Data, openflights.org/data#airport, accessed 11-18-2025). Heights are from 2014. In (3)-(5) the dependent variable is the log of the number, total revenue (billion USD) or number of employees of headquarters in 2012 considering the 2,000 largest public corporations in the world (Global Command and Control Centres Database 2006/2009/2012, gawc.lboro.ac.uk/gawc-worlds/gawc-data/dataset-26/, accessed 11-19-2025). Heights are from 2012. In (6) the dependent variable is the log number of branches in 2016 of the top services firms in the world (World City Network 2016: Service Value Matrix and Global Network Connectivities Database, gawc.lboro.ac.uk/gawc-worlds/gawc-data/dataset-28/, accessed 11-20-2025). The data includes branch data from the 25 largest accountancy firms, the 25 largest advertising firms, the 75 largest financial services firms, the 25 largest law firms, and the 25 largest management consultancy firms. Heights are from 2016. In (7)-(10) the dependent variable is the log total number of mentions of selected GDELT events in 2000-2005 (Global Database of Events, Language, and Tone 1.0 Database, blog.gdeltproject.org/the-datasets-of-gdelt-as-of-february-2016/, accessed 11-08-2025). GDELT is an open-source collection of real-time information from global news media. Changes in data collection methodology after 2006 toward more internet-based and "local" sources of information, reducing the prevalence of reported "international" economic events. In cols. (7)-(8), we only select business-related events. In cols. (9)-(10), we only select events related to multinational corporations. In cols. (8) and (10), we only select events related to "material cooperation". GDELT defines such events as events that involve tangible, physical, or functional support. It is one of the four main "Quad Classes" used to categorize events, specifically highlighting concrete actions rather than just words. Heights are from 2000.

Table A9: Land-Use Changes Inside 2015 Urbanized Boundaries

| Dependent Variable: | Δ Log ... Area 1982-2015 | | |
|---|---|---|---|
| | Bare Vegetation | Tree Cover | Short Vegetation |
| Coeff. on Δ ln Height | 0.21*** | -0.24*** | -0.03** |
| | [0.03] | [0.04] | [0.01] |
| Avg Frac of Area, Base Year | 0.21 | 0.07 | 0.72 |
| First Stage F-Statistic | 22.83 | 22.83 | 22.83 |

*Notes:* Each column is associated with a separate IV regression of the growth rate in land with the use indicated at top on the change in log heights using the same specification as in Table 2. Total urban area is decomposed into bare vegetation area (which includes urbanized area), tree cover area, and short vegetation area. Height growth is measured between 1975 and 2015. See the text for data sources. Robust standard errors in brackets.

Table A10: IV Results: Alternative Thresholds for Tall Building Heights

| | (1)-(5): Δ ln Population | | | | | (6)-(10) Δ ln Built Area | | | | |
|---|---|---|---|---|---|---|---|---|---|---|
| Cutoff (m) | 55 | 80 | 100 | 200 | 300 | 55 | 80 | 100 | 200 | 300 |
| Δ ln(Heights+1) | 0.13*** | 0.12*** | 0.13*** | 0.22*** | 0.45*** | -0.16*** | -0.15*** | -0.16*** | -0.26*** | -0.56*** |
| | [0.03] | [0.03] | [0.03] | [0.06] | [0.13] | [0.04] | [0.03] | [0.04] | [0.08] | [0.18] |
| Standardized | 0.17 | 0.13 | 0.13 | 0.12 | 0.12 | -0.21 | -0.16 | -0.16 | -0.14 | -0.15 |
| Observations | 11,257 | 11,257 | 11,257 | 11,257 | 11,257 | 11,257 | 11,257 | 11,257 | 11,257 | 11,257 |
| F-statistic | 22.84 | 23.94 | 20.76 | 9.663 | 7.720 | 22.84 | 23.94 | 20.76 | 9.663 | 7.720 |

*Notes:* (1) and (6) have baseline results. (2)-(5) and (7)-(10) use higher thresholds for the selection of tall buildings in Emporis. Standardized effects shown in the row labeled "Standardized" are z-scores for the log sum of heights.

Table A11: IV Results: Bedrock Depth Data

| | (1)-(4): Δ ln Population | | | | (5)-(8) Δ ln Built Area | | | |
|---|---|---|---|---|---|---|---|---|
| Specification | Baseline | Red/Blue Dot in City | Wgt: 1/(Dist. Red/Blue) Linear | Square | Baseline | Red/Blue Dot in City | Wgt: 1/(Dist. Red/Blue) Linear | Square |
| Δ ln(Heights+1) | 0.13*** | 0.12*** | 0.12*** | 0.12*** | -0.16*** | -0.13*** | -0.13*** | -0.13*** |
| | [0.03] | [0.03] | [0.03] | [0.03] | [0.04] | [0.04] | [0.04] | [0.04] |
| Observations | 11,257 | 8,388 | 11,255 | 11,255 | 11,257 | 8,388 | 11,255 | 11,255 |
| F-statistic | 22.84 | 19.87 | 20.02 | 19.95 | 22.84 | 19.87 | 20.02 | 19.95 |

*Notes:* Shangguan et al. (2017) uses three sources of information for bedrock depths: (i) soil profiles (∼1.3 million locations, red dots in their Figure 2) (ii) boreholes (∼1.6 million locations, blue dots) (iii) "pseudo observations, i.e., points inserted using expert knowledge." (yellow dots). (2) uses cities with at least one red or blue dot within boundaries. (3) uses the inverse of the minimum distance from the city's central business district (CBD) to any red or blue dot as weights and (4) uses inverse distance-squared. CBDs are measured using the center of the brightest 3X3 megapixel in each city.

Table A12: Alternative Heights (H) Measures: IV Estimates

| H Growth Measure | 1(Δ$H$>0) | Δln(H+1) | | Δln(H+55) | Δasinh(H) | | Δasinh(H/1000) | |
|---|---|---|---|---|---|---|---|---|
| | | | | Panel A: Δ ln Pop | | | | |
| Heights (H) Growth | 1.16*** | 0.13*** | 0.09** | 0.24*** | 0.12*** | 0.08** | 0.40*** | 0.27*** |
| | [0.32] | [0.03] | [0.04] | [0.05] | [0.03] | [0.04] | [0.09] | [0.10] |
| | | | | Panel B: Δ ln Built Area | | | | |
| Heights (H) Growth | -1.43*** | -0.16*** | -0.13*** | -0.29*** | -0.15*** | -0.12*** | -0.48*** | -0.40*** |
| | [0.42] | [0.04] | [0.05] | [0.07] | [0.04] | [0.04] | [0.12] | [0.14] |
| Observations | 11,257 | 11,257 | 1,528 | 11,257 | 11,257 | 1,528 | 11,257 | 1,528 |
| First Stage F | 13.22 | 20.76 | 20.23 | 19.33 | 22.51 | 18.25 | 12.04 | 9.58 |
| SD of H Growth | 0.20 | 0.99 | 2.66 | 0.61 | 1.40 | 2.90 | 0.35 | 0.86 |
| Min Pop 1975 (,000) | 0 | 0 | 150 | 0 | 0 | 150 | 0 | 150 |
| Min Height | 55 | 100 | 55 | 55 | 55 | 55 | 55 | 55 |

*Notes:* Results are analogous to those in Table 2, except for the heights measure and sample. Equation (5) shows the regression specification used. Each column uses the measure of heights growth indicated in the top row. The first column shows extensive margin results. "H" and "Heights" in column headers both indicate city aggregate heights in meters. asinh is the inverse hyperbolic sine transformation and uses heights expressed in m or km.

Table A13: Bedrock Quality Instruments: Local Identification

| | Δ ln(H+1) | Δ ln Pop 1975-2015 | | | Δ ln Built Area 1975-2015 | | |
|---|---|---|---|---|---|---|---|
| Bedrock for IV: | Both | Both | Shallow | Deep | Both | Shallow | Deep |
| | (1) | (2) | (3) | (4) | (5) | (6) | (7) |
| Δ Log Height (H) 1975-2015 | | 0.158*** | 0.172*** | 0.159*** | -0.216*** | -0.352*** | -0.229*** |
| | | (0.029) | (0.048) | (0.029) | (0.042) | (0.090) | (0.042) |
| Bedrock$^{deep}$ × ln Pop 1975 | 0.043*** | | -0.001 | | | 0.005* | |
| | (0.006) | | (0.002) | | | (0.003) | |
| Bedrock$^{shallow}$ × ln Pop 1975 | 0.033*** | | | 0.000 | | | -0.004** |
| | (0.008) | | | (0.001) | | | (0.002) |
| First Stage F-stat | _ | 26.6 | 18.5 | 53.0 | 26.6 | 18.5 | 53.0 |

*Notes:* N = 11,269 observations. Specifications are analogous to those in Tables 1 and 2, except that the quadratic in mean bedrock depth is replaced by a linear spline in mean bedrock depth. Regression in (1) is the first stage for the IV regressions in (2) and (5). Regressions in (3) and (6) use variation within shallow bedrock (up to 20 meters) and those in (4) and (7) use variation within deep bedrock (beyond 20 meters) only for identification. Robust standard errors in parenthesis. The R-squared for the first stage regression in the first column is 0.30.

Table A14: Robustness Checks on Functional Form

| | Δ ln Population (Pop) | | | ln Pop | Δ ln Built Area (BA) | | | ln BA |
|---|---|---|---|---|---|---|---|---|
| Period: | 1975-2015 | 1975-2015 | 1990-2015 | 2015 | 1975-2015 | 1975-2015 | 1990-2015 | 2015 |
| Test: | Bedrock Vars in IV | Built Area Ctrl 1975 | Pop 1975 in IV | Cross Section | Bedrock Vars in IV | Built Area Ctrl 1975 | Pop 1975 in IV | Cross Section |
| Δln(Heights+1) | 0.13*** | 0.07*** | 0.09*** | | -0.16*** | -0.11*** | -0.23*** | |
| | [0.03] | [0.03] | [0.03] | | [0.04] | [0.04] | [0.05] | |
| ln(Heights+1)$_{2015}$ | | | | 0.13*** | | | | -0.12*** |
| | | | | [0.03] | | | | [0.04] |
| First Stage F-Stat | 18.53 | 18.92 | 14.57 | 19.91 | 18.53 | 18.92 | 14.57 | 16.31 |

*Notes:* Specifications match those in Table 2 except as indicated. (1) and (5) "Bedrock Vars in IV": Mean bedrock depths and its square enter as instruments instead of as controls. (2) and (6) "Built Area Ctrl 1975": Additional control for log city built area in 1975 (in addition to log city population in 1975). (3) and (7) "Pop 1975 in IV": 1990 is the base year though instruments are constructed using log city population in 1975. (4) and (8) "Cross Section ": Dependent variables and heights are for 2015 only. Instruments are constructed using log city population size in 1975. Column (8) includes an additional control for log city built area in 1975. Robust standard errors in brackets.

Table A15: Displacement Effects: Robustness to Different Fixed Effects and Samples

| | | | | | |
|---|---|---|---|---|---|
| | Panel A: Δ ln Population | | | | |
| Δ ln Height | 0.13*** | 0.10*** | 0.16*** | 0.14*** | 0.13*** |
| | [0.03] | [0.03] | [0.03] | [0.02] | [0.04] |
| | Panel B: Δ ln Built Area | | | | |
| Δ ln Height | -0.16*** | -0.21*** | -0.25*** | -0.22*** | -0.08 |
| | [0.04] | [0.05] | [0.04] | [0.03] | [0.05] |
| Level of FE | Baseline | Subregion | Admin 1 | Admin 2 | Baseline |
| Sample | Full | Full | Full | Full | <20% Urb |
| Observations | 11,257 | 11,269 | 10,606 | 7,439 | 4,594 |
| IV F-stat | 22.84 | 20.02 | 28.96 | 35.23 | 9.77 |

*Notes:* Results of variants of the baseline empirical specification in Table 2 with the following alternative fixed effects (FE). Subregion: 2018 United Nations Geoscheme, grouping countries into 20 world regions (e.g., South America, Central America, and North America). We do not include country FE. Admin 1: First-level administrative divisions that subdivide countries into large sub-national units (e.g., provinces for China) (1,584 divisions). Admin 2: Second-level administrative divisions that subdivide countries into smaller sub-national units (5,176 divisions). The final column only uses cities that were less than 20% urbanized in 1975 (source: World Urbanization Prospects database of the United Nations).

Table A16: Displacement Effects: Controls for Heights-Based Changes in Market Potential (MP)

| | (1)-(5) Δ ln Population | | | | | (6)-(10) Δ ln Built Area | | | | |
|---|---|---|---|---|---|---|---|---|---|---|
| | Panel A: IV for Δ ln(Hgt+1), OLS for Δ ln($MP^H$) | | | | | | | | | |
| Δln(Hgt+1) | 0.13*** | 0.13*** | 0.13*** | 0.13*** | 0.14*** | -0.16*** | -0.16*** | -0.16*** | -0.15*** | -0.16*** |
| | [0.03] | [0.03] | [0.03] | [0.03] | [0.03] | [0.04] | [0.04] | [0.04] | [0.04] | [0.04] |
| Δln($MP^H$) | -0.01* | -0.01* | -0.01** | -0.00 | 0.04*** | -0.01 | -0.00 | 0.00 | 0.04*** | 0.08*** |
| | [0.00] | [0.00] | [0.00] | [0.00] | [0.00] | [0.00] | [0.00] | [0.00] | [0.00] | [0.01] |
| 1st Stage F | 21.88 | 21.96 | 22.18 | 22.59 | 23.12 | 21.88 | 21.96 | 22.18 | 22.59 | 23.12 |
| | Panel B: IV for Δ ln(Hgt+1), IV for Δ ln($MP^H$) | | | | | | | | | |
| Δ ln(Hgt+1) | 0.07 | 0.10** | 0.10*** | 0.09** | 0.18*** | -0.00 | -0.03 | -0.13** | -0.09** | -0.14*** |
| | [0.04] | [0.04] | [0.03] | [0.04] | [0.04] | [0.12] | [0.11] | [0.05] | [0.04] | [0.04] |
| Δ ln($MP^H$) | -0.05 | 0.05 | 0.14*** | 0.02 | 0.08 | 0.81** | 0.79*** | 0.35*** | 0.17*** | 0.19*** |
| | [0.13] | [0.09] | [0.04] | [0.02] | [0.06] | [0.39] | [0.29] | [0.07] | [0.03] | [0.07] |
| 1st Stage F | 1.83 | 3.03 | 16.83 | 11.12 | 13.60 | 1.83 | 3.03 | 16.83 | 11.12 | 13.60 |
| Decay Param | 0.33 | 0.5 | 1 | 2 | 3 | 0.33 | 0.5 | 1 | 2 | 3 |
| Country FE | Yes | Yes | Yes | Yes | Yes | Yes | Yes | Yes | Yes | Yes |

*Notes:* Regressions have the same specification as in Table 2, except that we also include the log change in heights-based market potential 1975-2015 (Δ ln($MP^H$)). We instrument Δ ln($MP^H$) using similarly constructed instruments as for Δ ln(Hgt+1). See the text for details of MP calculation and included controls. Robust standard errors in brackets.

Table A17: Counterfactuals: Illustrative Examples

| | 20% higher cost of height | Binding height limit | Binding height limit under 20% higher cost of height |
|---|---|---|---|
| Total population | -9.1% | -20.1% | -14.6% |
| Total area | 15.6% | 16.1% | 8.7% |
| Average commuting cost | 2.6% | 7.9% | 5.6% |
| Average residential rent | -0.4% | -15.0% | -12.1% |
| Average commercial rent | 7.5% | 0.8% | -2.4% |
| Average productivity | -0.9% | -5.1% | -4.3% |
| Wage | -2.5% | -6.6% | -4.9% |
| Total land value | -0.5% | 3.6% | 2.9% |
| Urban utility ($\bar{U}$) | -2.8% | -6.2% | -4.5% |
| Expected utility ($\mathcal{V}$) | -1.4% | -2.8% | -2.1% |

*Notes:* Scenarios in the first two columns directly correspond to the counterfactuals in the second and third rows of Figure 6. The scenario in the third column shows impacts of imposing a binding height limit on a simulated city that begins at a 20% greater cost of height than the baseline. Averages are weighted by the number of workers.

Table A18: Welfare Effects of Tall Buildings by World Region

| | | City characteristics | | | Expected utility ($\mathcal{V}$) | | Agg land rent ($\mathcal{R}$) | |
|---|---|---|---|---|---|---|---|---|
| World region | Urban pop. (BN) | In cities >1 mill. | Cost of height $\theta$ | Est. height gap | No tall building | No height limit | No tall building | No height limit |
| Africa, G | 0.55 | 34.7% | 0.42 | 47.5% | –0.4% | 5.6% | –0.2% | –4.8% |
| Asia, G | 1.95 | 44.5% | 0.59 | 41.5% | –0.9% | 3.0% | –0.8% | –3.3% |
| Europe, G | 0.04 | 29.2% | 0.46 | 50.9% | –0.4% | 0.8% | 0.3% | –1.3% |
| LAC, G | 0.33 | 52.9% | 0.40 | 62.0% | –1.5% | 5.5% | –1.3% | –6.4% |
| Mean, G | 2.87 | 43.3% | 0.53 | 44.9% | –0.9% | 3.7% | –0.7% | –3.9% |
| Asia, D | 0.19 | 77.2% | 0.38 | 65.2% | –3.6% | 13.7% | –0.1% | –13.4% |
| Europe, D | 0.25 | 41.4% | 0.31 | 84.5% | –0.6% | 4.6% | –2.5% | –5.9% |
| LAC, D | 0.02 | 48.6% | 0.91 | 61.8% | –0.2% | 0.9% | 0.2% | –1.3% |
| North America, D | 0.17 | 67.4% | 0.42 | 76.4% | –1.3% | 6.4% | –3.4% | –8.3% |
| Oceania, D | 0.01 | 64.2% | 0.33 | 89.1% | –0.2% | 7.9% | –0.1% | –7.9% |
| Mean, D | 0.64 | 59.6% | 0.37 | 77.9% | –1.4% | 7.0% | –2.1% | –8.1% |
| Mean, all | 3.51 | 46.3% | 0.50 | 50.7% | –1.0% | 4.3% | –1.0% | –4.6% |

*Notes:* Entries are population-weighted averages across cities in each indicated world region (G = developing economies; D = developed economies). Results are analogous to those in Table 5, calculated by world region.

Table A19: Welfare Costs of Limiting Tall Building Construction: Sensitivity Analysis

| | | | | Expected utility $\mathcal{V}$ | | Share adj. rent | | Agg land rent $\mathcal{R}$ | |
|---|---|---|---|---|---|---|---|---|---|
| | $\zeta$ | $\beta^R$ | $\mathcal{T}$ | No tall building | No height limit | No tall building | No height limit | No tall building | No height limit |
| 1. Baseline parameters | 6.4 | –0.11 | 3.0 | –1.0% | 4.3% | 0.78 | 0.49 | –1.0% | –4.6% |
| 2. Calib congest disamen | 5.7 | –0.09 | 3.0 | –1.1% | 4.7% | 0.68 | 0.45 | –1.0% | –4.7% |
| 3. No congest disamen | 3.4 | –0.00 | 2.9 | –1.9% | 7.2% | 0.39 | 0.30 | –0.8% | –5.1% |
| 4. Calib low mig elas | 4.8 | –0.07 | 3.0 | –1.3% | 5.4% | 0.57 | 0.40 | –0.9% | –4.8% |
| 5. Calib high mig elas | 9.0 | –0.14 | 3.0 | –0.7% | 3.4% | 1.17 | 0.61 | –1.1% | –4.3% |
| 6. Flrspc prod shr 0.10 | 6.4 | –0.08 | 3.1 | –0.9% | 4.3% | 0.88 | 0.64 | –0.7% | –6.1% |
| 7. Flrspc prod shr 0.20 | 6.4 | –0.13 | 2.7 | –1.0% | 4.4% | 0.70 | 0.35 | –1.2% | –3.2% |
| 8. City agglom elas 0.00 | 6.4 | –0.07 | 2.5 | –1.0% | 4.1% | 0.65 | 0.44 | –0.7% | –3.5% |
| 9. City agglom elas 0.06 | 6.4 | –0.14 | 3.5 | –1.0% | 4.5% | 0.94 | 0.53 | –1.3% | –5.7% |
| 10. Amenity decay 20%↑ | 6.4 | –0.12 | 3.4 | –1.0% | 4.4% | 0.87 | 0.52 | –1.0% | –4.8% |
| 11. Amenity decay 20%↓ | 6.4 | –0.08 | 2.5 | –0.9% | 4.2% | 0.68 | 0.45 | –1.0% | –4.3% |
| 12. Sao Paolo decay | 6.4 | –0.1 | 2.9 | –0.9% | 4.1% | 0.81 | 0.57 | –0.9% | –4.9% |
| 13. Spline for $\theta$ | 6.4 | –0.11 | 3.0 | –0.9% | 4.0% | 0.75 | 0.48 | –0.9% | –4.3% |
| 14. Spline for $\theta$ deep | 6.4 | –0.11 | 3.0 | –0.9% | 4.1% | 0.76 | 0.48 | –1.0% | –4.5% |
| 15. Housing exp shr 0.25 | 6.4 | –0.07 | 3.0 | –1.0% | 4.0% | 0.46 | 0.26 | –0.9% | –4.4% |
| 16. Housing exp shr 0.40 | 6.4 | –0.13 | 3.0 | –0.9% | 4.5% | 1.00 | 0.63 | –1.0% | –4.9% |
| 17. Ht gap $75^{th}$ pctile | 6.4 | –0.11 | 3.0 | –1.6% | 2.3% | 0.74 | 0.47 | –0.1% | –2.8% |
| 18. Set $\theta$ 20% lower | 6.4 | –0.11 | 3.0 | –1.1% | 5.3% | 0.86 | 0.52 | –1.1% | –6.0% |
| 19. No commercial ht lim | 6.4 | –0.11 | 3.0 | –1.0% | 2.3% | 0.78 | -0.43 | –1.0% | 3.5% |
| 20. No residential ht lim | 6.4 | –0.11 | 3.0 | –1.0% | 0.1% | 0.78 | -5.26 | –1.0% | –5.2% |

*Notes:* Entries are analogous to those in Table 5 for "All Economies" (developing + developed) except using indicated alternative parameter values. Entries in "Share adj. rent" columns are fractions of changes in urban utility $\bar{U}$ accounted for through changes in the adjusted rent (i.e., rents plus commuting costs). This share is negative if utility increases and these components sum to a negative contribution. Rows 2-3 use estimated preference heterogeneity $\zeta$ given indicated calibrated values of the congestion elasticity $\beta^R$ whereas rows 4-5 use estimated congestion elasticity $\beta^R$ for alternative calibrated values of preference heterogeneity $\zeta$. The third block of results show sensitivity of the baseline in the top row to changes in other parameters, one at a time. In rows 13-14, we use the specification for $\theta$ estimated in Table A13 Column (1). The bottom three rows show results given a 20% lower cost of height, a counterfactual in which only the commercial height limit is lifted (holding residential height limits at those calculated in Section 3.5), and a counterfactual in which only the residential height limit is lifted (holding residential height limits at those calculated in Section 3.5), respectively.